Morphology, mineralogy and surface chemistry of manganiferous oxisols near Graskop, Mpumalanga Province, South Africa

Catherine Elaine Dowding
Bsc Agric (Stellenbosch)

A thesis submitted in partial fulfilment of the requirements for the degree of

Master of Science (Agriculture)

Department of Soil Science
Stellenbosch University

August 2004

ABSTRACT

In the humid Graskop region of Mpumalanga Province, South Africa, there is an anomalous body of highly weathered black, manganiferous oxisols derived from dolomite. With Mn contents as high as 17%, potential large-scale Mn release is an environmental concern under current, acid generating, forestry practices. This study aims at establishing the factors which may affect the stability of the manganiferous oxisols of Graskop and in the process, investigating some of the morphological, mineralogical and chemical properties of these unique soils.

Typically, the soils show a reddish, nodule-rich horizon, containing 3-4% Mn, grading through a red and black mottled zone into a black (5YR 2.5/1) apedal subsoil with >7% Mn. The Mn gradient down the profile as well as the abundant nodule content of the upper subsoil horizons implies that Mn mobilization and redistribution are active pedogenic processes. The exceptional Mn content of these soils is complemented with Fe and Al concentrations of up to 10 and 8%, respectively, and anomalously high trace element levels in particular Ni and Zn (as high as 541 and 237 mg kg^{-1}, respectively) which are at the upper limit of cited world natural maxima for soils. The Mn mineral lithiophorite [$(Al,Li)MnO_2(OH)_2$], dominates the mineralogy of the soils with accessory amounts of birnessite, gibbsite, goethite, hematite, maghemite, kaolinite, aluminous chlorite and mica - a mineral suite reflecting that of well weathered soils.

With the pH of the soil being at or close to the point of zero charge (4.5-5.5) the soils show isoelectric equilibrium. The very low buffer capacity results in metal dissolution commencing with the first increment of titrated acidity. Manganese dissolution is relatively minor considering the large potential for release and is highly overshadowed by Al release. The apparent resilience of the Mn phase to added acidity may relate to the overwhelming poise of the soils which maintains robust, oxic conditions despite the usual instability of Mn oxides at low pH.

Manganese release and soil redox properties are substantially affected by drying especially in the organic rich topsoils. Using various redox analyses, evidence is shown for involvement of Mn(III)-organic complexes in the drying reactions. Using this and information gained in a real time, attenuated total reflectance Fourier transform infrared

(ATR-FTIR) spectroscopic study, a mechanism is suggested which may account for the observed Mn release and the loss of Cr oxidising capacity commonly observed in dried soils. The information provided by the ATR-FTIR study showed the decrease in surface pH of a clay film, from 5 to below 2, as well as the shift in coordination nature of sorbed oxalate from a more outer-sphere association to a more inner-sphere association concomitant with the removal of free water from the clay surface. This spectroscopic evidence for these chemical changes which accompany surface drying not only provides further insight into the reactions involving Mn oxides in soils but also highlights the suitability of ATR-FTIR for real time, *in situ* investigation into the chemistry of the drying water interface.

From these results it is concluded that Mn release from the manganiferous oxisols, under acid generation of the kind known to occur in pine plantations, is less that anticipated. On the other hand, desiccation of the topsoil results in substantial Mn release with a suggested mechanism which involves a Mn(III) intermediate.

UITTREKSEL

'n Onreelmatige grondliggaam van hoogs verweerde, swart, mangaanhoudende oxisols wat uit dolomiet ontwikkel het, word in die humiede Graskop streek van die Mpumalanga Provinsie van Suid-Afrika aangetref. Die hoë Mn-inhoud (tot 17%) van hierdie oxisols is van groot omgewings-belang weens die potensiële grootskaalse Mn-vrystelling onder huidige, suur-genererende bosbou praktyke. Hierdie studie beoog om die faktore wat die stabiliteit van die mangaanhoudende oxisols van Graskop affekteer, vas te stel. Tesame hiermee word die morfologiese, mineralogiese en chemiese eienskappe van hierdie unieke gronde ondersoek.

Kenmerkend van hierdie gronde is 'n rooi, nodule-ryke horison met 3-4% Mn aan die oppervlakte. Bogenoemde horison verander met toename in diepte in 'n rooi en swart gevlekte sone wat weer in 'n swart (5YR 2.5/1) apedale ondergrond met >7% Mn oorgaan. Die Mn gradiënt in die profiel sowel as die hoë nodule-inhoud van die boonste grondhorison dui daarop dat Mn-mobilisasie en -herverspreiding huidige aktiewe pedogenetiese prosesse in die profiele is. Fe en Al, met konsentrasies van 10% en 8% onderskeidelik, word saam met die onreelmatig hoë Mn inhoud aangetref. Baie hoë vlakke van Ni en Zn (so hoog as 541 en 237 $mg.kg^{-1}$ onderskeidelik) wat hoër is as aangehaalde wêreld natuurlike maksimum waardes, word ook aangetref. Die mineralogie van die gronde word deur die Mn mineraal litioforiet [$(Al,Li)MnO_2(OH)_2$] gedomineer. Bykomstige hoeveelhede van birnessiet, gibbsiet, goethiet, hematiet, maghemiet, kaoliniet, aluminiumryke chloried en mika word ook aangetref. Hierdie minerale samestelling is kenmerkend van hoogs verweerde gronde.

Met die pH van die grond in die omgewing van die punt van geen lading (4.5 – 5.5), word 'n iso-elektriese ekwilibrium by die gronde aangetref. Die baie lae bufferkapasiteit het metaal-oplossing aangehelp wat met die eerste inkrement van titreerbare suurheid 'n aanvang geneem het. Mangaan-oplossing is baie klein indien die groot potensiaal vir vrystelling asook die groot mate van Al-vrystelling in ag geneem word. Die skynbare teenwerking van die Mn fase tot toegevoegde suurheid, mag toegeskryf word aan die

sterk ewewig van die gronde om sterk, oksiese kondisies, ten spyte van die normale onstabiliteit van Mn oksiedes by lae pH, te onderhou.

Mangaan vrystelling en grond redoks eienskappe word beduidend deur uitdroging beïnvloed en veral in die organies-ryke bogronde. Deur van verskeie redoks analises gebruik te maak is daar bewyse van die betrokkenheid van Mn(III)-organiese komplekse in die uitdroging-reaksies gevind. Dit. en data ingesamel in ‘n “*real time, attenuated total reflectance Fourier transform infrared* (ATR-FTIR)” spektroskopiese studie, is gebruik om ‘n meganisme voor te stel wat die waargenome Mn vrystelling en die verlies aan Cr oksidasie kapasiteit (algemeen waargeneem in droë gronde) te kan verklaar. Die data verkry met die ATR-FTIR studie het ‘n afname in oppervlak pH van 5 na 2 van ‘n klei film asook die verskuiwing in koördinasie toestand van die gesorbeerde oksalaat van ‘n meer buite-sfeer assosiasie tot ‘n meer binne-sfeer assosiasie, gepaardgaande met die verwydering van vry water van die klei oppervlaktes, uitgewys. Die spektroskopiese bewyse vir die chemiese veranderinge wat die oppervlak uitdroging vergesel, gee nie net meer insig in die reaksies rakende Mn oksiedes in gronde nie maar onderstreep ook die toepasbaarheid van die ATR-FTIR vir intydse (“real time”), *in situ* ondersoeke na die chemie van die uitdrogende water kontakvlak.

Pectora roborant cultus recti

Vanuit hierdie resultate kan afgelei word dat Mn vrystelling vanuit mangaanhoudende oxisols onder suur genererende denne plantasies laer is as wat verwag is. Aan die ander kant sal uitdroging van die bogrond tot aansienlike Mn vrystelling, met ‘n verwagte meganisme wat Mn (III) as intermediêre toestand insluit, lei.

Acknowledgments

I am greatly indebted to my supervisor Prof. Martin Fey, for his endless support and encouragement and for introducing me to the Graskop soils, as well as to my co-supervisors Dr Freddie Ellis and Prof. Don Sparks for their valuable advice and input into this study.

A very special thanks to my financial sponsors, the NRF and the University of Stellenbosch and especially to the Skye Foundation, who gave me generous financial support which allowed me the privilege of study abroad.

I would also like to offer sincere thanks to the following people and institutions:

At Stellenbosch University: to Matt Gordon for countless analyses, to Herschel Achillies, Judy Smith, Kamiela Crombie, Kenneth Davidse, Philisiwe Shange, Ilsa Mathys, Ailsa Hardie and Michele Francis for friendly assistance in the lab, Richard O'Brien for XRD analysis, Dr Paul Verhoeven for IR analysis, Mr Willem de Clercq, Mr Jan Lambrechts and Dr Eduard Hoffman for suggestions and technical advice.

A big thanks to Prof. Don Sparks and the Environmental Soil Chemistry group at the University of Delaware: Jerry Hendricks, Amy Broadhurst, Kristin Staats, Dave McNear, Jen Seiter, Kristian Paul, Ted Peltier, Shinwoo Lee, Ryan Tappero and Jeff Everhart for their generous assistance and kindness during my 6 month visit. A special thanks to Markus Gräfe for his time and patience in collecting and processing the XAS data and to Mike Borda for making the ATR experiments possible.

To everyone at the department of Soil Science and Agronomy at Natal University for allowing me to use their labs, in particular Chris Bester, Essack Abib and Jeff Hughes.

To Lorraine McNamara and Global Forest Products for generous assistance during mapping and sampling and for providing information on the Driekop plantation.

To Willem Kirsten and Christl Bühmann at ISCW for allowing me to make use of the XRD facilities.

To Dr Darrell Schultz and Dr Don Ross for assistance with XANES analysis procedures and to Sam Clarke and Torsten Scheidt for their mathematical advice.

Very special thanks to my family for their tireless support and encouragement especially during the more trying periods of this study.

And finally I would like to thank the Graskop soils for their companionship and stimulation over the last two years. It has been a true privilege to work with what must be some of the most beautiful soils in the world.

TABLE OF CONTENTS

Pectora roborant cultus recti

LIST OF FIGURES

LIST OF TABLES

Pectora roborant cultus recti

INTRODUCTION

Manganese is an essential element in plant nutrition. It can be present in both toxic and deficient quantities in soils depending on the total concentration available and the prevalent chemical conditions. Manganese is considered fairly mobile in many acid soils (Kabata-Pendias and Pendias, 2001) and because of this mobility, many well weathered, acid soils have very low concentrations of Mn (Sumner et al., 1991). The high lability of Mn oxides under intense weathering conditions is probably one of the reasons many oxisols are deficient in Mn and it is this lability which may be a cause for concern when highly weathered soils do contain Mn in appreciable amounts.

Many soils of the Graskop region in the Mpumalanga Province of South Africa are exceptionally enriched in Mn oxides. These soils are very old, highly weathered oxisols which have formed through the congruent weathering of Mn-rich dolomite (Hawker and Thompson, 1988). Exotic forest plantations have been established in the region during the last century and soil acidity is becoming an increasing concern in these highly weathered soils (Nowicki, 1997). Very little information is available on the manganiferous oxisols of Graskop and their suitability to host acid generating crops like pine trees. This study aims at elucidating some of the mineralogical and chemical properties of the Mn-rich oxisols, as well as investigating the factors which may influence their chemical stability under the current environmental conditions.

The large pool of Mn in the Graskop soils is a potential source of phytotoxicity and, if certain pedogenic thresholds were to be exceeded, large-scale dissolution of Mn oxides might result. The manganiferous oxisols of Hawaii can be likened to the Graskop soils in that they have a very high Mn content, between 1 and 4%, and are fairly acidic (Fujimoto and Sherman, 1948). Manganese toxicity is a serious constraint to many crops grown on the acid soils of Hawaii (Fujimoto and Sherman, 1948; Asghar and Kanehiro, 1981; Vega et al., 1992; Hue et al., 2001) and soluble Mn has been shown to increase 100-fold for every unit decrease in pH (Hue et al., 2001). While manganese toxicity has not been reported in the Graskop area, it is also fair to say little work has been done to assess any cases of phytotoxicity. It is also possible that Mn toxicity in these soils has not drawn much attention because *Pinus patula*, one of the most widely planted species in the area, shows a high tolerance for Mn with foliage concentrations of up to 2000 mg kg^{-1} being

tolerated before growth is adversely affected (Schutz, 1990). In the latter study foliar Mn concentrations of trees grown on the dolomitic soils were shown to be close to 2800 mg kg^{-1} while on the granitic soils of the region the foliar concentrations were only 300 mg kg^{-1} which clearly indicates that Mn in the soil may reach phytotoxic levels. Although the pine trees may tolerate high Mn levels, metal concentrations entering the ecosystem through drainage water could be of concern. Manganese encrustations have been observed along quartzitic streambeds which drain from the transition zone between the quartzite and dolomite (De Waal, 1978) indicating that Mn concentrations in stream waters may be substantial. A further consideration is the mobilization of any trace elements associated with the Mn oxide phase. Some trace elements are known to have a high affinity for Mn oxides (Kabata-Pendias and Pendias, 2001). Thus the mobility of any sorbed trace elements will also depend on the stability of the Mn phase. For these reasons it is important to establish the factors affecting Mn mobilization in the Graskop soils and to determine the vulnerability of these soils under current land use practices.

The effect that drying has on Mn release is one of the ambiguities surrounding our understanding of Mn chemistry in soils. Drying a moist but well aerated soil has been shown to result in substantial enhancement of exchangeable Mn (Bartlett and James, 1979; Bartlett and James, 1980; Goldberg and Smith, 1984; Berndt, 1988; Haynes and Swift, 1991; Ross et al., 1994; Bunzl et al., 1999; Makino et al., 2000; Ross et al., 2001a), which is almost counter-intuitive as drying would naturally increase the aeration of the soil and should, if anything, result in Mn oxidation and precipitation. From the perspective of the Graskop soils, drying may play an important role in Mn mobilisation as has been shown in Hawaiian oxisols (Fujimoto and Sherman, 1945). Graskop experiences a long dry season during the winter and early spring months. Continual transpiration of the evergreen pine plantations throughout the dry winter period may result in significant soil desiccation and drying could be an important mechanism of Mn release. Grassland soils, may also dry out substantially especially with the event of *veld* fires which are common in late winter. The Graskop soils with their exceptional Mn content make them ideal for investigating some of the chemistry surrounding the drying induced Mn release which is still highly speculative.

It is also important to investigate the manganiferous oxisols of Graskop for their own sake. They are a true freak of nature and are surrounded by intrigue and paradoxes. With the abundance of Mn they provide a unique opportunity to elucidate some of the important

characteristics of soil Mn oxides that have eluded many researchers due to the very low Mn oxide content of most soils. Generally studies of Mn oxides are confined to local accumulations such as nodules or dendrites and various pretreatments are normally required to concentrate Mn oxides prior to investigation. The Graskop soils provide an abundance of Mn for studying the fundamental mineralogical and chemical characteristics of Mn oxides in highly weathered soils. They also provide a very good opportunity for elucidating the changes that occur in Mn oxides as the soil dries. It is hoped that by investigating this extreme case of Mn enrichment, insight may be gained into some of the subtleties not readily evident in soils with more moderate Mn concentrations.

This study highlights some of the fundamental chemistry and mineralogy of the Graskop soils and then assesses the stability of the Mn phase under current environmental conditions. To achieve a more holistic approach to understanding the pedogenic processes active in these soils the study encompasses a wide range of investigation from landscape to atomic scale. The main objective is to establish the factors which affect the stability of the manganiferous oxisols at Graskop. In order to achieve this an attempt has been made to answer the following questions:

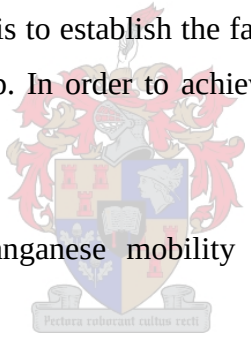

1. Is there evidence of manganese mobility within the profile and within the landscape?
2. What are the chemical and mineralogical properties of these unusual soils?
3. What is the buffer capacity of the soil, and how is metal release affected by addition of acids?
4. What is the effect of drying the soil and, given the abundance of Mn oxides, is it possible to unravel the mechanism which results in enhanced Mn release from dried soils?

The study has been divided into five chapters. The first two deal mainly with morphological, chemical and mineralogical characteristics of the soils and the last three then focus on the effects of added acidity and drying on metal release.

CHAPTER 1

1 Mapping, classification and chemical analysis

1.1 Introduction

Finding considerable amounts of manganese in any soil is uncommon. This is primarily due to a lower total concentration of Mn compared to Fe and Al but it is also largely due to the high lability of Mn under many soil conditions. Manganese oxides are stable under conditions of high pH and high redox potential, and it is likely that any soils, or localized zones within soils containing Mn oxides must have experienced such conditions at one or other time during their development. When soils weather and acidify, Mn oxides become less stable, especially when organic matter is present. This usually results in the mobilisation and migration of Mn to lower parts of the profile where both pH and pe increase. The high lability of Mn under intense weathering conditions typically results in Mn deficiencies being a common problem in many oxisols and the term ‘manganiferous oxisol’ might almost be considered an oxymoron. Therefore finding acidic, highly weathered soils with a mineralogy dominated by Mn oxides is very exciting. The following review highlights some of the geographical, geological and pedological circumstances which have combined uniquely to produce the extremely weathered manganiferous oxisols of Graskop.

Pectora roborant cultus recti

1.1.1 Geomorphology

Graskop is a high lying town on the eastern escarpment of Mpumalanga Province in South Africa. The eastern escarpment, also known as the Great or Mpumalanga escarpment, is the most prominent geomorphic feature of the region, separating the elevated interior from the coastal hinterland, which stretches eastwards towards Mozambique. The formation of the escarpment is said to have been a result of uplift during the breaking up of Gondwana (Partridge and Maud, 1987). It has survived aeons of weathering largely as a result of the resistant Black reef quartzite which has been cut back rather than incised. The relatively steep escarpment rises to elevations over 2000 m.

1.1.2 Climate and vegetation

The extreme relief and high altitude of the eastern escarpment results in the area being one of the highest rainfall regions in South Africa, generally receiving more than 1000mm y^{-1}. As is the case for much of the eastern seaboard, rainfall on the eastern escarpment is confined to the summer months, receiving most of its rainfall between November and March. This is followed by a dry, cool winter and a dry, warm spring between September and October. Rainfall usually occurs in the form of thunderstorms although there are also occasional extended periods of light drizzle. Fog is common during summer in the high altitude areas, which helps reduce evapotranspiration. The dry season usually starts with the onset of winter, which is cold and dry. Early morning frosts often occur in the lower parts of the valleys.

The steep slopes render the area unsuitable for agriculture but the humid climate and deep soils make it a prime region for commercial forestry. This has seen much of the deciduous natural grassland being converted into pine and eucalyptus plantations during the course of the last century. The dry winter and frequent frosts cause much of the grassland vegetation to die back and dry out during winter. This becomes a fire hazard and in late winter and early spring, *veld* fires are frequent in the natural grassland areas. There are interment pockets of indigenous, semi-deciduous rainforest scattered throughout the grasslands and plantations, usually in sheltered ravines or along cliff lines. This natural forest is said to have been much more extensive prior to the development of the mining and forestry industries.

1.1.3 Geology and soils

The geology of the Mpumalanga escarpment is dominated by the Wolkberg group, which consists of resistant quartzite exposed on many of the cliffs which define the edge of the escarpment. This is overlain by the Chuniespoort group which leads up to the higher mountain ranges of the Pretoria group. The Chuniespoort group comprises a number of dolomite formations which were deposited in a shallow, clear water sea (Viljoen and Reimond, 1999). Of these formations it is the Eccles formation, known as Malmani dolomite, which dominates the region around Graskop (Fig.1.1). The Eccles formation is differentiated from the other dolomites of the Chuniespoort group by its higher content of

chert which forms resistant lenses throughout the dolomite. It has been suggested that the higher chert content may be one of the reasons the dolomite has persisted in such a humid climate (Schutz, 1990). The topography around Graskop is typical of carbonate solution weathering, with steep sided valleys dominating the landscape (Fig. 1.2) and the regular occurrence of sink holes and caves.

The Malmani dolomite is fine-grained and grey-blue in colour. The weathering front of the dolomite is often black due to Mn oxides. The dolomite is composed of Ca and Mg carbonate with accessory amounts of manganese, iron, silicon and traces of lead and zinc (Schutz, 1990). Congruent weathering of the dolomite has lead to the dissolution of much of the soluble carbonate components, while Mn and Fe have accumulated as a residual enrichment of their oxides (Hawker and Thompson, 1988). Generally the soils which weather from the dolomite are dark red, although there are intermittent patches within the landscape which show extreme Mn accumulation and these are very dark, even black in colour. The localised pockets of Mn-rich soils probably relate to variation in parent material composition because there is little correlation between landscape position and the occurrence of black soils.

Figure 1.1 Dolomite cliffs of the Eccles formation

Figure 1.2 Steep sided valleys typical of carbonate weathering in humid environments

Some of the residual manganese material is found relatively deep in the solum (down to 2m; Fig. 1.3) and has had little pedogenic alteration with much of the overlying soil material being considered colluvial (Hawker and Thompson, 1988).

Figure 1.3 Black Mn 'wad' overlain by colluvial soil material.

This fairly porous, manganese residuum is commonly known as ‘wad’ and was mined in the past as a manganese ore (Schutz, 1990). Some of this wad, itself a product of weathering, is found close to the soil surface and has been exposed to further pedogenic alteration which has resulted in deep, highly weathered soils with extreme Mn enrichment. These soils have clearly visible horizons and can best be described as manganiferous oxisols.

Although there is very little information available about the physical and chemical properties of the dolomitic soils, there have been various studies which have highlighted some of the general properties of the eastern escarpment soils (Von Christen, 1964; Schutz, 1990; Louw, 1995). Typically the soils are deep and well drained, with very weak structure (Schutz, 1990). They have been likened to the intensely weathered soils of the humid tropics (Von Christen, 1964) where ferralisation is the dominant pedogenic process. They are dystrophic, infertile and usually acidic (Schutz, 1990). Despite potential fertility shortcomings, however, their great depth and favourable physical properties make them highly suitable for tree growth (Schutz, 1990; Louw, 1995).

This chapter focuses on a field investigation of the morphology and the subsequent chemical characterisation of a selected body of Graskop soils which showed extreme Mn accumulation, with the main objective of providing visual and chemical evidence which may pertain to Mn mobility throughout the landscape and within selected profiles

1.2 Materials and methods

1.2.1 Site location and description

The soils, on which this study is based, occur on the Driekop plantation which borders the towns of Graskop and Pilgrims Rest (Fig. 1.6). Driekop is one of the oldest plantations in the region, with the earliest records of afforestation dating back to 1904 when wattle and gum plantations were established to supply timber for the increasing demands of the Transvaal Gold Mining Estates. It soon became evident that the area was well suited to afforestation, and *Pinus* species were introduced in 1919. In 1946, forestry practice broke away from the mining industry and Driekop was placed under professional forest management. Currently, Global Forest Products owns and manages Driekop. *Pinus* stands

constitute nearly 95% of the total afforestable land with eucalypts comprising the remainder.

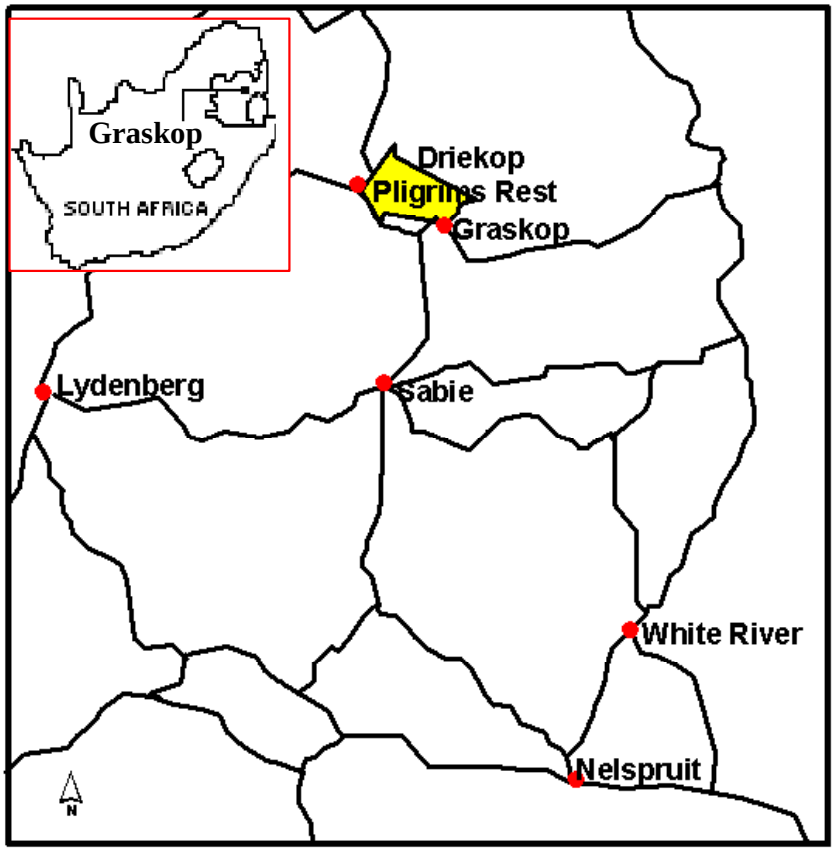

Figure 1.4 Driekop plantation in relation to neighbouring towns

Most of the Driekop plantation is situated on Malmani dolomite and only a small section on the eastern corner lies on quartzite. Pockets of the black manganiferous soils are abundant throughout the plantation and especially along the south-facing slope of the central catchment (Fig 1.5), which was chosen as the main sampling and mapping area.

The climatic conditions in Graskop are similar to those described above for the general eastern escarpment region. Some geographical information on Driekop plantation is provided in Table 1.1.

Table 1.1 Geographic information for the Driekop plantation provided by Global Forest Products

Altitude gradient	1220-1795 m
Mean annual rainfall	1253 mm
Mean annual temperature	15 – 17 ^{o}C

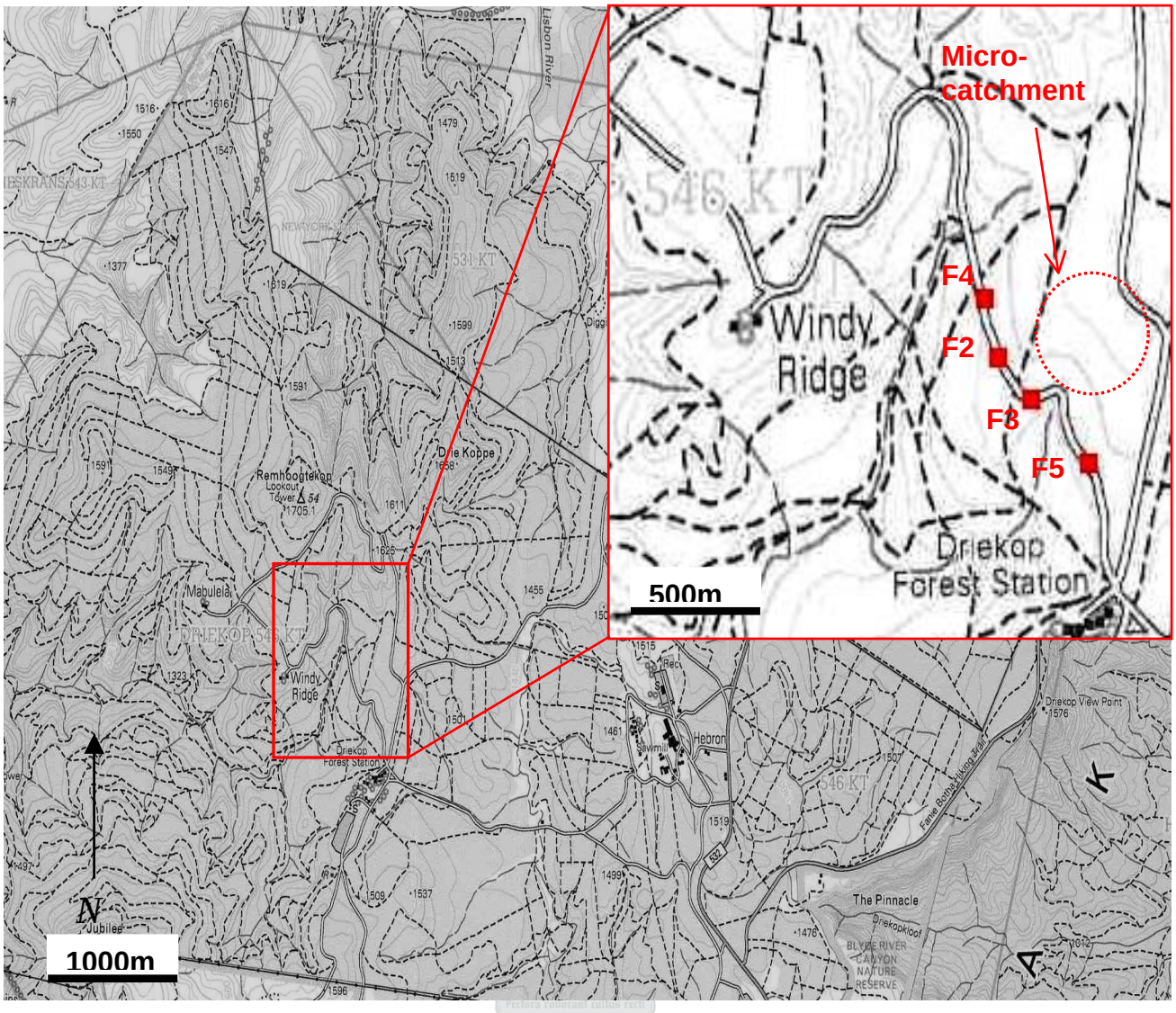

Figure 1.5 Driekop plantation, Graskop. The highlighted area and inset demarcate the southern slope of the major catchment where soils where sampled and mapped.

1.2.2 Mapping and sampling

A micro-catchment was mapped on the south-facing slope of the central Driekop catchment (Fig. 1.5). The soils of the south-facing slope are mainly very dark to black, representing one of the larger pockets of manganiferous soils. A micro-catchment within this pocket was chosen for mapping to get an idea of Mn mobility and distribution on a landscape scale. The micro-catchment was mapped with respect to soil colour, nodule content and nodule size. This was achieved by augering pits on a 25 x 25 m grid across the micro-catchment. Nodule content and Munsell colour values were recorded for each horizon.

Soil samples were collected from a transect along the south face of the main Driekop catchment, as shown in Figure 1.5 (Inset). Samples were taken from four soil profiles which occur along a road cutting. All of these profiles were found under mature pine stands between 20 and 25 years old. Prior to sampling, a fresh face of the profiles was exposed by digging 15-20 cm into the road cut. Representative samples were taken from each horizon and placed in thick polyethylene bags. The bags were well sealed to prevent moisture loss and stored away from direct sunlight.

The redox status of the soils was determined whilst sampling. To achieve this the tetramethylbenzidine and Cr oxidation field tests were performed as described by Bartlett and James, (1995).

Sample handling and storage has been shown to cause important chemical changes, especially in the case of Mn oxides where extractable Mn and redox properties can be substantially altered by air-drying samples (Bartlett and James, 1980; Ross et al., 2001). To avoid this, the soils were sieved (< 2mm) in their moist state and stored in air-tight containers for the duration of the study to prevent moisture changes. Periodic Cr tests (Bartlett, 1999) were conducted on the soils to ensure the redox properties of the soils were not being altered by storage. All chemical analyses were performed with the soils in their field moist state unless otherwise stated. The moisture content of the soils, determined by weighing the soils before and after oven-drying at 104^{o}C, was used to calculate the equivalent mass of oven-dried soil used in the various chemical analyses. All soil masses reported in this study refer to the oven-dry mass.

1.2.3 Chemical analysis

Manganese and easily reducible Fe were determined by successive washings using acidified hydroxylamine hydrochloride (Chao, 1972). Briefly, 0.5g soil was reacted with 25 ml hydroxylamine hydrochloride (0.1 M $NH_2OH.HCl$, 0.01M HNO_3) for 30 min. Three successive washings were performed and the extracts were analysed for Mn, Fe and Al.

Total, reducible, Mn and Fe concentrations were determined using dithionite-citrate (Holmgren, 1967). Material, from the fine earth fraction (<2 mm) and from pisolithic nodules, was analysed from each horizon as follows: nodules and fine earth from each

horizon were ball milled to a fine powder, 0.4g powdered sample was reacted with 40 ml, 0.3M Na-citrate and 2g Na-dithionite at 78^{o}C. The procedure was repeated to ensure total oxide dissolution. The remaining sediment was light grey in colour indicating that most Mn and Fe oxides had been removed. All extracts were analysed for metal concentration using a Varian Spectra AA atomic absorption spectrometer.

Carbon and nitrogen analyses were performed on finely milled soil powders using a Eurovector element analyser.

X-ray fluorescence (XRF) spectrometry for total elemental analysis was performed on a Phillips 1401 XRF spectrometer.

1.3 Results and Discussion

1.3.1 Manganese distribution within a micro-catchment

In order to achieve a three dimensional picture of Mn distribution within the landscape a micro-catchment, which occurs within one of the larger bodies of black soil, was mapped. Not only would this allow the effects of topography on soil formation to be assessed, but it would also capture signs of Mn mobility in areas characterised by varying degrees of drainage. The soils were mapped on the basis of soil colour, nodule content and nodule size as it was assumed that these parameters would be the best indicators of Mn mobility and distribution.

Generally the soils throughout the catchment show a similar sequence of horizons. Typically, the A horizon is dark reddish brown and has a 3-4% organic matter content (Table 1.2). The texture has a silty feel and consistence is friable. The dark colour of the topsoil is probably more a result of a high organic matter than high Mn content, because the A horizon typically has the lowest Mn content (Table 1.2). The nodule content of the topsoil is less than 30% of the soil volume and the nodules are coarse to medium in size. Colluvation is likely to be an important process in the topographical position of these soils and so it is hard to assess whether the nodules found in the topsoil are of residual or colluvial origin.

The transition from the A horizon into the upper subsoil horizon is gradual but is generally marked by an increase in clay content, a redder colour and a higher nodule content. The nodules may occupy as much as 80% of the soil volume and are fine to medium in size. As depth increases the soil becomes darker and the nodules decrease in size and abundance. A zone of transition exists where the red horizon with black mottles grades into the very dark horizon with red mottles. Within this zone, incipient nodule formation is apparent. This mottled horizon then grades into a moist, friable black, apedal horizon containing very fine nodules (<2mm) in the transition zone. Small lithiorelics of white siliceous material (probably weathered chert) are evident in almost all the black apedal horizons.

On a landscape scale certain trends were observed. Soils along the valley floor are deeper, redder and contain more nodules than soils on the valley slopes. The soils on slopes are generally shallower, but show the same sequence of horizons as the lower lying soils. Along the rim of the catchment the soils are very shallow and have very few nodules. There are no red horizons in these soils, with the silty A horizon grading directly into a very friable, black apedal B horizon which is shallow and overlies unweathered dolomite. The transition between the soil and unweathered dolomite is abrupt.

Figure 1.6 shows the spatial variation in soil colour and nodule content throughout the micro-catchment. It appears from these plots that soil nodule content and chroma have some kind of inverse relationship, with the soils of reddest colour having the highest nodule content and the very dark soils having the lowest nodule content. It would almost appear then that nodule formation may have taken place at the expense of Mn pigmentation or, viewed in another way, the manganese in the soil matrix shows signs of redistribution into nodules as a result of pedogenic processes.

1.3.2 Profile descriptions

The preceding section describes the typical appearance of the dark Mn rich soils. The soil profiles selected for detailed description and sampling occur below the catchment and so are more typical of the deeper soils along the valley floor.

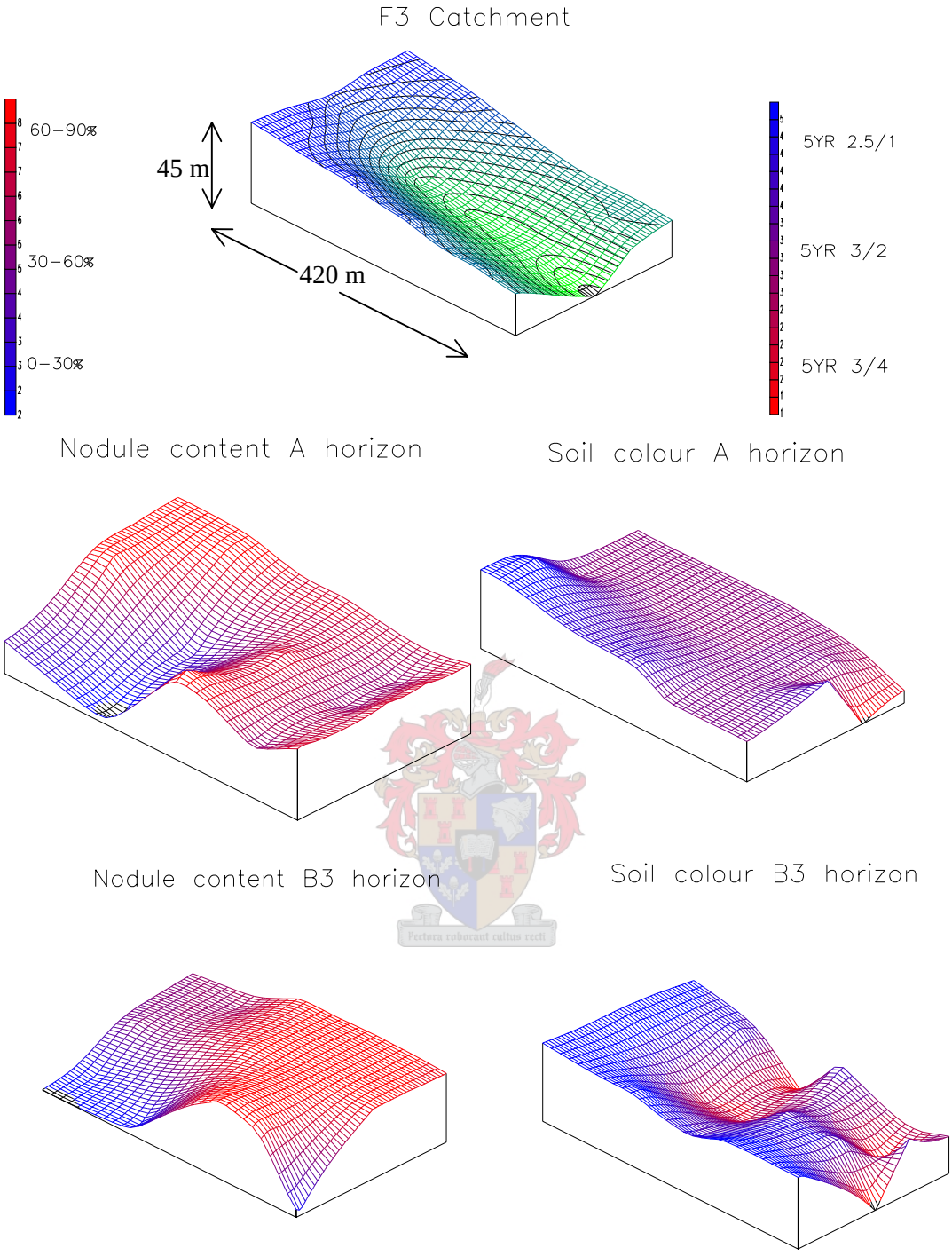

Figure 1.6 Plots of soil colour and nodule content for the F3 catchment

Classification of the soils using the local and various international classification systems has been attempted. However, due to their uniqueness it is hard to place them into a classification category. The South African system (Soil Classification Working Group, 1991), is especially difficult as many of the diagnostic criteria involve morphological

features (especially colour). However, if Mn is considered analogous to Fe with regard to colour formation, classification is still feasible. The international classification systems are slightly easier because they rely largely on diagnostic properties that are chemical and mineralogical.

The sampling sites are shown in Figure 1.5. All the profiles are situated under mature stands of pine trees. Pine needles, grass and weeds were present on the soil surface. Descriptions of each profile are presented below, with the horizons that were sampled being indicated by the sample name in parentheses in the right-hand column. References to soil classification systems used to identify the soils are abbreviated as follows: SCWG: Soil Classification Working Group (1991); ST: Soil Taxonomy (Soil Survey Staff, 1999); WRB: World Reference Base, FAO (1998).

Profile

F2

Deep, dark, porous soil with little horizon development. Gentle, south-facing, colluvial midslope. Black Mn-rich variant of *Inanda Form* (SCWG); *Mesic Anionic Acrustox* (ST); *Posic Ferralsol* (WRB).

Depth (cm)	Description	Horizon (sample no.)
0-20	Moist, dark reddish brown (5YR 4/3); gravelly clay loam; weak, fine, crumb structure; loose to friable; highly porous, abundant fine and coarse roots, many Mn nodules; clear, wavy transition.	A (F2A)
20-70	Moist; black (5YR 2.5/1) gravelly clay loam; weak, coarse subangular blocky, friable; many fine, medium and coarse stone fragments with bleached, white siliceous interiors and black, brown and red staining on periphery; moderately porous, few fine and coarse roots; gradual wavy transition.	B1 (F2B1)
70- 110	Moist; reddish black (10R 2.5/1) with very dusky red (10R 2.5/ 2) fine, vesicular mottles; loamy clay; apedal, massive; soft to friable; very few, fine roots; highly porous; clear, wavy transition.	B2 (F2B2)
110-140+ :	As above, but moister and lacking dusky red mottles; common, coarse, soft, bleached, white, powdery saprolite inclusions. Few, fine roots; highly porous; silty, wet feel when rubbed.	B3 (F2B3)

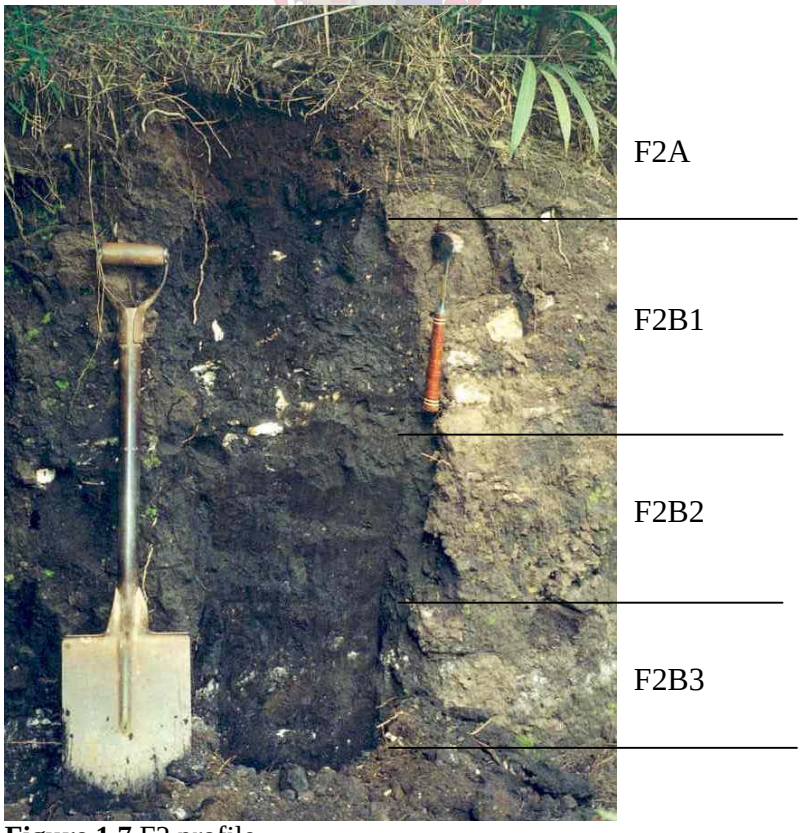

Figure 1.7 F2 profile

Profile

F3

The profile F3 lies on the interfluve at the base of the mapped catchment (Fig 1.5).

Forest profile: well developed with distinct horizons on gently sloping, south-facing convex creep slope on spur. Thick grass, ferns and weeds, under mature pines; Black Mn-rich variant of *Kranskop Form* (SCWG); *Mesic Anionic Acrustox* (ST); *Posic Ferralsol* (WRB)

Depth (cm)	Description	Horizon (sample no.)
0-30	Slightly moist, dark brown (7.5YR 3/4); gritty clay loam; weak, fine, crumb structure; soft; abundant, fine and medium roots, many, fine and medium, pisolitic concretions near lower boundary; highly porous; diffuse, smooth transition.	A (F3A)
30-60	Slightly moist; dark reddish brown (7.5YR 3/3); gravelly clay loam; apedal, massive; friable; many fine roots, abundant, fine and medium, black pisolitic nodules, porous; gradual, smooth transition.	B1 (F3B1)
60-95	Moist, black (5YR 2.5/1); loamy clay; apedal, massive; soft to friable; few, fine roots, few, fine and medium concretions and stone fragments; highly porous; gradual, irregular transition.	B2 (F3B2)
95-110+	As above, but with common fine, medium and coarse fragments of weathered dolomite, commonly bleached white with brown and black staining.	B3

Figure 1.8 Profile F3

Profile

F4

Forest profile: well developed with distinct horizons on a 5% southeast facing, neutral slope. Thick grass, ferns and weeds, under mature pines. Many nodules showed magnetic properties. Black Mn-rich variant of *Kranskop Form* (SCWG); *Mesic Anionic Acrustox* (ST); *Posic Ferralsol* (WRB)

Depth (cm)	Description	Horizon (sample no.)
0-20	Moist, (5YR 3/2) dark reddish brown; loamy silt; apedal; very loose; non-sticky; many coarse and fine roots, 40% medium + coarse nodules; gradual, wavy transition.	A (F4A)
20-50	Moist; (5YR 3/4) dark reddish brown; clay loam; very fine, weak, subangular blocky; loose, friable; many coarse roots, 70% coarse + medium nodules; gradual, wavy transition.	B1 (F4B1)
50-100	Moist; (5YR 2.5/2) dark reddish brown; loam clay; fine, weak subangular blocky; crumbly; very few, fine roots; 80% fine to medium nodules; gradual wavy transition.	B2 (F4B2)
100+	Moist; (5YR 2.5/1) black; loam clay; weak, subangular blocky; friable, sticky; few, fine siliceous fragments, 60% very fine nodules, 10% medium nodules, few (5YR 2.5/2) mottles; gradual transition to black apedal material containing weathering siliceous material.	B3 (F4B3)

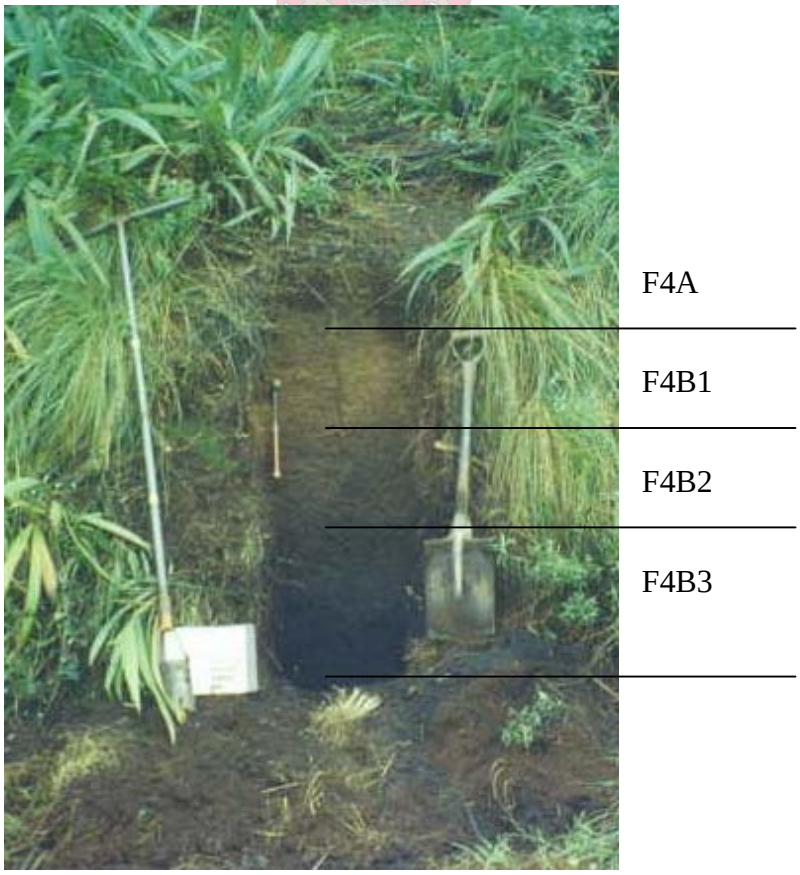

Figure 1.9 F4 profile

Profile

F5

Forest profile: Extremely deep well developed profile, many degrees yellowier than previously described soils, on a 5% south facing neutral slope. Thick grass, ferns and weeds, under mature pines. Nodular variant of *Kranskop Form* (SCWG); *Mesic Anionic Acrustox* (ST); *Posic Ferralsol* (WRB)

Depth (cm)	Description	Horizon (sample no.)
0-15	Moist, (10YR 4/6) dark yellowish brown; loam; apedal, massive; loose; non sticky; many coarse and fine roots, 5% medium + coarse nodules; gradual, smooth transition.	A (F5A)
15-35	Moist; (7.5YR 3/4) yellowish brown; gravelly loam; apedal; loose, non-sticky, non-plastic; many coarse and fine roots, 70% medium pisolitic nodules; gradual, wavy transition.	B1 (F5B1)
35-100	Moist; (5YR 3/4) dark reddish brown matrix with 40% yellowish brown (7.5YR 4/6) mottles; gravelly loamy clay; fine, weak, subangular blocky; friable, plastic; few coarse roots; 80% medium pisolitic nodules; gradual wavy transition.	B2 (F5B2)
100-140	Moist; (5YR 3/2) dark reddish brown matrix with 5-10% yellowish brown (7.5 YR 4/6) mottles; loamy clay; weak, medium, subangular blocky; friable, sticky; 60% medium pisolitic nodules.	B3 (F5B3)
140-160	Moist; (5YR 4/3); clay; subangular blocky; friable, sticky, plastic; 60% medium pisolitic nodules.	
160-180	Moist; (5YR 2.5/2); clay; weak subangular blocky; friable, sticky, plastic; 60% fine pisolitic nodules.	
180+	Moist; (5YR 2.5/1); clay; weak coarse subangular blocky; friable, sticky, plastic; 5% very fine pisolitic nodules	

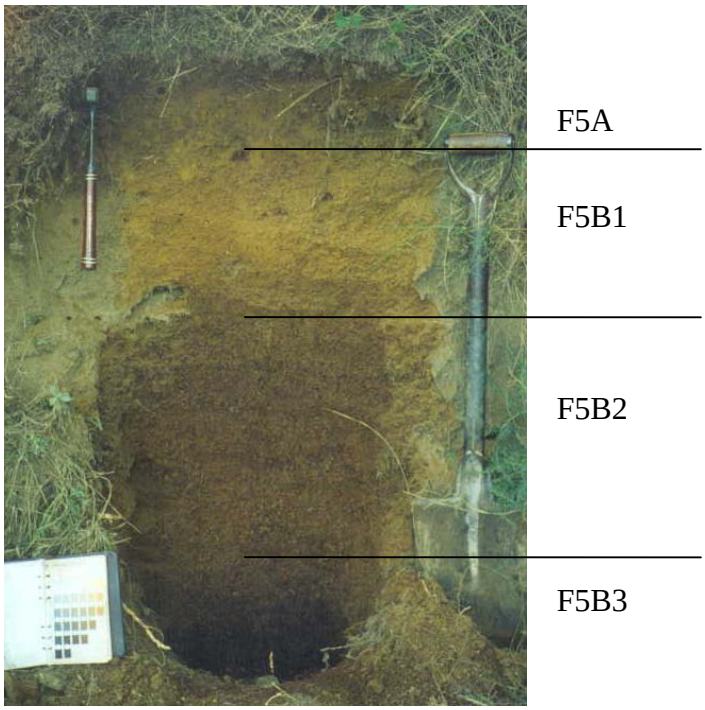

Figure 1.10 Profile F5

The redox status of these soils was assessed in the field using the field tetramethylbenzidine (TMB) and the Cr oxidation test (Bartlett and James, 1995). All the soils gave a positive yellow or green TMB test (Figure 1.11) and a positive pink Cr test. Normal oxic soils usually give a light blue TMB test, the intense yellow and blue colours seen in Figure 1.11 are clear evidence that the redox status of these soils can be classified as *Super oxic* (Bartlett and James, 1995).

Figure 1.11 Testing redox status in the field, intense yellow and blue are indicative of a super oxic redox status.

1.3.3 Pedogenic processes

Observations made during mapping and sampling provided important information on Mn mobility within the soil profile and the landscape. The mapping has revealed that the soils on the valley floor are deeper, redder and contain abundant nodules. Considering the landscape position, colluviation should always be kept in mind; however, there is evidence for the red soils having formed *in situ*, perhaps the most convincing being the red and black mottled zone within the red or black matrix. The fact that the red soils are so enriched with nodules is also very strong evidence for *in situ* formation. If colluviation were the dominant process, it might be expected that the nodule content would decrease with depth, which is not the case. It would appear that the nodules may be forming through the enrichment of Mn, and possibly Fe, which is gradually being redistributed from the soil matrix to the nodules. The mottled zone is most likely an indicator of incipient nodule formation, which signals the encroachment of pedogenesis upon the less weathered, underlying wad material. The nodular and mottled zones provide two important pieces of information. Firstly, the nodules reflect Mn redistribution and secondly, the mottled zone suggests that this Mn mobilization is occurring under present-day conditions – i.e. the nodules are not relict.

From field observations the following theory of pedogenesis is suggested: Mn is mobilized close to the surface of the profile, probably as a result of the reductive environment created by the organic-rich topsoil. This mobilised Mn then percolates through the soil profile until it precipitates through oxidation at a node of raised redox potential, as was suggested for Fe nodule formation by Blume (1967). Typical nodes may be fragments of unweathered dolomite, since often the nodules have a light grey core. If reduced Mn comes into contact with the high pH surface of dolomite, the Mn is likely to precipitate out and coat the surface. This centre of high redox potential then becomes enriched with Mn while the less stable (lower redox potential) matrix is stripped of Mn through reductive dissolution and in the process, the dominating pigment of the Mn oxides is gradually removed from the matrix and the less dominant pigments of Fe oxides can then be expressed, which may account for the more reddish colour of soils having abundant nodules. If this is indeed the case then red and black colour relationship may be considered analogous to the yellow and red colour relationships of other highly weathered soils described by Fey (1981), where

less stable hematite is selectively removed, through organically fuelled reduction, exposing the more stable goethite.

Many of the nodules and even some of the fine earth fraction of these soils showed magnetic properties, which can probably be attributed to maghemite which is frequently found in highly weathered soils of South Africa (Fitzpatrick, 1981).

1.3.4 Chemical properties

To get an idea of the chemical make-up of the Graskop soils, total elemental analysis was performed on the fine earth fraction (<2 mm), using dithionite-citrate (DC) and hydroxylamine hydrochloride (HAHC) extractions as well as XRF elemental analysis. Nodules taken from the horizons of the F3 and F4 profiles were analysed for DC extractable Mn and Fe.

Table 1.2 Organic C and N contents and dithionite-citrate (DC) and hydroxylamine hydrochloride (HAHC) extractable metal contents. All expressed as a percentage of dry mass.

	Organic		DC		HAHC		
Sample ID	C	N	Mn	Fe	Mn	Fe	Al
F2A	3.67	0.088	4.7	6.6	5.1	0.6	0.4
F2B1	0.20	0.025	9.5	6.4	10.0	1.3	0.4
F2B2	0.24	0.023	17.2	8.3	15.6	1.9	0.7
F2B3	0.25	0.017	11.6	5.7	11.4	2.3	0.7
F3A	3.22	0.290	6.2	10.0	4.3	0.6	1.1
F3B1	1.28	0.139	5.2	8.7	3.6	0.8	0.8
F3B2	0.25	0.032	7.2	7.6	6.8	1.4	0.7
F4A	3.37	0.256	6.9	8.6	4.4	0.6	0.9
F4B1	0.63	0.024	5.9	9.0	5.4	0.9	0.9
F4B2	0.23	0.001	6.0	8.4	4.7	1.0	1.0
F4B3	0.17	0.001	8.6	9.8	7.2	1.2	0.8
F5A	3.62	0.224	0.9	10.3	1.2	0.2	1.0
F5B1	2.02	0.122	1.0	10.0	1.2	0.3	0.8
F5B2	0.51	0.014	1.2	10.6	1.5	0.4	0.3
F5B3	-	-	2.0	10.6	2.6	0.6	0.4

Hydroxylamine hydrochloride (HAHC) and dithionite-citrate (DC) extractable metal concentrations as well as organic C and N contents are shown in Table 1.2. The DC extractable metal content of the nodules are shown in Table 1.3.

Dithionite-citrate is used to remove crystalline Fe and Mn oxides (Loepert and Inskeep, 1996) and thus should give an indication of total Mn and Fe oxide contents in the fine earth fraction. In profiles F2, F3 and F4 the Mn contents are exceptionally high especially in the F2 profile (Table 1.2). The Mn contents of the F5 profile are two to three times lower although still high by normal standards (range of worldwide means 0.008 and 0.13%; McBride, 1994). The general trend is for the Mn content in the fine earth fraction to increase with depth, although the F3 and F4 profiles show a slight decrease in Mn content in their middle horizons which may relate to the very high nodule content of these soils. The deeper subsoil horizons in all profiles show the highest Mn content. The general increase in Mn content with depth relates well to the change of colour down the profile, with the subsoils being much darker than the topsoils. This colour change is also related to the nodule content of the soil. The nodule content, expressed as a weight percentage of the whole soil, is typically around 50% in the topsoil, 60-70% in the upper subsoil and less than 30% in the dark subsoil (data not shown) so the reddest middle soil horizons also have the highest nodule content. The Mn concentration in the nodules is substantially higher than the soil matrix showing an enrichment ratio (ratio of nodule Mn/ fine earth Mn) of between 2 and 3 (Table 1.3). This adds chemical evidence to support the field observations (Fig 1.6) that suggested that Mn is being mobilized and redistributed from the matrix to the nodules, thus exposing the less pronounced Fe pigmentation.

Hydroxylamine hydrochloride (HAHC) is meant to be an extractant specific for Mn oxides (Chao, 1972). As can be seen in Table 1.2, small amounts of Fe and Al were also extracted with the HAHC. The Fe may originate from poorly crystalline Fe minerals or alternatively from mixed Fe-Mn phases. A surprising amount of Al is present in the HAHC extract but this may merely be a result of gibbsite dissolution due to the acidified nature of the HAHC which had a pH around 2.3. A certain portion of this released Al may also represent Al which is incorporated in the Mn mineral structure. Lithiophorite, the dominant Mn mineral in these soils (Chapter 2), hosts an Al-hydroxy interlayer between MnO_2 layers. Reductive dissolution of lithiophorite may therefore also account for this Al release.

Table 1.3 Manganese and Fe content of fine earth fraction (<2 mm) and nodules using dithionite-citrate as the extract, all expressed as dry weight percentage.

	Mn			**Fe**		
Sample ID	soil	nodules	Enrichment ratio*	soil	nodules	Enrichment ratio*
F3A	6.2	16.4	2.7	10.0	9.1	0.9
F3B1	5.2	16.2	3.1	8.7	8.5	1.0
F3B2	7.2	14.8	2.1	7.6	7.5	1.0
F4A	6.9	16.8	2.4	8.6	6.2	0.7
F4B1	5.9	16.4	2.8	9.0	6.4	0.7
F4B2	6.0	17.3	2.9	8.4	6.6	0.8
F4B3	8.6	17.2	2.0	9.8	6.4	0.6

* nodule metal concentration/fine earth metal concentration

The total Fe contents of the soils are also very high although a concentration gradient down the profile is not evident as it is with Mn (Table 1.2). In the redder, non-manganiferous, soils of the region a typical profile may have a yellow-brown B1 horizon directly below the A, which grades into a red apedal B2 horizon as shown for a profile close to Mac-Mac falls (Fig 1.12).

Figure 1.12 Typical soil profile of non-manganferous soil (Mn < 0.017%), close to the Mac-Mac falls, DC extractable Fe in yellow and red horizon is 5 and 10%, respectively.

This horizon sequence is largely attributed to hematite being more prone to reductive dissolution than goethite. Organically fuelled reduction selectively removes hematite exposing the less dominant pigment of the more stable goethite (Fey, 1981). This generally

results in an increase in Fe content down the profile as is indeed the case for the Mac-Mac profile (Fig. 1.12) which contains 5% Fe in the yellow horizon and 10% in the red subsoil (Fig 1.12). In the manganiferous soils the absence of this Fe concentration gradient with depth may be a result of high redox poise created by the abundant Mn oxides. Theoretically all the Mn would need to be removed before reductive dissolution of Fe would occur. So perhaps the poise of the Mn oxides 'protects' the Fe against organically fuelled reductive dissolution resulting in very little Fe redistribution throughout the profile. A further ramification of this is seen in the Mn and Fe concentrations in the nodules. As mentioned above, the Mn concentration in the nodules is 2 to 3 times higher than in the soil matrix, Fe on the other hand has an enrichment ratio of ≤ unity (Table 1.3) which suggests that the Fe mobility and thus redistribution is highly limited in these soils.

The total elemental analysis for the four profiles is shown in Table 1.4. Also included in this table are results from the study of Hawker and Thompson (1988) showing the total element analysis for Mn wad, taken close to the weathering front, and unweathered dolomite. Although the exact sampling locations of this earlier study were not the same as that of the soils sampled in this study, relative accumulations or depletions may aid in understanding the pedogenic processes active in the soils.

Weathering of the dolomite to the wad causes marked enrichment of Mn and Fe which are present in only minor amounts in the parent material. The soils show a decrease in total Mn content compared with the wad material while the Fe content is generally higher in the soils. The soils, relative to the wad, show an increase in Al and a decrease in Ca and Mg contents. This change can probably be accounted for by the pedogenic alteration of the wad material. The Al content of the F5 profile is exceptionally high, being close to bauxite grade (M. Fey, pers. comm.) and is indicative of how advanced the degree of weathering is in these soils.

Table 1.4 XRF total chemical analysis (%) expressed on a dry weight basis for B2 horizons of the F2, F3, F4 and F5 soil profiles and a wad and dolomite sample

	F2	F3	F4	F5	Wad[a]	Dolomite[a]
SiO_2	64.63	59.27	43	41.03	10.1	0.9
Al_2O_3	7.87	14.48	22.02	30.29	5.62	0.14
Fe_2O_3	7.95	10.65	16.71	20.19	10.2	0.65
MnO	15.1	10.75	13.4	3.77	26.5	1.72
MgO	1.13	1.18	1.26	0.58	7.1	20.9
CaO	0.18	0.03	0.001	0.001	10.94	29.2
Na_2O	0.1	0.08	0.03	0.001	-	-
K_2O	2.03	2.7	2.17	0.29	1.8	<0.01
TiO_2	0.25	0.74	1.31	3.59	-	-
P_2O_5	0.03	0.05	0.08	0.22	-	-
TOTAL	99.27	99.93	99.99	99.97	98.9	99.6
L.O.I	8.46	8.7	11.68	14.84	26.3	46.1

[a] Results from the study by Hawker and Thompson (1988). Wad sample was taken close to the weathering front and the dolomite sample from the underlying unweathered dolomite.

From the data in Tables 1.2, 1.3 and 1.4 it would appear that the concentration range of Mn in the Graskop soils lies between 1 and 17%. The F2 profile appears to contain twice as much Mn as do the other profiles. In fact it generally has properties more similar to wad than to the other soils (Table 1.3). It also shows less horizonation than the other profiles, and perhaps it would be better classified as a developing soil. Even with the omission of the F2 profile, the Mn range is still nearly 100-fold greater than the range of world means which is between 0.008 and 0.13% (McBride, 1994). A body of soils that shows a similar Mn enrichment is the manganiferous oxisols of Hawaii. These contain between 1 and 4 % Mn (Fujimoto and Sherman, 1948). The Mn content in the Graskop soils is much higher than this indicating that these soils must represent some of the most Mn enriched soils in the world.

1.3.5 Trace elements

The trace element concentrations for subsoil samples from the four soil profiles are compared with values reported elsewhere, including those for other oxisols, in Table 1.4. It

can be seen that the trace element content for the soils is high, with most soils having trace element values above the South African (SA) median (Herselman et al., 2004, manuscript in preparation) as well as the world mean (Kabata-Pendias and Pendias, 2001). The trace element composition of a well weathered oxisol from Cerrado (Marques et al., 2003) has been included, in Table 1.4, to compare the trace element content of a soil at a similar stage of weathering. The data from the Cerrado oxisols clearly suggests that there is an anomalous enrichment of trace elements in the Graskop soils.

The Zn and Ni levels are very high for all soils except the F5 profile, which also has the lowest Mn oxide content (Table 1.2). In profiles F2, F3 and F4, Ni is 1.5 to 4 times higher than the 95th percentile SA maximum. Soils with such high Ni levels would usually be considered contaminated in South Africa (Herselman et al., 2004). Cobalt, Cu, Cr, V, La and As levels are also high, all generally being above average for most local and world soils whereas Pb, while exceeding the SA median, is in accord with the world average.

Table 1.5 Trace element analysis of upper subsoil (B2) samples from the four profiles determined by XRF (mg kg^{-1}) and compared with values reported elsewhere.

Element	F2	F3	F4	F5	SA median[a]	SA-Max 95th percentile[a]	Cerrado oxisol[b]	min-mean-max for surface soils worldwide[c]
Zn	160	237	111	31	39	115	22	17-67-236
Cu	31	68	157	128	18	117	10	6-24-80
Ni	225	541	387	35	22	159	8	6-24-92
Cr	100	199	158	138	47	353	118	12-67-221
V	67	132	214	474	-	-	175	18-100-220
La	52	44	51	10	-	-	18	5-31-55
As	5	8	14	17	-	-	-	2.2-7-25
Pb	21	29	37	32	14	66	9	8-29-67
Co	26	35	80	55	9	69	3	1.4-10-27

[a] Taken from Herselman et al. (2004)
[b] Values from Cerrado oxisols derived from sedimentary rocks (Marques et al., 2003)
[c]Minimum, mean and maximum of the means for mineral surface soils from various countries, as tabulated by Kabata-Pendias and Pendias (2001) and displayed by Marques et al. (2003)

In the study of the Cerrado oxisols (Table 1.5) it was observed that elements stable in their trivalent state in acid conditions, like V and Cr, had accumulated during weathering and are in concentrations above the world mean. This was accounted for by the capacity of these elements to substitute for metals such as Fe and Al in oxide minerals (Marques et al., 2003). Elements that are stable in their divalent forms in acid environments, such as Mn, Zn, Cu, Co and Pb, were depleted in the Cerrado soils, being lower than their worldwide means (Table 1.2; Marques et al., 2003). This relationship is almost completely reversed in the Graskop soils, with Zn, Ni, Co and Cu (and of course Mn) levels being exceptionally elevated in most cases. It appears that, in the Cerrado soils, oxidation state may have played an important role in the relative accumulation and depletion of specific trace elements. Apart from the known affinity of Mn oxides for certain trace elements, the highly oxidative environment in the Graskop soils may also have played a role in the extreme accumulation of trace elements. Certain elements such as Co and Pb are relatively immobile in their higher oxidation state while other elements such as Cr form soluble anions which may readily leach from the soil. Despite this, Cr appears to accumulate in Mn nodules (McKenzie, 1972), and it appears to have done the same in the Graskop soils (Table 1.2). The presence of relatively high levels Cr in these soils raises environmental concerns due to the high toxicity of Cr(VI) which is likely to be the most common species in such super oxic soils.

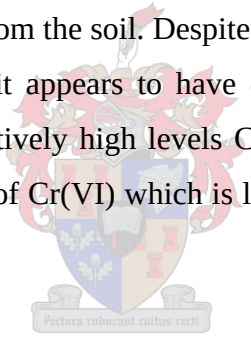

The close association of many trace elements and Mn oxides is well known (McKenzie, 1980; Kabata-Pendias and Pendias, 2001; Dixon and White, 2002). Cobalt has been shown to have a very high affinity for Mn oxides, with the mobility of Co being highly dependent on Mn oxide content (Kabata-Pendias and Pendias, 2001). The specific adsorption of Co has been related to its oxidation (McKenzie 1970) and Co^{2+} has been shown to oxidise to Co^{3+} (Murray and Dillard, 1979) which can then be incorporated in the Mn mineral lattice (McKenzie, 1970; Manceau et al., 1987). Zinc and Ni are also known to have a high affinity for Mn oxides (Kabata-Pendias and Pendias, 2001). The Graskop soils appear to be highly enriched in both Ni and Zn, although the variability between soils is high (Table 1.2). It is interesting to note how much lower the concentrations of Ni and Zn are in the F5 profile. This profile has a much lower Mn content than the other three profiles (Table 1.2) which may be responsible for the lower Zn and Ni concentrations. However, drawing firm conclusions on element distribution in relation to Fe and Mn oxide content cannot be made due to the limited number of samples that were analysed.

The mineralogical study in Chapter 2 has identified lithiophorite, an Al-hydroxy interlayered Mn oxide, as being the dominant mineral in the subsoils. Nickel, Zn and Co have been found in varying proportions in the mineral structure of lithiophorite (Ostwald, 1984; Golden et al., 1993) with concentrations of these elements in the mineral being inversely proportional to the Al concentration (Ostwald, 1984). Following this observation, two types of lithiophorite have been proposed, a transition metal-poor species and a transition metal-rich species. In study of trace element partitioning between various minerals, Ni was found to associate strongly with lithiophorite as did Zn but Zn was also distributed between goethite, phyllosilicates and birnesstite (Manceau et al., 2003). Considering the high trace metal content of the Graskop soils, the lithiophorite constituent may house a large proportion of these trace elements in its structure and the special affinity of Ni for lithiophorite may explain the extremely high Ni content of some of these soils. Element and mineral mapping would be necessary to develop a clear correlation but such work falls beyond the scope of this study. The accumulation of trace elements is a very interesting property of these soils and with the number of different sesquioxide phases present (to be reported in Chapter 2) the study of trace element distribution among different minerals could be very rewarding.

Despite the unusual accumulation of trace metals in these soils, most of the trace elements present may be strongly sorbed to, or structurally included in, the Fe and Mn phases which may render them unavailable to plants. It may even be speculated that certain trace elements, such as Co the plant availability of which is dramatically decreased in the presence of Mn oxides (Adams et al., 1969), may even become deficient. On the other hand, dissolution of the Mn oxide phase may render many of these trace elements mobile which could create phytotoxic conditions.

1.4 Conclusions

The soils of the Driekop plantation, Graskop, show extreme accumulation of Mn, Al and Fe oxides. Soils within a mapped micro-catchment show a similar sequence of horizons, with soil depth being the largest variable. Typically the soils have a dark reddish brown topsoil which grades through a red and black mottled nodular zone into a black, apedal, Mn-rich subsoil. There appears to be a rough correlation between soil colour and nodule

content, with the redder horizons having the highest nodule content. This may be indicative of the redistribution of Mn from the soil matrix to the nodules. Chemical data support these field observations with the Mn content in the nodules being 2 to 3 times higher than the Mn content of the soil. There is a general decrease in Mn content down the profile, which may be attributable to organically fuelled reductive dissolution in the topsoil and redistribution of this mobilized Mn further down the profile, where the redox potential is higher.

The Graskop soils are highly enriched in trace elements, with most trace element levels being above the SA- 95th percentile maximum as well as the world maximum. Zinc and nickel are extraordinarily high and may be associated with lithiophorite, the dominant Mn mineral. Cobalt, V, Cu, As, Cr and La are also highly enriched. This means the stability of these soils is not only important for release of large quantities of Mn but also for the release of large reserves of latent phytotoxicity which is present in the form of sorbed or occluded trace elements.

CHAPTER 2

2 Mineralogical investigation of the Graskop soils

2.1 Introduction

It is important to establish the mineralogical make up of the Graskop soils in order to get some idea about their pedogenic background. The mineralogy of the soil is a reflection of the degree of weathering the soils have been exposed to. This is fundamental to understanding the behavior of the soil and the stability of the manganese minerals as many of the chemical properties of soils such as buffer capacity and charge characteristics are a function of mineral composition. This chapter aims at providing an outline of the mineralogy of the Graskop soils, with the main focus being on the Mn oxides.

Identification of Mn minerals in soils is usually troublesome due to their poor crystallinity, fine particle size, low concentrations and the close proximity of layer silicate and Mn mineral XRD peaks (Taylor et al., 1964). The typically low concentration of Mn oxides in soils has led to most mineralogical studies being conducted on localized Mn accumulations such as dendrites or nodules (McKenzie, 1977). In such accumulations the chemical environment is likely to be different to that of the surrounding soil matrix and the minerals that form in such accumulations may not be representative of the minerals present in the matrix. A further problem in Mn mineral analysis is that it may often require some kind of chemical pre-concentration method prior to analysis. This pre-concentration can produce artifacts. Pre-treatment of Mn oxides using concentrated NaOH has been suggested for removing silicates. This is a harsh treatment and some Mn minerals such as lithiophorite may become unstable (Dixon and Skinner, 1992) while crystallization of birnessite may be enhanced (Ross et al., 1976).

Identification of Mn minerals using x-ray diffraction is made difficult by the fact that many of the diagnostic peaks for Mn minerals coincide with other minerals. Birnessite peaks have d-spacings similar to those of kaolinite; those of todorokite are close to mica and gibbsite; and nsutite has its major peak close to that of maghemite. Researchers have overcome this difficulty by employing sequential selective dissolution. Tokashiki et al. (1986; 2003) compiled a succession of dissolution procedures that could be used to give a

rough indication of the type of Mn oxide mineral that is present in a sample. This includes boiling the soil in 5 M NaOH to remove kaolinite, washing in unacidified hydroxylamine hydrochloride to remove birnessite and finally removing all remaining reducible oxides by treating the soil with citrate-bicarbonate-dithionite.

Another alternative or supplement to XRD is to use Fourier transform infrared (FTIR) analysis. In many aspects IR is more suitable to the study of Mn oxides than XRD because it is sensitive not only to crystalline materials but also amorphous components with short-range order. Another benefit of IR is that it is sensitive to the structural environment of hydrous components which is often diagnostic of Mn oxide mineralogy. Potter and Rossman (1979a) have published a compilation of IR powder absorption spectra for a number of synthetic and naturally occurring tetravalent and trivalent oxides as a basis for the identification of these minerals. They used crystalline mineral species to calibrate their technique, and once a mineral's characteristic IR spectrum had been established, it could be used to identify the phases present in less crystalline samples. It was established that the spectra provide information on polymerisation in the form of edge-sharing by MnO_6 octahedra, from which structural information could be drawn.

Using the various techniques mentioned above, lithiophorite, birnessite and todorokite have been identified as common soil Mn minerals. Lithiophorite has been identified as the most stable Mn mineral in acid conditions (Taylor et al., 1964; Uzochukwu and Dixon, 1986; Golden et al., 1993) while birnessite is more common under neutral to alkaline conditions and todorokite is commonly associated with carbonates (Ross et al., 1976; Taylor et al., 1964). A brief discussion of these minerals and their chemistry may be useful in understanding the conditions under which the minerals form.

Birnessite [$(Na,Mg,Ca,Mn^{2+})Mn_7O_{14}$] has a layer structure composed of sheets of edge-sharing MnO_6 octahedra alternating with planes of cations (mainly Ca, Mg, Na and Mn^{2+}). There are vacancies in one in every six MnO_6 octahedra within the sheet, with Mn^{2+} and Mn^{3+} ions situated between the sheets above and below these vacancies. In synthetic birnessite, pH of synthesis plays an important role in the geometry and chemical composition of the birnessite mineral formed (Silvester et al., 1997). It can be imagined that soil pH will play a similarly important role in determining the birnessite structure and chemistry.

Lithiophorite [(Al,Li)$MnO_2(OH)_2$] has a layer structure like that of birnessite except that the interlayers between the MnO_6 octahedra consist of Al-hydroxy sheets, the ideal structure containing Li in the Al octahedral vacancies. The cation sites in the Mn octahedral layer are fully occupied with 2/3 of the sites occupied by Mn^{4+} ions and the remaining 1/3 occupied by Mn^{3+} ions. The layers are cross-linked by hydrogen bonds between the hydroxyl H of the Al/Li layer and the O atoms of the Mn sheet (Post, 1999). Other transition metals such as Ni, Cu and Co have been observed as substituting in the structure of lithiophorite (Ostwald, 1984). Lithiophorite has been identified in old, highly weathered soils. The Al interlayer suggests formation under acid conditions (Golden et al., 1993).

Todorokite [$(Na,Ca,K,Ba,Mn^{2+})_2Mn_5O_{12}.3H_2O$] has a tunnel structure formed from triple chains of edge-sharing MnO_6 octahedra linked to form 3x3 tunnels which contain Na, Ca, K, Ba, Sr and water molecules (Post and Bish, 1988). The octahedra at the edge of the triple chains are slightly larger than those near the middle and can probably accommodate the larger, lower-valence cations found by Post and Bish (1988) in todorokite samples. Todorokite synthesis from birnessite was most successful in the presence of the Mg^{2+} ion (Dixon, 1988). Magnesium is also the most common constituent of natural todorokites (Turner, 1982). The apparent role of Mg in the formation todorokite, as well as its fibrous morphology, suggests that todorokite may be sensitive to weathering and would not be expected to occur in highly weathered, acid environments (Dixon, 1988).

The manganiferous soils of Graskop provide a good opportunity to study Mn minerals in highly weathered soils, as Mn is typically found in trace quantities in most oxisols (Marques et al., 2003). The high Mn content (up to 17%) provides abundant Mn for mineralogical analysis. The Mn minerals in the soils are not limited only to nodules. Manganese oxides form a large proportion of the clay minerals and will be influenced by the chemical conditions that define the pedogenic environment of the soil. Pre-concentration is not necessary due to the high Mn content so a mineralogical study can be performed on the soils in their natural state.

An earlier study by Hawker and Thompson (1988) was conducted to determine the mineralogy of the Graskop dolomite and its manganiferous alteration products. Soil

material that lay above the manganese wad was not investigated. Elemental analysis from their study revealed that Fe and Mn constitute only a minor fraction of the dolomitic parent material. The accumulation of Mn and Fe in the weathering products had been the result of residual enrichment through removal of Mg and Ca carbonates. From XRD patterns Hawker and Thompson (1988) concluded that the dominant Mn minerals present in the residuum are birnessite (7.2, 2.46, 2.33 Å), nsutite (2.44, 2.15, 1.66 Å) and todorokite (9.69, 4.8 Å) while the dominant iron mineral is goethite (4.18 Å). The minerals identified were confirmed by IR spectroscopy, using the spectra published by Potter and Rossman (1979a) as a reference. The IR bands were broad and not clearly resolved, indicating crystal disorder. They were able, however, to identify bands representative of birnessite, nsutite and poorly ordered todorokite.

The present study aims at investigating the mineralogy of the soils that are enriched with Mn, and not simply the Mn wad which is seen as an extreme alteration product of dolomite weathering. It can be hypothesized that pedogenic alteration of the wad, especially through interaction with soil organic matter, will result in a mineral assemblage different from that of the Mn oxide residuum, the initial dolomite weathering product.

2.2 Materials and methods

2.2.1 Sample pretreatment

Soil material was taken from the A and B2 horizons of the F3 profile. The clay faction was extracted from the bulk soil using acid dispersion as follows: 10 g soil was suspended in 1 liter of deionized water and the pH of the suspension adjusted to pH 4 using 0.1 M HCl. After shaking the suspension for 5 min it was allowed to stand for 16 h in order for coarse material to settle. The dispersed colloidal fraction (<2 μm) was removed by siphoning and then flocculated using a few drops of 0.5 M $MgSO_4$ solution. The clay separate was washed several times with deionized water to remove salts, and concentrated slurry was collected for pre-treatment.

Subsamples (0.5 ml aliquot) of clay slurry were treated for selective removal of various constituents as summarized in Table 2.1:

Table 2.1: Selective dissolution pre-treatments for mineralogical analysis

Constituents dissolved	Method	Source
Amorphous Al and Fe minerals	20 ml 0.2M Ammonium oxalate in the dark	Jackson et al., 1986
Fe and Mn oxides	20 ml 0.3 M Na-citrate and 2 g Na-dithionite at 78^{o}C	Holmgren, 1967
Mn oxides¶	10ml, 0.1M hydroxylamine hydrochloride + 0.01M HNO_3	Chao, 1972
Kaolinite and gibbsite	5M NaOH heating	Tokashiki et al., 1986

¶ Separate subsamples washed either 1, 2 or 3 times

2.2.2 X-ray diffraction

X-ray diffraction patterns were obtained on a Philips PW1710 diffractometer using CoKα radiation generated at 45 kV and 30 mA (divergence slit = 1^{o}; receiving slit = 0.1 mm). Clay fractions of treated and untreated samples were mounted on glass slides using sedimentation.

Powder mounts of soils from the other three profiles were also analyses to check for soil variability these patterns are shown in Appendix A.

2.2.3 Infrared analysis

Infrared spectra were obtained with a Thermo Electron® Nexus 670 spectrometer, fitted with a liquid-N_2 cooled MCT-A detector, in diffuse reflectance mode. The spectrometer was fitted with COLLECTOR® apparatus for DRIFT spectroscopy. Spectra were collected using 64 co-added scans at 4 cm^{-1} resolution. Approximately 2.5 mg of powdered sample was dispersed in 500 mg KBr. Spectra were obtained for untreated, and citrate-dithionite treated samples. The lower frequency region (400-1200 cm^{-1}) could not be observed using the MCT-A detector and so spectra were also obtained of samples dispersed and compressed in KBr using a DTGS detector.

Differential spectra were obtained by subtracting the spectrum of the DC treated sample from the spectrum of the untreated sample with prior normalization of the quartz peak at 1030 cm^{-1}. All manipulations were carried out using OMNIC software.

Synthetic birnessite, prepared by the method of McKenzie (1971) and synthetic lithiophorite, prepared by the method of Yang and Wang (2003) (from mineral collection of Environmental Soil Chemistry laboratory, University of Delaware) were used as standards for IR peaks associated with each mineral.

2.2.4 Scanning electron microscopy

To assist in mineral identification Scanning electron microscopy (SEM) was performed using a LEO 1430VP SEM. Images were obtained of a small undisturbed, carbon-coated soil aggregate from the F3B2 horizon.

2.3 Results and discussion

2.3.1 X-ray diffraction analysis

X-ray diffraction patterns of clay separates from the top and subsoil are shown in Figure 2.1. Lithiophorite (9.45; 4.74 and 3.14 Å) is the only Mn mineral that can be identified unambiguously. The presence of birnessite is hard to infer from these patterns because of the close proximity of kaolinite peaks (7.16 and 3.4 Å). Gibbsite, mica, quartz, goethite and hematite peaks are also identifiable. Patterns representing the top and subsoil differ mainly in the intensity of the lithiophorite peak, which increases substantially in the subsoil and, quite remarkably, dominates the mineralogy. The intensity and sharpness of the lithiophorite peaks implies a fairly crystalline mineral. Lithiophorite was not amongst the minerals identified in an earlier study of the wad material (Hawker and Thompson, 1988). The XRD patterns of powder mounts from the other soil profiles are given in Appendix A. Patterns similar to those for profile F3 were obtained for all soils except for the F5 profile where the gibbsite peak had the highest intensity.

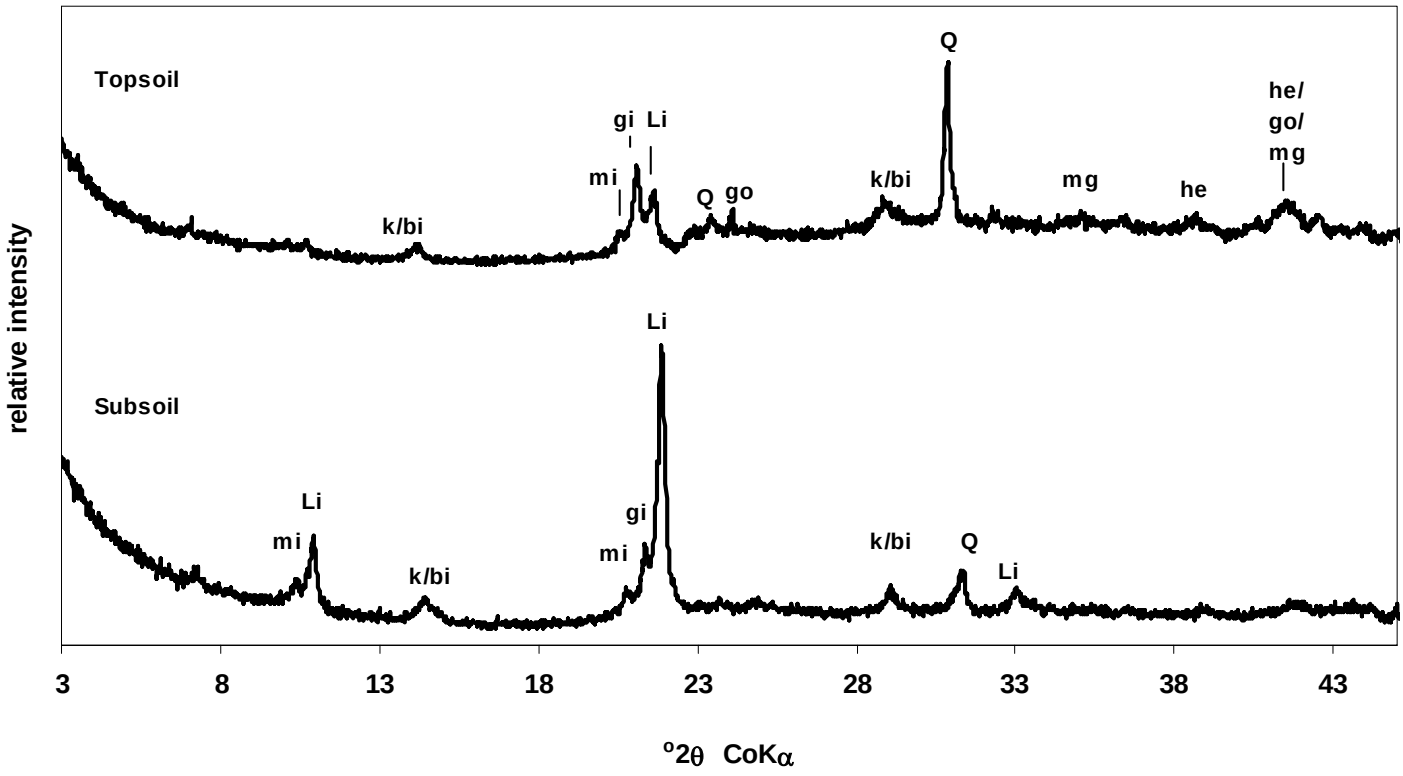

Figure 2.1 X-ray diffraction patterns of clay separates extracted from top and subsoil (B2) of profile F3. k= kaolinite (7.16, 3.57, 2.34 Å); bi = birnessite (7.14, 3.57, 2.52 Å); mi= mica (10.0, 4.98, 3.34 Å); gi= gibbsite (4.85, 4.37, 4.32 Å); Li = lithiophorite (4.71, 9.43, 2.37, 3.14 Å); Q = quartz (3.34; 2.46 Å); go = goethite (4.18, 2.69, 2.43 Å); mg = magnetite/maghemite (2.52, 2.95 Å) and he = hematite (2.69, 3.68, 2.52 Å).

All pretreatments were performed on the subsoil clay separates. Figure 2.2 shows XRD patterns of dithionite-citrate (DC) and NaOH treated samples. The DC treatment shows the presence of kaolinite, mica, gibbsite and quartz. The peak at 14.14 Å is common for 2:1 layer silicate minerals. Positive identification would require a number of heating and chemical treatments which are beyond the scope of this study. The highly weathered nature of the soil would suggest the most likely mineral to be aluminous or so-called pedogenic chlorite, as noted in other well-weathered soils in South Africa (le Roux, 1973; Bühmann, 1986). Perhaps additional evidence for this mineral is the disappearance of the peak when treated with NaOH (Fig. 2.2) which would destroy the Al interlayer. Hawker and Thompson (1988) identified muscovite in the wad material, and related it back to lenses of muscovite found in the dolomitic parent material. This would probably also account for the mica peaks found in this study (Fig. 2.2).

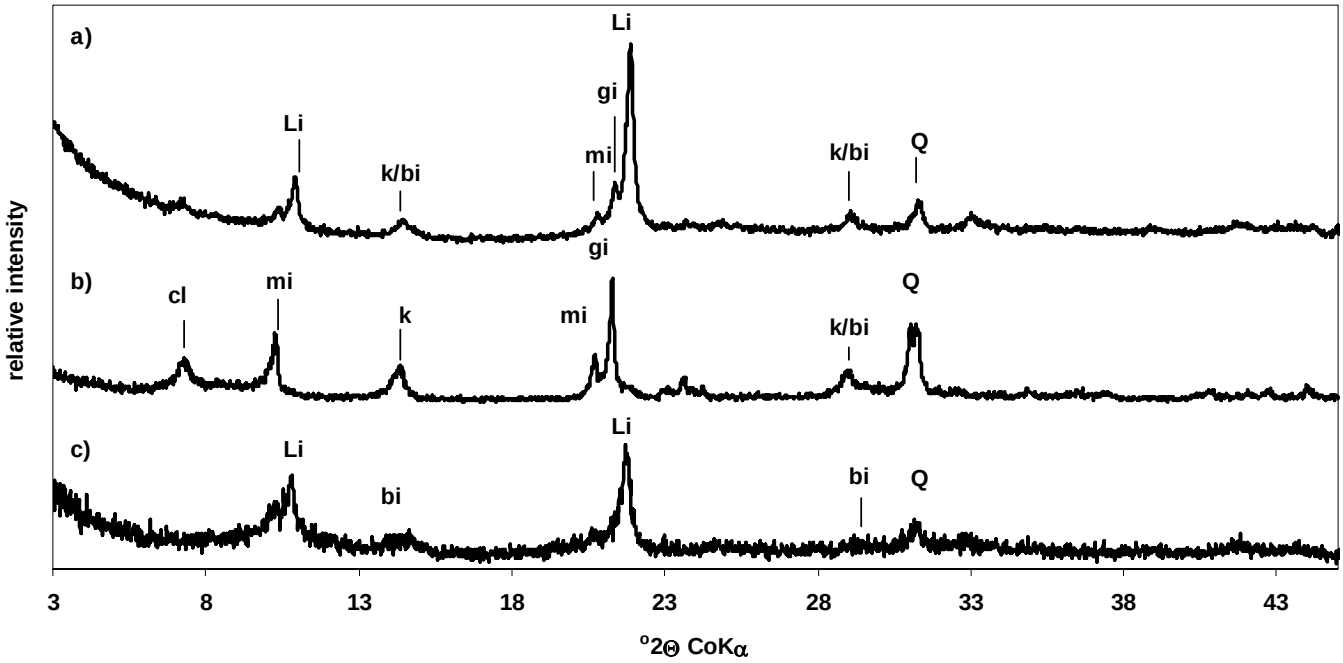

Figure 2.2 X-ray diffraction patterns of a) untreated, b) dithionite-citrate (DC) and c) NaOH treated clay separates extracted from the subsoil (B2) horizon. cl = chlorite; k= kaolinite; bi = birnessite; mi= mica; gi= gibbsite; Li = lithiophorite; Q = quartz (d-distances of minerals are specified in Figure 2.1).

The NaOH treatment is designed to remove silicate clays and gibbsite and concentrate Mn oxides (Tokashiki et al., 1986 and 2003). Removal of kaolinite and gibbsite would allow diffraction peaks representing birnessite and todorokite to be identified. Figure 2.2a shows the peaks at 7.2 and 3.4 Å representative of birnessite are present after the removal of kaolinite. However, the major peak at 4.8 Å for todorokite is not evident. Dissolution of lithiophorite Al-interlayers by strong alkali has been reported (Dixon and Skinner, 1992). The lithiophorite clearly persists after the NaOH treatment (Fig. 2.2). The high crystallinity of the lithiophorite may account for this, or alternatively, the lithiophorite in the soil could be of the kind described by Ostwald (1984), that hosts other cations such as Co, Ni or Cu in the interlayer which might stabilize the mineral in strong alkali.

Figure 2.3 shows the clay separates from the subsoil horizon before and after treatment with HAHC and acid oxalate. Washing with HAHC causes a distinct loss in intensity of the lithiophorite peaks while the other peaks appear unaffected. Acid oxalate has little effect on the intensity of the lithiophorite peaks but does increase the relative intensity of other peaks. The chlorite peak at 14.14 Å and goethite peak at 4.18 Å only become evident after washing the clay with oxalate or HAHC. Acid oxalate and HAHC should remove all

amorphous Mn and Fe minerals from the clay, which would enhance peak intensities of the remaining minerals. This could explain why certain peaks only become evident after the clay surface has been 'cleaned' of poorly crystalline material.

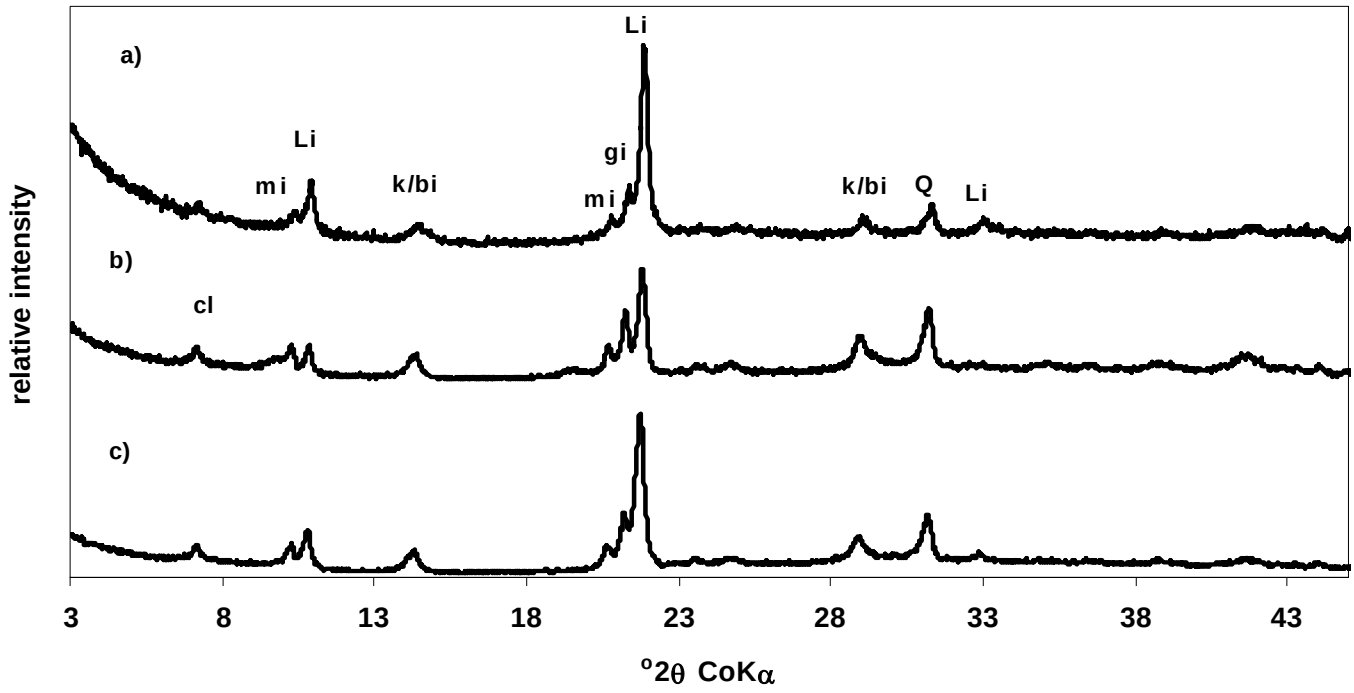

Figure 2.3 XRD patterns of a) untreated, b) hydroxylamine hydrochloride (HAHC) and c) acid oxalate treated clay separates from the subsoil (B2) horizon. cl = chlorite; k= kaolinite; bi = birnessite; mi= mica; gi= gibbsite; Li = lithiophorite; Q = quartz (d-distances of minerals are specified in Figure 2.1).

The XRD patterns of the clay separates after successive HAHC treatments are shown in Figure 2.4, while the corresponding quantities of Mn and Fe removed in each HAHC extraction are shown in Table 2.2.

Table 2.2 Metal release from successive hydroxylamine hydrochloride (HAHC) washings of F3B2 soil material expressed as a weight percentage of soil and percentage DC extractable metal concentration.

No. HAHC washings	Weight % soil		% DC extractable	
	Mn	Fe	Mn	Fe
1	5.5	0.4	80.3	6.4
2	0.8	0.5	8.6	8.6
3	0.6	0.5	8.6	8.6

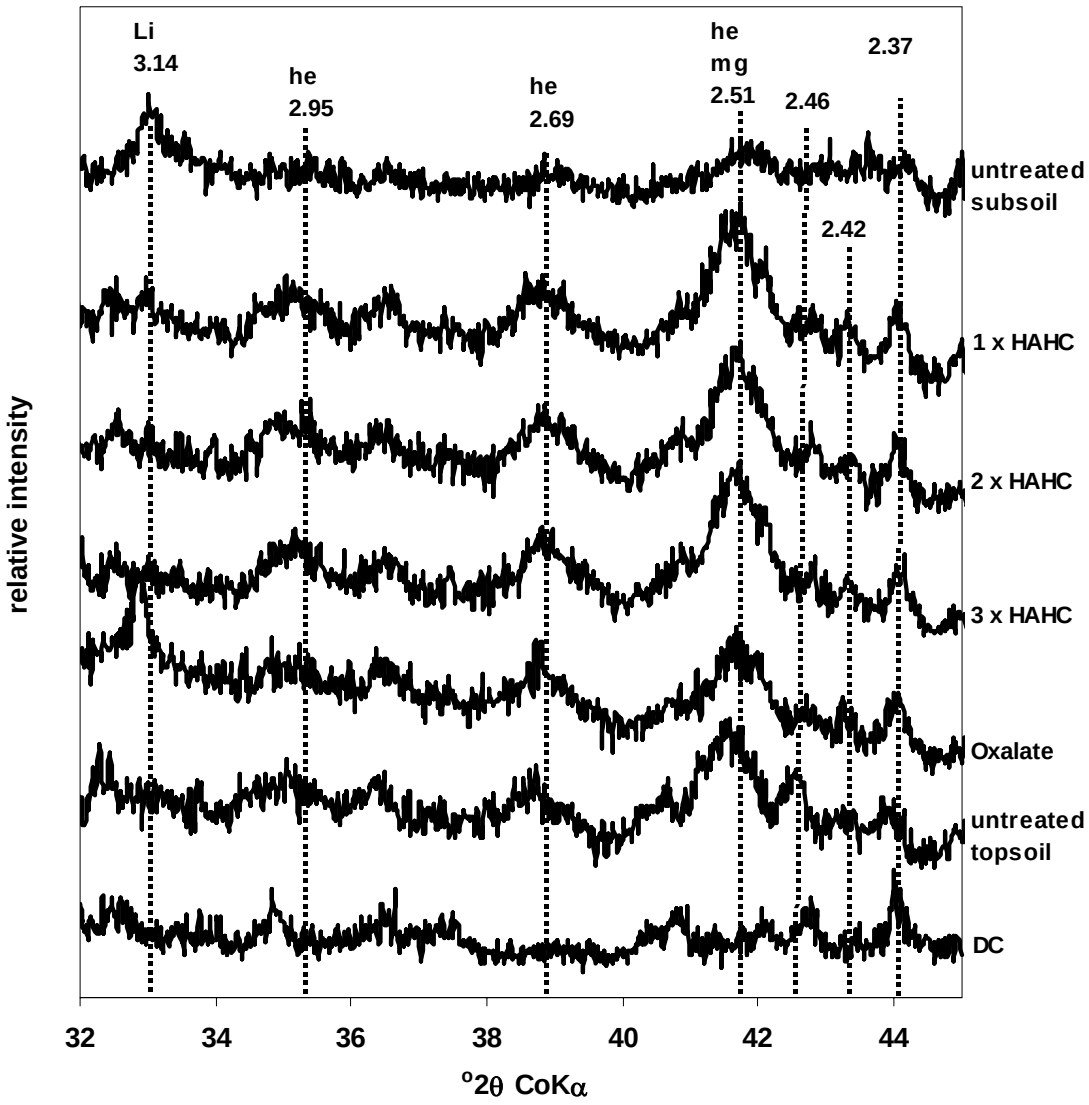

Figure 2.4 X-ray diffraction patterns of clay separates from the subsoil (B2) after treatment with acid oxalate and successive washings with acidified hydroxylamine hydrochloride (HAHC) compared to untreated top and subsoil clay and dithionite-citrate (DC) treated separates.

The first washing removes the most Mn (Table 2.2) and causes a discernible enhancement of the maghemite and hematite peaks at 2.95 and 2.69 Å, respectively. The presence of maghemite is not unexpected given the magnetic behaviour of the soil described in Chapter 1 (the allocation of maghemite rather than magnetite is based on the expectation that, in the colloidal size range, magnetite would be unstable and unlikely to occur (Schwertmann and Taylor 1977)). Subsequent HAHC washings increase the intensities of these peaks and diminish the 3.14 Å lithiophorite peak (Figure 2.4). Treatment of the clay separates with HAHC and acid oxalate increases the intensity of peaks at 2.46, 2.42 and 2.37 Å.

Lithiophorite has a peak at 2.37 Å, but the 3.14 Å lithiophorite peak decreases in intensity with HAHC treatments while the 2.37 Å peak increases in intensity, making lithiophorite an unlikely candidate. The pattern of the DC treated clay has been included to indicate peaks from the non-reducible fraction. This shows peaks at 2.46 and 2.37 Å which could explain these peaks after HAHC and acid oxalate treatments. The small 2.42 Å peak is absent in the DC sample and could indicate goethite. A peak for nsutite (2.44 Å) could be present but it is not possible to make this assignment on the basis of XRD analysis alone.

Some concern has been raised over the use of acidified hydroxylamine hydrochloride because of increased Fe oxide dissolution at low pH (Neaman et al., 2004). The Fe oxides in the Graskop soils may be quite crystalline and appear to be unaffected by the HAHC washings although increasing amounts of Fe were extracted with successive HAHC washings (Table 2.2). This Fe release could be attributed either to dissolution of poorly crystalline ferrihydrite or to the release of Fe housed in the structure of Mn minerals. Acid oxalate has a similar effect on the Fe oxide peaks but unlike the HAHC treatment, it does not remove the lithiophorite peak. The enhancement of Fe oxide peaks with acid oxalate and HAHC treatments could simply be a result of the removal of poorly crystalline material (mainly Mn oxides). The XRD pattern of the untreated topsoil, shows many characteristics of the HAHC and acid oxalate treated subsoil, having clearly evident hematite and maghemite peaks. This 'cleaner' topsoil pattern may be a result of the higher reducing potential of the topsoil, which ensures only the more crystalline minerals persist.

From the XRD analysis it is evident that lithiophorite is the dominant Mn mineral in the clay fraction, birnessite may also be present but there is little evidence for the presence of todorokite and nsutite. Further mineral investigation of the Mn phase was carried out using infrared spectroscopy and scanning electron microscopy. The pedogenic significance of the XRD data will be discussed after consideration of the IR and SEM data.

2.3.2 Infrared-spectra

The differential infrared spectra are shown in Figure 2.5. The birnessite and lithiophorite standards correspond well to the IR spectra obtained by Potter and Rossman (1979a). Lithiophorite shows the resolved band around 3400 cm^{-1} which the above-mentioned workers attributed to a single type of hydroxyl band. The peak around 3300 cm^{-1}

corresponds to one of the gibbsite peaks (White and Roth, 1986) and is probably a result of Al-OH stretching in the lithiophorite. The birnessite spectrum shows the characteristic broad band around 3200 cm^{-1} (Potter and Rossman, 1979a).

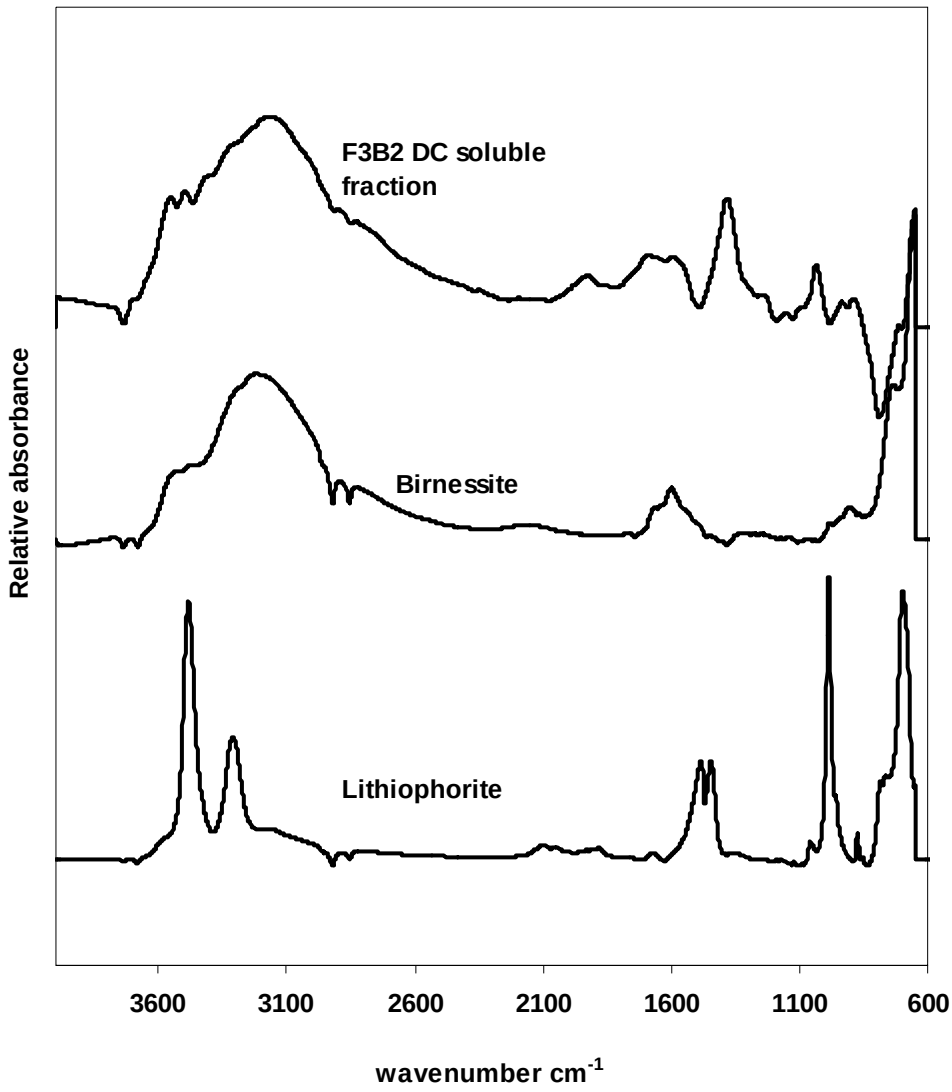

Figure 2.5 Diffuse reflectance infrared Fourier transform (DRIFT) spectra showing the reducible fraction of the clay separate (top), and synthetic birnessite (middle) and lithiophorite (bottom) standards. The spectrum of the reducible fraction was obtained by subtraction of spectra collected from the untreated and DC treated clay separate.

The differential spectrum representing the reducible fraction of the subsoil clay separate is shown in Figure 2.5. This represents the phase removed by DC treatment. The broad band around 3200 cm^{-1} of birnessite as well as a shoulder at ~3400 cm^{-1}, characteristic for lithiophorite, is evident in the differential spectrum. The peak at 1600 cm^{-1} corresponding to birnessite and the peaks at 1500 and 990 cm^{-1} corresponding to lithiophorite are also evident. Although, the information obtained in the DRIFT spectra is useful, most

researchers (Hawker and Thompson, 1988; Golden et al., 1993; Kim et al., 2002) use the region between 1400 and 400 cm^{-1} for the identification of Mn minerals. To investigate this region spectra were collected of the DC and untreated clay separate using compressed KBr pellets. The subtraction result is shown in Figure 2.6.

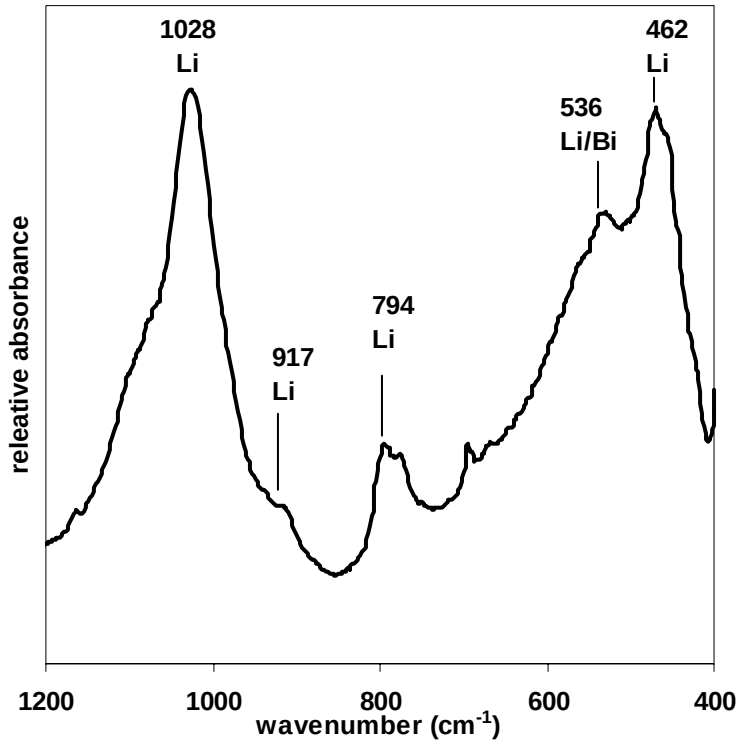

Figure 2.6 Infrared Fourier transform spectrum obtained by subtracting spectra collected from the untreated and DC treated clay separates. Li = lithiophorite and Bi = birnessite.

The absorption bands, shown in Figure 2.6, between 400 and 1200 cm^{-1} correspond reasonably well to those reported for lithiophorite identified in the Hawaiian oxisols (474, 546, 666, 791 and 1026 cm^{-1}; Golden et al., 1993). The characteristic broad band around 500 cm^{-1} for birnessite is not evident and only one other peak, (around 530 cm^{-1}) characteristic for birnessite, can be identified and coincides with a lithiophorite band. Hawker and Thompson (1988) observed a broad band around 580 cm^{-1} in the wad material which was assigned to nsutite. This band is not evident in the present data.

2.3.3 Scanning electron microscopy

Figure 2.7 shows a series of SEM images of an undisturbed aggregate from the F3B2 horizon at different magnifications. The image at lower magnification is useful for highlighting the extremely porous nature and high surface area of these soils. At higher

magnifications platy mineral structures can be identified within a mass of less crystalline material. These hexagonal platy minerals may represent well-crystallized lithiophorite as they resemble such minerals identified in a Hawaiian oxisol (Golden et al., 1993), adding further confirmation to the XRD and IR evidence for lithiophorite.

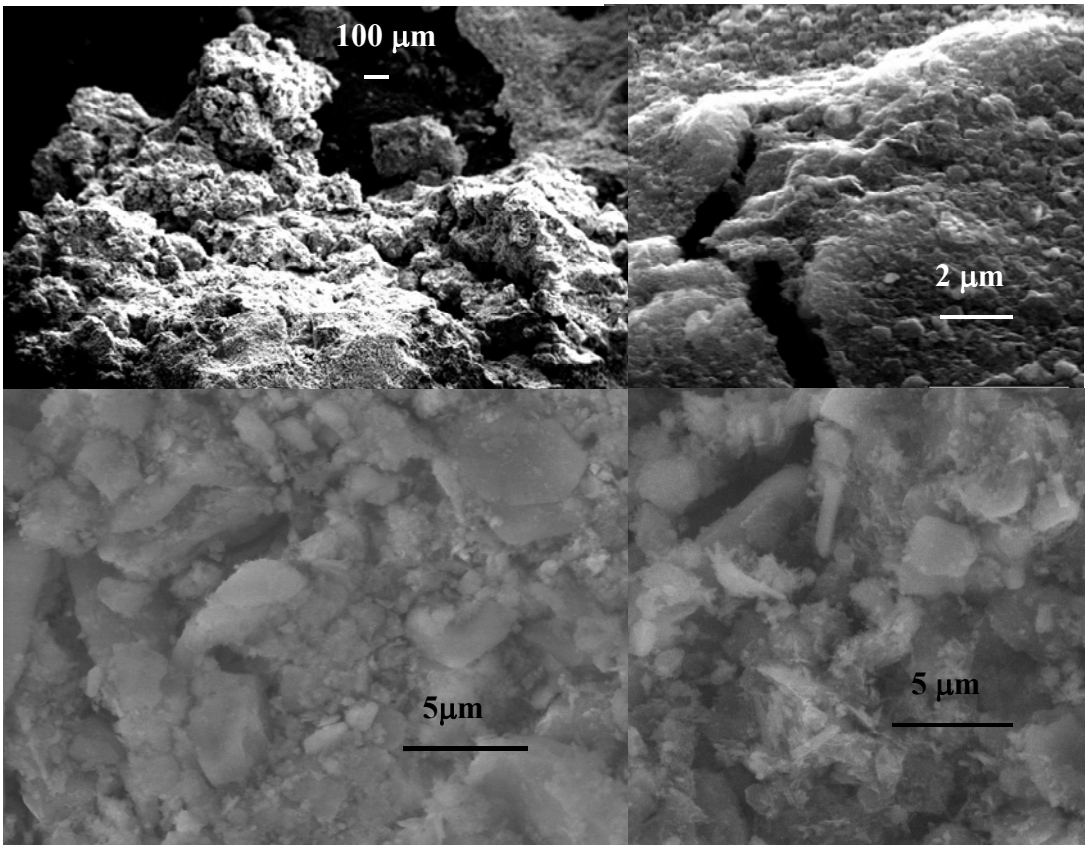

Figure 2.7 Scanning electron microscope images of an undisturbed soil aggregate from the F3B2 horizon at varying magnifications.

2.3.4 Pedogenic significance

From the XRD, IR and SEM data, it appears that lithiophorite is the dominant manganese mineral in the clay fraction. Birnessite may also be present in smaller amounts, but there is little evidence for todorokite and nsutite. Other minerals in the clay fraction include gibbsite, goethite, hematite, maghemite, kaolinite, quartz and a 14 Å mineral, probably aluminous chlorite.

Lithiophorite has been identified in highly weathered or acid soils as being the most stable Mn mineral (Taylor et al., 1964). Golden et al. (1993) suggested that the formation of

lithiophorite was favoured by acid conditions because of high Al concentrations needed for formation. Perhaps another way of interpreting it would be to imagine gibbsite sheets, present in well weathered soils, acting as templates and locally reducing the activation energy for Mn oxidation. Thus Mn weathered from less stable minerals may oxidize out in association with Al-hydroxy sheets to form lithiophorite. Whatever the role of Al is in the structure it appears to add to the stability of the mineral. In the weathering sequence of Mn minerals, lithiophorite is considered the final weathering product (Dixon, 1988; Parc et al., 1989) and weathers to gibbsite through reductive dissolution (Golden et al., 1993). Neaman et al. (2004) observed the resistance of lithiophorite to dissolution in acid hydrogen peroxide. Kim et al. (2002) concluded that lithiophorite was a weaker oxidizing agent than birnessite, pyrolusite and todorokite. They related it to the higher proportion of Mn^{3+} in the structure. An alternate view may be that Al in the structure somehow stabilizes the mineral against reductive dissolution. Perhaps the structural Al disrupts electron flow within the mineral reducing the semi-conducting properties of Mn oxides. The fact that lithiophorite displays a weaker oxidizing capacity than other Mn oxides is probably the reason it persists in acid weathered soils, while other Mn minerals are removed.

The study of Hawker and Thompson (1988) showed birnessite, todorokite and nsutite in the wad material. They did not investigate the soil material overlying the wad. The current study has shown that the overlying soil material, which is exposed to pedogenic processes, has practically reached the end point in the sequence of Mn oxide weathering, with all Mn minerals in the wad weathering to lithiophorite in the soil. This is a nice illustration of Mn mineral evolution in the weathering sequence suggested by (Parc et al., 1989) where most birnessite, todorokite and nsutite minerals have weathered to lithiophorite and will eventually weather to gibbsite as depicted by the series:

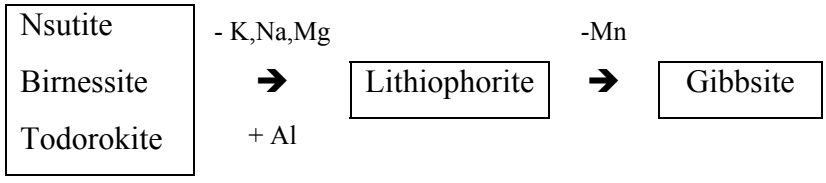

The iron minerals identified were goethite, hematite and maghemite. The latter two Fe oxides generally form in warm environments (Schwertmann and Taylor, 1977). Maghemite has diffraction peaks at 2.52 and 2.95 Å as does manganite. Manganite found in soils is

usually considered lithogenic while pedogenic maghemite is commonly reported (Schwertmann and Taylor, 1977; Bigham et al., 2002). In dolomitic parent material it is not expected to find magnetite, which is usually associated with an igneous origin, so it is assumed that the magnetic material present is pedogenic maghemite. A large proportion of the nodules displayed magnetic behavior and in the F4 profile much of the fine earth fraction is also magnetic. The possibility of a contribution by paramagnetic Mn minerals was not investigated.

After removal of Mn and Fe oxides, an intense, sharp XRD peak for gibbsite was evident. Table 1.4 shows that some soils have a total Al_2O_3 content as high as 30%. Gibbsite usually appears at a later stage of weathering than Fe oxides (Hsu, 1989). It is generally considered the end product of primary and secondary silicate weathering, analogous to lithiophorite being the end member in Mn mineral weathering. The data therefore provide mineralogical confirmation of very advanced weathering and that these unusually manganiferous soils probably belong in the oxisol order of the USDA Soil Taxonomy.

2.4 Conclusions

The mineralogical analysis of the Graskop soil shows that lithiophorite dominates the mineralogy of the clay fraction with accessory amounts of birnessite, gibbsite, goethite, hematite, maghemite, mica, kaolinite and aluminous chlorite. This mineral suite shows an extreme degree of weathering with the mineral composition dominated by sesquioxides. Comparing the results of this study to earlier work on the wad material it appears that the weathering sequence of Mn minerals is also very advanced with most Mn minerals having transformed to lithiophorite, an aluminous Mn oxide which is widely considered to be the end member of Mn mineral weathering.

This mineralogical information is important for understanding the chemical properties of the soil. Sesquioxides are amphiprotic and so a large proportion of the charge is likely to be pH dependent. The low proportion of permanently charged minerals usually infers a low CEC which has important implications for the soil's buffer capacity. The charge characteristics and buffer capacity are addressed in the next chapter.

CHAPTER 3

3 Soil acidity and its influence on metal mobility

3.1 Introduction

The manganiferous soils of the Driekop plantation have supported forestry practices for over 60 years. The effects of afforestation on soil acidity in South Africa (du Toit, 1993 and Nowicki, 1997) and North America and Europe (Lutz and Chandler, 1946; Ovington and Madgwick, 1957) have been well documented. Nowicki (1997) investigated the impact of forestry practices on soils of the eastern escarpment. It was shown that the pH was lower and dissolved metal (mainly Al and occasionally Mn) concentrations were higher for forest soils compared to soils of adjacent grassland, although the natural grassland soils were also found to be fairly acidic. The sampling by Nowicki (1997) did not include soils derived from dolomitic parent material and so little information is available on how the manganiferous soils react to inputs of acidity, and how acidity affects metal mobility in these soils.

The highly leached Graskop soils have lost the alkalinity of the dolomitic parent material and long periods of weathering have converted most primary minerals to sesquioxides and kaolinite (Chapter 2). These minerals are largely considered to be the final products of mineral weathering, and are generally associated with infertile, poorly buffered soils which have very low cation exchange capacity. It is important to establish the buffering capacity of the highly weathered Graskop soils and establish how additions of acidity will affect the release of metals from the solid phase. With such a high Mn oxide and associated trace metal content (Chapter 1), the stability of the Mn oxides is of particular concern. The high nodule content of the soil, as discussed in Chapter 1, is a clear indication that Mn can be remobilised. It is important to identify the factors that affect the mobility of the Mn in order to predict the stability of the Mn phase under current land use practices.

3.1.1 Sources of acidity in forest soils

The process of soil acidification under commercial pine plantations is well documented (Lutz and Chandler, 1946; Ovington and Madgwick, 1957). Disruption of nutrient cycling through the harvesting of accumulated biomass is believed to be a major contributor

(Ulrich, 1991; Johnson and Todd, 1987; Richter, 1986). This has the effect of gradually depleting the soil of basic cations, mainly Ca and Mg. Another source of acidity comes from the preferential uptake up of ammonium-nitrogen by pines (Keltjens and van Loenen, 1989) which leads to the exudation of protons to maintain charge balance in the root. Additions of acidity and removal of base cations is especially important in poorly buffered soils. The high water requirement of pine plantations results in areas of high rainfall being used for their cultivation. High rainfall areas in South Africa, such as the eastern escarpment, usually have well leached, poorly buffered soils and so soil acidification through afforestation can have important implications for metal mobility (Nowicki, 1997).

3.1.2 The mobility of Mn, Fe and Al in acid soils

Manganese, aluminium and to a lesser extent iron can become mobile in acid soils creating potentially phytotoxic conditions. Manganese toxicity is generally considered less of a problem than Al toxicity due to Mn only being found in trace quantities in most acid soils. Iron, although ubiquitous, is very insoluble except under reducing conditions (Sumner et al., 1991). If Mn is present, however, it can become mobile and cause toxic conditions at a higher pH than Al (Hue et al., 1987; Sumner et al., 1991). The mobility of these metals is controlled by a number of factors and conditions suitable for the immobilization of one metal may enhance the toxicity of another. These factors are reviewed in the ensuing section.

Manganese usually comes into solution in the form of Mn^{2+} (Norvell, 1988). Soluble complexes of Mn^{3+} may occur in the presence of stabilizing ligands but, if uncomplexed, Mn(III) rapidly undergoes disproportionation to Mn(II) and Mn(IV) ions (Dion and Mann, 1946). Tetravalent manganese is highly insoluble and its contribution to soluble Mn is generally considered negligible. Thus the dissolution of Mn from the solid phase is likely to proceed through reduction of Mn(IV) and Mn(III) to Mn(II) or via release of Mn(II) from the mineral lattice. Considering this, soil pH can influence the mobility of Mn in two ways. Firstly, the redox parameter (pH + pe), as defined by Lindsay (1979) will decrease with pH allowing Mn reduction to occur at a higher pe. It has been observed that lowering the pH below 5 permitted reduction of Mn oxides even at a redox potential of +500 mV whereas at pH 6 reduction only occurred when the potential dropped below +200 mV (Gotoh and Patrick, 1972). More recent studies have suggested that the Mn^{2+} released from

birnessite as the pH is decreased is actually due to direct proton attack on the Mn mineral structure which releases Mn^{2+} housed in the birnessite lattice (Banerjee and Nesbitt, 2001). This highlights a second influence of pH. Proton promoted dissolution of oxides has been described by Furrer and Stumm (1986) and involves the weakening and eventual cleavage of the M-O bonds as protons bind to and polarize the oxygen atom. Ligand promoted dissolution, in the case of Fe oxides, also requires protons to aid in M-O bond weakening (Zinder et al., 1986). Proton attack will probably only occur in moderate to strongly acid soils, while lowering the redox parameter may result in Mn mobilization in mildly acid conditions.

Certain oxisols in Hawaii have a low pH <5.6 (Hue et al., 2001) and contain 1-4 percent Mn (Fujimoto and Sherman, 1948), which is comparable to the Graskop soils which have a pH around 5 and Mn content between 1 and 17 percent (Table 1.3) Manganese toxicity is a problem in the manganiferous oxisols of Hawaii (Fujimoto and Sherman, 1945) and it has been shown to be enhanced by low pH and the addition of organic matter (Vega et al., 1992; Hue et al., 2001). Work on Hawaiian oxisols has illustrated how certain management practices used to ameliorate Al toxicity, such as additions of manure or sewage sludge, can enhance Mn toxicity. The pH required to eliminate Al toxicity is lower (5.2-5.5) than that (5.8-6.2) required to prevent Mn toxicity (Fox et al., 1991).

The factors affecting mobility of Fe in soils are similar to those affecting Mn, except that more extreme conditions of acidity and electron activity are required to bring Fe into solution (Sumner et al., 1991). In well drained soils most Fe is found as very sparingly soluble Fe(III), usually in the form of iron oxides such as goethite, hematite, maghemite and ferrihydrite. Reduction and complexation can bring ferric iron into solution, both mechanisms being favoured by fulvic acids and low pH (Paterson et al., 1991). In acid soils fulvic acids appear to play a more important role in reducing rather than complexing ferric iron due to the very high fulvic acid concentrations required to maintain significant levels of Fe in the complexed form (Goodman and Cheshire, 1987). The reduction of Fe, like Mn, is highly dependent on pH. In acid soils the redox potential can be lowered enough to allow reduction to occur in micro-environments even in fairly well drained soils (Paterson et al., 1991). However, in well poised soils, such as those rich in Mn oxides, Fe reduction will be less likely to occur due to the presence of stronger oxidising agents (McBride, 1994). This could result in lower concentrations of plant available Fe.

Unlike Mn and Fe, pH has a much simpler effect on the solubility of Al with proton promoted dissolution being the most important mechanism of dissolution. This is shown by the following hydrolysis reactions:

$$Al(OH)_3 + H^+ \Leftrightarrow Al(OH)_2^+ + H_2O$$

$$Al(OH)_2^+ + H^+ \Leftrightarrow Al(OH)^{2+} + H_2O$$

$$Al(OH)^{2+} + H^+ \Leftrightarrow Al^{3+} + H_2O$$

Below a pH of 5 Al starts to appear in solution and its concentration increases with decreasing pH (McBride, 1994). Once in solution this Al competes for exchange sites on both clay minerals and soil organic matter, the latter being important in preventing Al toxicity in weathered topsoils (Hue et al., 1986) by reducing Al solubility (Bloom et al., 1979). Aluminium toxicity is a common fertility problem in old, weathered soils especially under crops that naturally acidify the soil. Acid subsoils have been shown to have higher soluble Al concentrations than overlying topsoils, which is mainly attributed to the sequestering of soluble Al by organic matter (Ruth et al., 1998).

While organic matter appears to be vital in the control of soluble Al, it plays the opposite role for Mn. Organic matter provides a source of electrons which are capable of reducing Mn oxides both indirectly, through microbial processes, or directly, though metal-ligand charge transfer (Stone and Morgan, 1984a+b; Stone, 1987). This means that while organic matter may relieve Al toxicity it can generate Mn toxicity. Further, Mn^{2+} forms only weak outer-sphere complexes with organic functional groups (McBride, 1978; McBride, 1982) and can easily be displaced by other metals ions (Norvell, 1988) and become plant available. In the subsoil the lack of organic matter and raised redox potential may result in the opposite scenario and conditions may be more suitable for soluble Al than soluble Mn.

3.1.3 Soil buffer capacity and proton sinks in highly weathered soils

The buffer capacity of a soil usually refers to its capacity to minimise the effect of additions of acidity or alkalinity. When a soil becomes acidified there are a few mechanisms of buffering. In weathered soils carbonate buffering is generally of less importance and in such soils the buffer capacity usually involves proton or proton generators being sequestered by the solid phase of the soil. The most important phases include soil organic matter, silicate clays and oxide minerals.

Soil organic matter is probably the biggest contributor to buffer capacity in highly weathered topsoils (Bloom, 2000). This capacity arises from the wide range of proton-accepting functional groups of soil organic matter and, just as important, its ability to complex Al. This not only buffers the pH of the soil but helps remove phytotoxic Al which becomes soluble below pH 5 (McBride, 1994). Organic rich soils are well buffered against pH change when limed, and this is partly because much of the alkalinity is consumed hydrolysing the complexed Al (Bloom, 2000).

Aluminosilicate clays, like organic matter, also provide exchange sites to accommodate protons and Al. In highly weathered soils, however, where most aluminosilicate minerals have been weathered to kaolinite and oxides, they make a limited contribution to buffer capacity. Dissolution of aluminosilicates also buffers the pH of moderately acid soils where part of the acidity is consumed breaking Si-O-Si and Al-O-Al bonds (McBride, 1994).

Charge generation on oxides and hydroxide minerals is another important sink for protons in highly weathered soils (Uehara and Gillman, 1982). The hydroxide or oxide groups in these minerals can act as proton donors or acceptors, and losing and gaining protons determines the charge on the minerals. These minerals can only accommodate a limited number of protons before mineral dissolution begins as the protons weaken the M-O bond (Furrer and Stumm, 1986). The Lewis acidity of the metal cation governs the capacity of oxides and hydroxides to accept or donate protons which in turn determines the point of zero charge (Parks and De Bruyn, 1962). Strong Lewis acids like Mn^{4+} strongly polarize the bonded oxygen atom and weaken the affinity of oxygen atoms for protons. Oxygen atoms of weaker Lewis acids like Fe and Al have a much high affinity for protons. This

results in Mn oxides generally having a lower pzc than Fe and Al oxides (McBride, 1994). In highly weathered soils where the mineralogy is dominated by sequioxides, buffering and charge development will go hand in hand.

The objective of this chapter is to investigate the response of the soil to additions of acidity. By measuring buffer capacity and charge characteristics of the soils it can be determined how readily acidification, and its associated release of Mn, Fe and Al, will take place.

3.2 Materials and methods

3.2.1 Exchangeable acidity and base saturation

Exchangeable acidity and basic cations were determined in the supernatant after shaking 5 g soil with 50 ml, 1M KCl for 30 min and filtering through Whatman no. 40 filter paper. Exchangeable acidity was determined by titrating the KCl extract with standardized 0.01 M NaOH to a phenolphthalein end-point. Basic cations (Ca, Mg and Na), together with Al and Mn were measured in the extract using flame atomic absorption spectroscopy (AAS) with a Varian Spectra AA.

3.2.2 Point of zero charge and buffer capacity

The point of zero charge (pzc) was determined using an approach similar to that of Hunter (1981). Potassium chloride was used as the indifferent electrolyte at concentrations of 0.01, 0.1 and 1.0 M. Field moist soils having the equivalent dry mass of 5 g were placed into polyethylene bottles and 50 ml of KCl solution was added. The soil suspensions, of different ionic strengths, were treated with 0.01 M NaOH or HCl (0-0.6 ml) and allowed to equilibrate on a reciprocal shaker overnight. A settling period of 30 min was allowed before pH was measured using a Metrohm 744 pH meter.

The supernatants from suspensions in 1 M KCl that had been acidified were analysed for Mn, Al and Fe concentrations using AAS.

3.3 Results and discussion

3.3.1 Exchangeable acidity and pH

Exchangeable cations and acidity and pH data are shown in Table 3.1. The soil pH range is 4.6-5.8 in H_2O, indicating that the acidity status is moderate to strong. Apart from the topsoils, the pH measured in H_2O is higher or equal to the pH measured in KCl which shows the soil pH is at or even slightly below the zero point of charge. This will be addressed in more detail in section 3.3.2, but it is important to consider when assessing the quantities of released exchangeable cations. The effective cation exchange capacity (ECEC), determined though the summation of total exchangeable acidity and basic cations, should be considered with caution due to the ambiguities involving exchangeable acidity and exchangeable Al (McBride, 1994). It can be used, however, as a guideline for understanding certain trends. The very low ECEC in the subsoils relates to the negative ΔpH ($pH_{H2O} - pH_{KCl}$) values (Table 3.1), which imply a net positive charge (AEC>CEC). The low exchangeable acidity in the subsoils, despite their pH being below that of Al hydrolysis, may be a result of a low ratio of exchangeable acidity to total acidity which is commonly found in soils with significant pH dependent charge (Sparks, 2003). This is largely a result of partially hydrolysed Al and Fe polymers blocking the CEC sites of permanently charged clays (Coleman et al., 1964). These polymers contribute to total acidity but cannot be extracted using a strong electrolyte like 1 M KCl. This may also explain the high base saturation of some of the subsoils (Table 3.1). There is also the corollary that when the soil is at its pzc there is no CEC to host exchangeable cations and the ratio between soluble and exchangeable cations becomes important. Some of the subsoils contained a higher concentration of exchangeable Al than exchangeable acidity (Table 3.1). The concentration of Al in these cases was low, however, and the inclusion of some polymeric Al in the KCl extracts might account for the discrepancy.

Table 3.1 Exchangeable cations, acidity and pH in horizons of the F3 and F4 soil profiles.

				----------$mmol_c kg^{-1}$----------							
Sample	**pH (KCl)**	**pH (H_2O)**	**Δ pH***	**Exch. Acidity**	**Al**	**Mn**	**Ca**	**Mg**	**Na**	**ECEC**	**Base saturation %**
F3A	4.3	4.9	0.6	6.3	4.3	0.34	3.0	2.5	1.1	12.8	51
F3B1	5.0	4.6	-0.4	1.3	0.7	0.08	0.5	0.4	0.2	2.4	47
F3B2	5.3	4.9	-0.4	0.2	0.3	0.08	0.5	0.4	0.2	1.3	81
F4A	4.4	4.9	0.5	6.9	5.6	0.18	2.0	1.6	0.7	11.2	39
F4B1	5.5	5.2	-0.3	0.2	0.7	0.06	1.7	1.4	0.6	3.9	94
F4B2	5.8	5.8	0.0	0.2	0.8	0.07	1.5	1.2	0.5	3.4	93
F4B3	5.6	5.6	0.0	0.2	1.2	0.07	2.5	2.1	0.9	5.7	96

* $\Delta\ pH = pH_{(H20)} - pH_{(KCl)}$

Exchangeable cations and acidity determined in 1M KCl (soil solution ratio 1:10). Effective cation exchange capacity (ECEC) determined through the summation of exchangeable acidity, Ca, Mg and Na. pH(KCl) and (H_2O) determined in 1:2.5 soil:solution ratio.

Exchangeable Mn in the topsoils is surprisingly low given their more acidic status and the abundance of Mn in these soils. This may have to do with the capacity of Mn to form only weak outer sphere bonds with organic compounds, allowing it to readily be displaced by other competing cations like Ca (Novell, 1988). An alternative explanation could be the autooxidation of Mn^{2+} when brought into contact with Mn oxide surfaces. Ross and Bartlett (1981) showed that the extent of Mn^{2+} oxidation was proportional to the amount of Mn oxide already present in the soil. With the exceptional concentration of Mn oxides in the Graskop soils it might thus be expected that exchangeable Mn is kept low through autooxidation, especially in the subsoils. The role of oxidising bacteria could also play an important role. The low levels of Mn^{2+} found in some acid soils has been attributed to the presence of oxidizing bacteria which can result in Mn^{2+} oxidation even though inorganic oxidation is unfavourable (Sparrow and Uren, 1987).

Table 3.1 shows the most acidic soils are the surface horizons, which also have the highest exchangeable acidity and lowest base saturation. The higher CEC, presumably related to humic substances, in these topsoils is still very low compared to less weathered soils and this together with the negative Δ pH in the subsoils supports the classification of these soils as *Anionic Oxisols* (Soil Taxonomy) or *Posic Ferralsols* (WRB).

Metal concentrations were determined in saturated paste extracts but are not shown here because almost all concentrations were below detection limits.

3.3.2 Point of zero charge and buffer capacity

Potentiometric titration was used to determine point of zero charge (pzc) of the A, B1 and B2 horizons of the F3 profile. The results are shown in Figure 3.1. A clear intersection point of the three isotherms (representing the pzc) can be identified for all three horizons, with the pzc for the A, B1 and B2 horizons being 4.5, 5.1 and 5.5, respectively. The increase in pzc down the profile almost certainly reflects the influence of organic matter which greatly enhances the CEC of highly weathered soils. The pzc of these soils falls beyond the range of 3.5-4.5 given for highly weathered soils by McBride (1994), which is consistent with the exceptionally high sesquioxide content and low proportion of permanently charged minerals reported in Chapter 2.

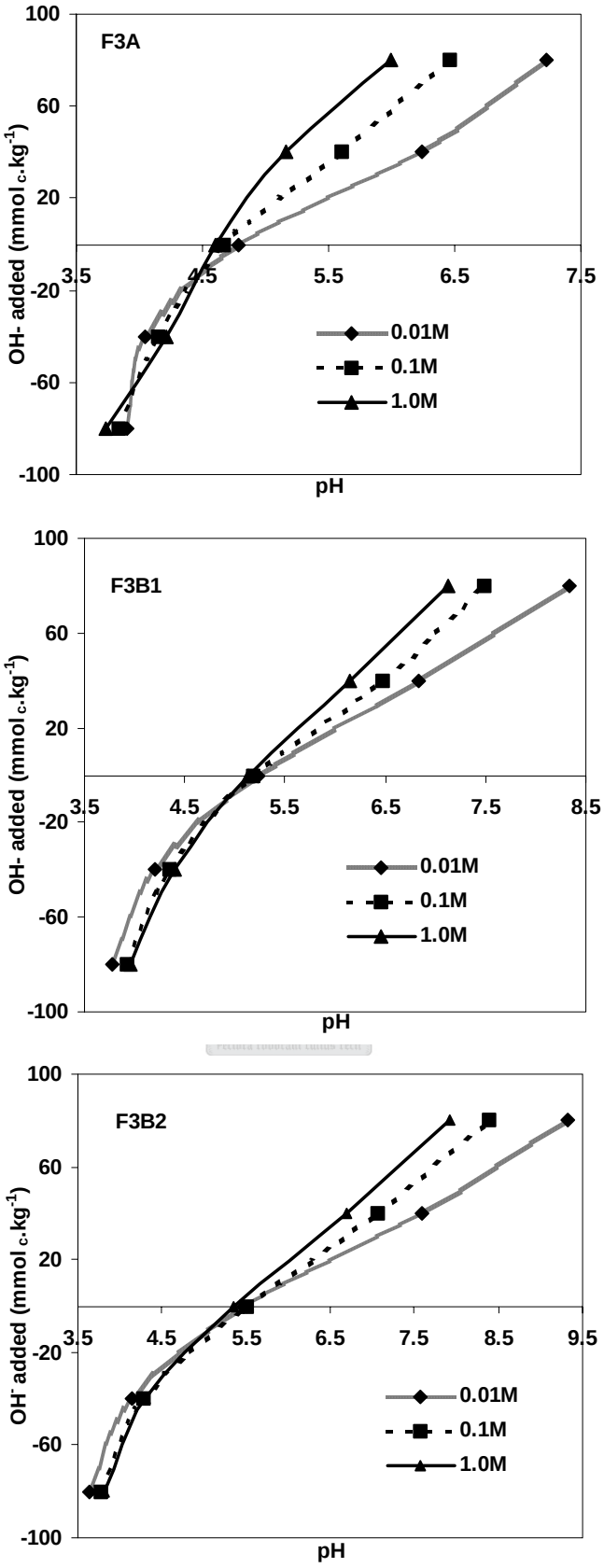

Figure 3.1 Potentiometric titration curves of F3A, F3B1 and F3B2 indicating the point of zero (PZC) charge for each soil using 1.0, 0.1 and 0.01 M KCl solutions as the indifferent electrolyte. The pzc for each soil is indicated by the intersection point of the three isotherms.

The measured pzc will represent the overall charge from the individual oxide species. Oxides of Al and Fe generally have a high pzc between 7.5 and 9 (McBride, 1994) while birnessite and lithiophorite have a pzc of around 2.3 and 6.9, respectively (Murray, 1974; Kim et al., 2002). The Mn mineralogy of the Graskop soils is dominated by lithiophorite (Chapter 2) which may account for the pzc being higher than expected for such Mn rich soils, as most Mn oxides have a pzc in the range 1.5 to 4.6 (Healy et al., 1966).

It is interesting to note that the pzc for all soils occurs close to the point of zero titration i.e. the point at which no acid or base is added (Fig 3.1), indicating that the pH of the soil is close to the point of zero charge. Table 3.1 shows that for most of the other soils, excluding the topsoils, the pH_{H2O} is the same as or slightly lower than the pH_{KCl} confirming that the subsoils are either at or just below their pzc. This has important pedogenic and stability implications. Hendershot and Lavkulich (1978) suggested that with increasing pedogenic development the pzc becomes more defined and approaches the natural pH of the soil. Further, when the pH of a solution reaches the pzc of a particular solid, the hydrolysis of the solid by OH^- and H^+ ions is at a minimum, therefore the solubility of the surface reaches a minimum (Parks and De Bruyn, 1962). When applied to soils, this means that when the pH of the solution reaches the pzc of the soil, as is the case in the Graskop soils, the mineral phase will be at its most stable against hydrolysis. The complex mineral associations and contributions to pzc may make this more complicated in soils but modifying the pH of the soil through added acidity may have some important implications for such a delicately poised, charged surface. Firstly, the uncharged, organic poor subsoil, will have little buffer capacity in the form of CEC to sequester protons and Al, and secondly, added acidity will immediately charge the soil which means oxides will begin to protonate, putting stress on M-O bonds and favouring metal release as described by Furrer and Stumm (1986).

The buffer capacity of the top- and subsoils after the addition of HCl is shown in Figure 3.2. The soils respond differently to the early addition of acid, shown by the initial gradients of the curves. Further additions result in similar responses which may indicate a similar buffering mechanism which most likely involves mineral dissolution.

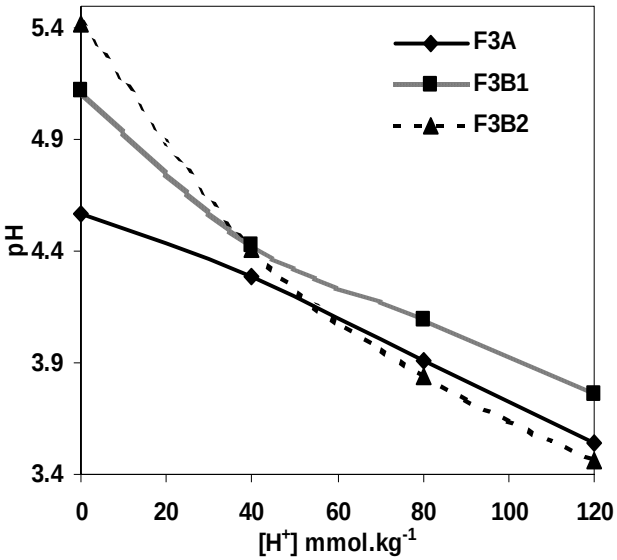

Figure 3.2 Buffer capacity curves (pH vs. added HCl) for the F3A, F3B1 and F3B2 soils, determined in 1M KCl after 24 h equilibration.

As expected, the A horizon shows the smallest pH deviation (lowest slope) with added acidity which is probably attributable to the buffer capacity of organic matter sequestering protons and releasing basic cations into solution. The buffer capacity decreases with depth, the B2 horizon being very poorly buffered, showing the greatest change in pH with added acidity (Fig. 3.2).

Figure 3.3 shows the Al, Mn and Fe release in the acidified solutions used in the determination of the buffer capacity (shown in Figure 3.2). Aluminium and Mn appear to have a similar release pattern in response to added acidity although the absolute amount of Al released is much higher than that of Mn. The Fe release appears somewhat anomalous and will be addressed later. Metal release in the A horizon with the unacidified KCl solution probably indicates the release of exchangeable metals associated with the organic fraction. The initial increment of acid added results in little change in the quantity of metal released in the topsoil in accord with its' higher buffer capacity. Metal release from the B1 and B2 horizons, however, occurs with the first input of acid and probably stems from the dissolution of the mineral phase. Subsequent additions of acid appear to satisfy the buffer capacity of the A horizon, and it too begins to release Mn and Al into solution.

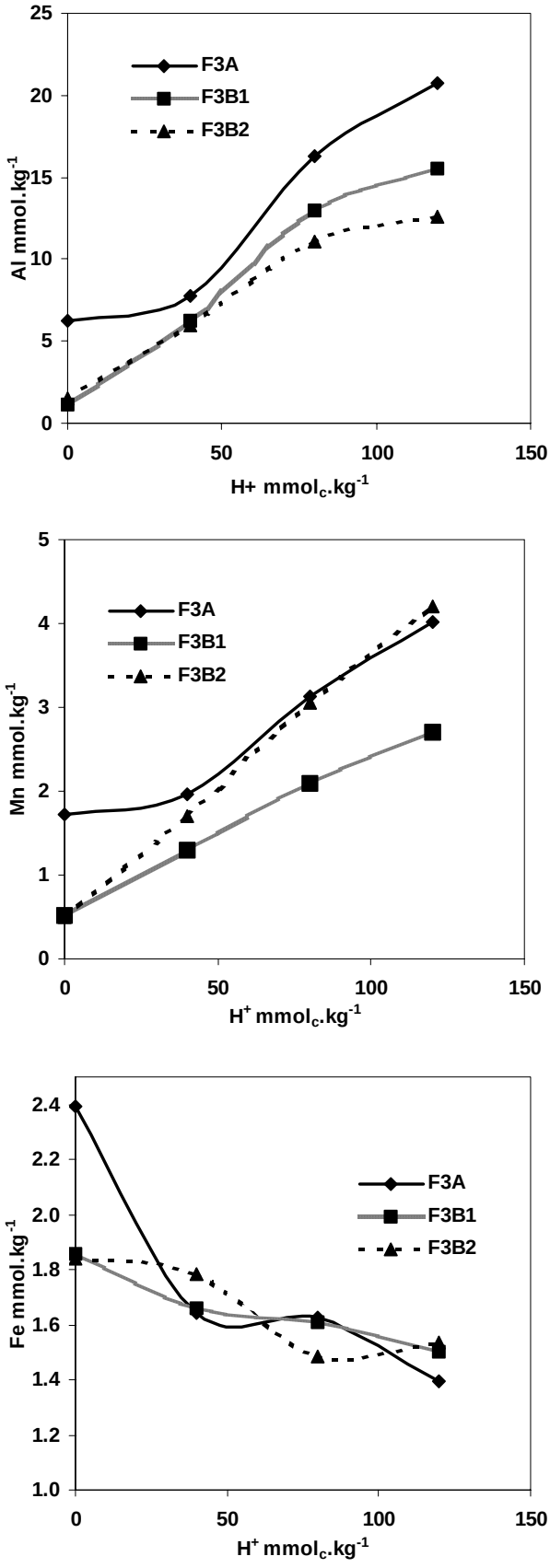

Figure 3.3 Dissolution of Al, Mn and Fe as a function of added acid in 1M KCl suspensions used to determine the buffer capacity in Figure 3.2

From the above it appears that the A horizon retains some buffer capacity by its ability to sequester protons before mineral dissolution begins. The subsoils, however, show minimal buffer capacity and are very sensitive to the addition of acidity with the first increment of acidity resulting in metal release.

The release of Fe shows an anomalous pattern, decreasing with the amount of acidity added (Fig. 3.3). The topsoil shows a higher KCl exchangeable Fe fraction than the subsoils as was the case with Al and Mn. However, the initial addition of acidity results in a decrease in exchangeable Fe for both the top and subsoils. This seems counterintuitive as acidification should result in Fe release according to both reductive and proton-promoted dissolution. Perhaps this result may have occurred due to an artefact arising from the strong KCl electrolyte which may have led to the formation of a Fe-Cl-solid ternary complex on the soil surface. The pzc determination has shown the soils to be at or close to their pzc. Therefore, the addition of acidity would cause the soils to become positively charged thus attracting the negatively charged chloride ions which at high enough concentrations can complex Fe^{3+} ions (Cotton and Wilkinson, 1966) thereby creating a ternary surface complex. Although a very interesting result, the actual quantities of Fe released in response to pH changes are small compared with Al and Mn.

Pectora roborant cultus recti

Metal release data in Figure 3.3 have also been plotted as a function of equilibrium pH in the KCl suspension (Figure 3.4). The Fe release once again shows the anomalous pattern possibly linked to the formation of ternary Fe-Cl-surface complexes discussed above. Manganese and Al show a similar release pattern to each other with the release of both metals as a function of pH increasing noticeably below pH 4.4 (Fig. 3.4). One notable difference between Mn and Al behaviour is the sharper increase in Al dissolution below pH 4.4 in the surface horizon than in the subsoils. This may be due to the combined effect of mineral dissolution together with a contribution from a more stable organically bound fraction of Al. This accelerated increase is not apparent in the Mn released from the topsoil (Fig.3.5) which may be related to the weak outer-sphere bonding of Mn to organic matter (McBride, 1978; McBride 1982) which would render most organically bound Mn exchangeable and therefore less responsive to a lowering of pH.

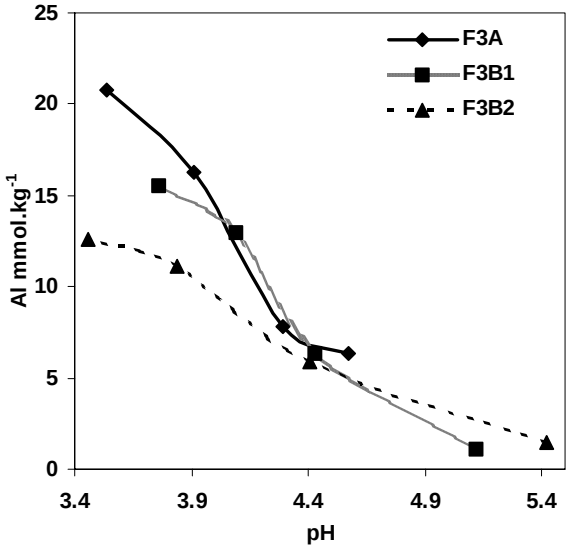

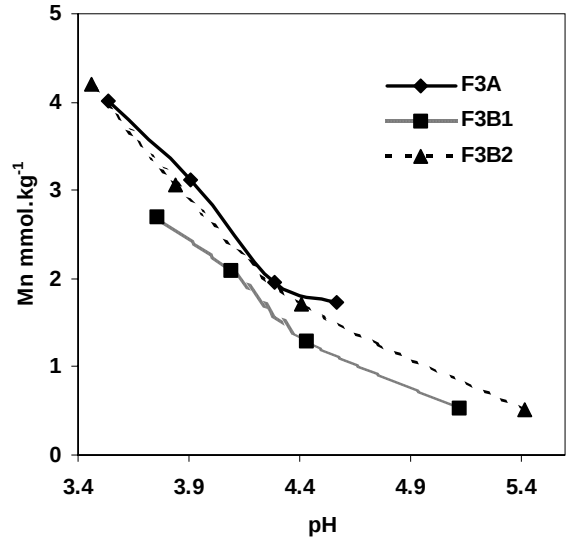

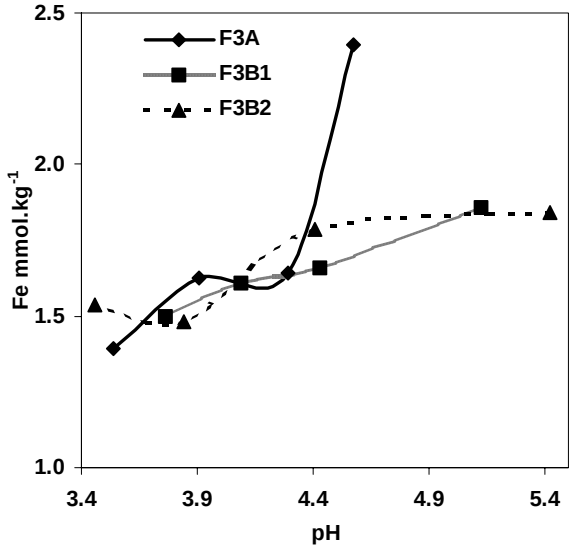

Figure 3.4 Dissolution of Al, Mn and Fe (from Fig. 3.3) as a function of pH after 24 h equilibration, in 1 M KCl suspensions used to determine the buffer capacity in Figure 3.2.

The quantity of Al released by acidification is much larger than that of Mn (Figs. 3.3 and 3.4) which is surprising considering the high Mn oxide content. In the unacidified KCl solutions, representing the exchangeable fraction, only 1.7 $mmol.kg^{-1}$ Mn was released compared to 6.4 $mmol.kg^{-1}$ Al (Fig. 3.3), this may again pertain to the weaker ability of Mn to form organic complexes. It might have been expected, however, that Mn release in the A horizon would increase more substantially with the addition of acidity as findings in the Hawaiian oxisols illustrated that organic ligands and low pH favour Mn release (Vega et al., 1992; Hue et al., 2001).

$$MnO_2 \text{ (solid)} + 4H^+ + 2e^- \leftrightarrow Mn^{2+} + 2H_2O$$

As the above reaction shows, the reduction of Mn oxides should be highly favoured in an acidified A horizon due to the electrons supplied by organic matter. It is clear, however, that this redox reaction is not responsible for the Mn release in the A horizon because the pattern and quantity of Mn release is no greater than in the subsoil horizons (Figs. 3.3 and 3.4). Rather, it appears that Mn released from the top- and subsoils is proton-promoted. A possible reason for the lack of reductive dissolution expected in the topsoil, could be the overwhelming redox poise of the soil due to its extremely high Mn oxide content. Released Mn may be rapidly re-adsorbed (Fendorf et al., 1993a; 1993b) and oxidised by the remaining oxides through autooxidation (Ross and Bartlett, 1981) although the high electrolyte concentration used (1 M KCl) would seriously hinder Mn re-adsorption. Perhaps a more feasible explanation could be that of solid state reduction, whereby electrons are delocalised within the oxide structure without the release of Mn^{2+} (McBride, 1994). Guest et al. (2002) observed a lowering of Mn oxidation state in XANES spectra, after decreasing the soil pH from 7-3, without the release of Mn^{2+} from the structure. They too attributed this to solid state reduction within the Mn oxide structure. Perhaps then, the large body of Mn oxides in the Graskop soils can be imagined as acting like a redox sponge, absorbing electrons and protons, with minimal release of Mn^{2+} until a critical threshold point is reached and large quantities of soluble Mn are released into solution. It is doubtful, however, that such conditions of high electron and proton activity would occur in such well drained oxisols and it appears that the Mn phase in the Graskop soils may be able to resist minor fluctuations in pH and pe without significant Mn release.

3.4 Conclusions

The results of this chapter reinforce the conclusion that the Graskop soils have reached a very advanced stage of weathering, in which the pH of the soil mirrors the point of zero charge. At this stage of weathering most of the buffer capacity is generated through organic matter in the topsoil and through protonation of sesquioxides in the subsoil. The response to additions of acidity, shown in both pH change and metal release, is much larger in the subsoil than in the topsoil, although the initial release of exchangeable metals is greater in the topsoil. Iron release in response to acidification was difficult to quantify due to a possible ternary complex formed between the positively charged oxides and Fe-Cl species in the concentrated KCl electrolyte. Acidification results in similar patterns of Mn and Al release although the absolute amount of Al released is much higher than that of Mn. The release of Mn from the solid phase appears to be surprisingly low, and probably stems from proton-promoted rather than reductive dissolution. Reductive dissolution may have been expected, from observations made in similar soils from Hawaii, as the pH is lowered in the topsoil. Mn release from the Graskop soils, however, was quite modest and heavily overshadowed by the release of Al. The apparent resilience of the Mn oxide phase to low pH conditions could stem from the semi-conductor properties of Mn oxides which may allow electrons to be sequestered in the oxide structure without the release of Mn into solution. The quantity of Al released, on the other hand, showed that toxic levels of Al are far more likely to occur with an onset of soil acidification. It may therefore be concluded that acidification generated through forestry practices may not have as big an impact on Mn release as originally expected, with a possible reason being the same redox poise of the Mn oxides that has made their persistence possible in an environment that is normally conducive to the mobilisation of Mn.

CHAPTER 4

4 The effects of drying on Mn release and speciation

4.1 Introduction

The previous chapter has shown the resilience of the Mn oxide phase of the Graskop soils to acidification and reductive dissolution. Another factor that has aroused interest in the chemistry of Mn oxides in soils is the enhancement of extractable Mn in dried soils compared to soils that remain moist. One of the first to observe this phenomenon were Fujimoto and Sherman (1945) who had noticed that during the hot dry summer months certain plants, grown on some Mn rich soils in Hawaii, showed chlorosis which abated during the wet, cooler winter months. They suggested that this chlorosis may, in part, be the result of increased exchangeable Mn which they observed in soils dried in the lab. Numerous other reports have been made of increased extractable Mn after soils have been dried and stored (Bartlett and James, 1979; Bartlett and James, 1980; Goldberg and Smith, 1984; Berndt, 1988; Haynes and Swift, 1991; Ross et al., 1994; Bunzl et al., 1999; Makino et al., 2000; Ross et al., 2001a). The mechanism of Mn release appears to be reductive in nature as it was established that when soils are air- and oven-dried, the water-soluble and exchangeable fractions of Mn are enhanced at the expense of the easily reducible fraction (Goldberg and Smith, 1984). The reduction of Mn during drying is somewhat hard to conceptualise because drying and oxidation are usually considered synonymous. Drying usually implies the introduction of oxygen into a system thereby increasing the redox potential which should, theoretically, increase the oxidation and thus precipitation of Mn. This is very true of soils and sediments which have experienced anaerobic conditions for extended periods of time. Drying anaerobic soils undoubtedly decreases the solubility of Mn oxides. However, the term drying used here and by previous workers who have noticed this Mn release refers to the drying of moist soils which are already well aerated and oxic (Bartlett and James, 1979 and Ross et al., 2001a).

Another related consequence of drying in soils is the decrease of Cr oxidising capacity. The oxidation of Cr(III) to Cr(VI) in soils was first observed by Bartlett and James (1979). It had not been assumed possible prior to this because analyses had always been conducted on soils dried in the laboratory. The above mentioned workers showed that field moist soils

which contain Mn oxides will readily oxidize Cr(III), but this capacity is rapidly lost after the soils have been air-dried. There are two schools of thought on the diminished Cr oxidising capacity of dried soils. Bartlett and James (1980) attributed the decreased Cr oxidizing capacity to the increase of reducing organics that they observed in extracts from dry soils. These reducible organics would then reduce Cr(VI) as soon as it had formed resulting in no apparent net Cr oxidation. An alternative hypothesis is that of Ross et al. (2001) who, after multiple washing to remove reducing organics, found little recovery of Cr oxidizing capacity from dried soils. They speculated that the Mn(II) released during drying blocks the sites available for Cr(III) bonding and oxidation, as added Mn(II) was shown to do by Ross and Bartlett (1981).

Organic matter has been implicated in playing a role in both the release of Mn and retardation of net Cr oxidation, with drying causing a very noticeable increase in dissolved organic carbon (Bartlett and James 1980; Ross et al., 2001). Further ramification of this comes from the observations of the drying effect being most prominent in topsoils (Makino et al., 2000). It has been proposed that this increased solubilization of organic matter may occur due to the physical rupture of organic molecules rendering them more soluble (Raveh and Avnimelech, 1978). An alternate hypothesis is the protonation of organics, as the clay surface acidifies with drying, which increases the solubility of the organic molecules (Bartlett and James, 1980). This builds on the mechanism, proposed by (Mortland and Raman, 1968), whereby the surface acidity of clay increases as it dries. The source of acidity, according to this mechanism, stems from hydrolysis of the last remaining water layers that surround exchangeable cations. As the water layer becomes increasingly thin the polarization forces of hydrolysing cations, which are usually ‘diluted’ in fully hydrated systems, are concentrated on the remaining water molecules. This results in the water molecules splitting and protons being released adjacent to the clay surface. The nature of the exchangeable cation obviously plays an important role in the generation of surface acidity and it has been shown that strongly polarizing cations, such as Fe^{3+} and Al^{3+} ions, generate a more acidic surface than Ca^{2+} and Mg^{2+} (Mortland and Raman, 1968; Frenkel, 1974). Although most of these workers used model, synthetic systems it is quite likely that these mechanisms can operate in soil environments and the substantial drop in pH at the mineral surface as it dries may be fundamental in understanding the release of Mn from dried soils.

Storage time and heating of soils have been shown to be paramount in both Mn release and degree of Cr oxidation (Bartlett and James, 1979, Bartlett and James, 1980; Berndt, 1988; Ross et al., 2001). The individual role of storage time and heating is hard to assess because they both result in soil dehydration. The general consensus is that dehydration is responsible for the chemical transformation (Fujimoto and Sherman, 1945; Bartlett and James, 1980; Makino et al. 2000, Haynes and Swift, 1991) and heating obviously enhances the degree of dehydration. Bartlett and James (1980) stated that heating a soil to 105^{o}C released an equivalent amount of Mn as air-drying the soil for 2 months. Berndt (1988) showed that soils oven-dried at 60^{o}C released more Mn than soils air-dried at 28^{o}C which in turn released more than the field moist soils and Ross et al. (2001) showed a linear trend in the amount of Mn released with air-drying time. Thus it is clear that the extent of dehydration plays an important role, and whether heating has an effect on its own is yet to be determined.

Most reports of enhanced extractable Mn have been made after soils have been dried and stored in the laboratory (Bartlett and James, 1979; Bartlett and James, 1980; Haynes and Swift, 1991; Ross et al., 1994; Bunzl et al., 1999; Ross et al., 2001). Air-drying a small quantity of soil on a lab bench may allow a degree of desiccation much greater than would be expected in a dry soil profile and thus extrapolation to field conditions may be difficult. Reports have been made, however, that exchangeable Mn released with soil drying is observed in surface soils of warmer climatic zones (Makino et al., 2000) and may even be responsible for poor plant responses (Fujimoto and Sherman, 1945). The manganiferous Graskop soils are located on the eastern escarpment which receives a high rainfall, although that rainfall is confined to the summer months with a long dry period during winter and early spring in which surface soils may dry out substantially. Yellowing of pine trees has been observed towards the end of the dry season (F. Ellis, pers. comm.) which has previously been attributed to drought stress. This chlorosis could also, however, be an indicator of Mn toxicity related to the increased Mn release from dry soils. *Veld* fires are a common occurrence in the dry grasslands in late winter. These fires could cause extensive heating and drying in the top few centimetres of soil, which could be an important factor in mobilising Mn in the natural grassland area.

From the above discussion it appears that there are still many uncertainties surrounding the mechanism of Mn release in soils. The Graskop soils with their high Mn oxide content may

be substantially affected by this drying phenomenon and it is an important consideration when assessing the stability of the Mn phase. In this chapter the effect of soil drying on Mn release was investigated. To achieve this, soils were dried by various means, and sometimes the soils were exposed to extreme desiccation which would exaggerate the effect and be unrealistic in extrapolation to field conditions. It was hoped, however, that by studying the effects of drying on such Mn rich soils, insight may be gained into possible mechanisms involved. In order to achieve this, various redox tests were conducted together with various spectroscopic techniques including x-ray at near edge structure (XANES) spectroscopy and attenuated total reflectance Fourier transform infrared (ATR-FTIR) spectroscopy. This latter technique will be dealt with in Chapter 5.

4.2 Materials and methods

Soils from the F3 profile were used in the redox as well as XANES experiments, while topsoils from the F2, F4 and F5 profiles were used for the extraction of organically bound metals. All these soils had been stored in air-tight containers to preserve their original moisture content. Periodic Net Cr tests (Bartlett and James, 1979) have shown that storage of these soils did not change their redox properties. The moisture content of the soils was measured and all subsequent reported mass refers to oven-dry mass (after drying to 105^{o}C).

Pectora roborant cultus recti

4.2.1 Extractable Mn

Extractable Mn was determined on soils at various stages of desiccation. Soils from the A, B1 and B2 horizon were oven-dried overnight at 40 and 80^{o}C. Extractable Mn was determined on the dried and moist samples by shaking the soils for 30 min in 0.5 M $CaCl_2$ (soil: solution ratio 1:20). Subsamples from the A horizon were allowed to dry in the dark for 7 days at 25^{o}C. Each day samples were analysed for gravimetric water content and exchangeable Mn using the above-mentioned method. All Mn concentrations were expressed on a dry weight basis.

Exchangeable Mn released from moist soils in response to acidification was measured in 0.5 M $CaCl_2$ after equilibrating separate suspensions (1:20 soil solution ratio) with 0.2, 0.4 and 0.6 ml 0.01 M HCl. After equilibration for 24 hrs the pH of the suspensions was

measured using a Metrohm 744 pH meter and Mn concentration in the extract was determined.

Organically bound Mn and Fe were determined by washing 1 g soil with 20 ml, pH 5, 0.05 M Na-pyrophosphate ($Na_4P_2O_7$). Exchangeable Mn and Al were determined in 1 M KCl (1:10 soil solution ratio shaken for 30 min) using moist soils and soils that had been air-dried for 4 days at room temperature.

All suspensions were centrifuged at 2000 rpm and extract analysis was performed with a Varian Spectra AA spectrometer. All metal concentrations were expressed on a dry weight basis.

4.2.2 Redox experiments

The change in oxidative capacity of dried and moist soils was investigated using a range of redox tests. Sub-samples from the A, B1 and B2 horizon were placed in the oven overnight at 40^{o}C and these, together with equivalent quantities of moist soil, were used in the redox experiments. A Net Cr test, as described by Bartlett (1999), was performed on the soils without modification, briefly, 20 ml, 0.001 M $CrCl_3$ solution was added to 0.5 g soil and shaken for 15 min. After centrifugation, supernatants were tested for Cr(VI) colorimetrically, using diphenylcarbazide as an indicator. The manganese electron demand (MED), as described by Bartlett (1999), was measured on the samples but because of the high Mn content of the soils, the reagents had to be more concentrated to prevent sublimation of I_2. Briefly, 0.5 g soil was shaken for 1 hr with 10 ml iodide solution (0.5 M KI and 0.5 M, pH 4, NH_4OAc). A 0.01 M $Na_2S_2O_3$ solution was used for the iodine-iodide titration using soluble starch as an indicator.

To determine the oxidation state of the Mn released in response to drying the soils were washed with pH 5, Na-pyrophosphate solution. It was hoped that Na-pyrophosphate would stabilize any Mn(III) present in the exchangeable or organically bound fraction. To ensure Na-pyrophosphate did not result in oxidation of Mn(II), 2 ml 0.001 M $MnSO_4$ solution was added to 10 ml, pH 5, 0.05 M Na-pyrophosphate solution and the oxidation state analysis (described below) was performed. No oxidation of I^- occurred so it was assumed that oxidation of Mn(II) to Mn(III) by Na-pyrophosphate at pH 5 is negligible.

The oxidation state of the Na-pyrophosphate extract was determined as follows: 0.5 g of oven dried (40^{o}C) soil and an equivalent mass of moist soil from the A, B1 and B2 horizons were washed with 10 ml 0.05 M Na-pyrophosphate (pH 5) for 30 min. The suspensions were centrifuged and the extract analysed for oxidizing capacity using the method of Murray et al. (1984). Briefly, 1 ml Na-iodide solution (8 M NaI + 8 M NaOH) was acidified using 2 ml 10 M H_2SO_4; 1 ml of the Na-pyrophosphate extract was added and titrated to a colourless endpoint using 0.001 M $Na_2S_2O_3$ and soluble starch as an indicator. Manganese and Fe concentrations were determined in the Na-pyrophosphate extract using AA spectroscopy. The O/Mn ration was calculated using the formulae given by Murray et al. (1984).

To further investigate some of the changes that occurred in the organic-rich horizons, topsoils from all four profiles (F2A, F3A, F4A and F5A) were dried at 40^{o}C and together with field-most samples washed in Na-pyrophosphate as described above. The redox status of these extracts was determined using tetramethylbenzidine (TMB). The TMB solution was prepared as described by Bartlett (1999), 0.5 ml TMB was added to 3 ml of extract from field moist and dried soils and the colour changes observed. The Cr reducing capacity of these extracts was examined using a method similar to the one described by Bartlett (1999). Briefly, 1 ml of extract was placed in a cuvette and 0.1 ml of Cr(VI) solution (5 x 10^{-4} M $K_2Cr_2O_7$ made up in pH 4, 0.6 M NH_4OAc) added, the volume was made up to 6 ml with deionised water and 0.5 ml diphenylcarbazide indicator added. The concentration of Cr(VI) was determined colorimetrically using absorbance at 540 nm.

4.2.3 XANES experiments

X-ray absorption at near-edge structure spectroscopy was performed at beam line X11A, National Synchrotron Light Source, Brookhaven National Laboratory, Upton, NY. This is a bulk XAS beam line and while usually not suitable for analysis of whole soils, the high Mn content of the Graskop soils allowed clean spectra to be obtained. Multiple scans showed no decrease in intensity or peak shifts so it was assumed beam-induced reduction was negligible (Ross et al., 2001b).

High resolution spectra were obtained of the XANES region using a 0.5 eV step size. All spectra were normalized with respect to the position of the pre-edge feature at 6.539 KeV. Data analysis was done using WinXAS software.

Soils and solid standards were diluted with boron nitride. The concentrations of aqueous and solid samples placed in sample holders were calculated using McMaster values. Samples and standards were mounted in X-ray transparent sample cups. Non-sticky Mylar tape was placed between the sample and the, X-ray transparent, Kapton® tape to prevent any reduction of Mn by the adhesive resin whilst the sample was in the beam.

Five oxidation state standards were used. An aqueous $MnSO_4$ solution was prepared for the Mn(II) standard; aqueous Mn-pyrophosphate, as prepared by Bartlett and Ross (1988), and manganite (γ–MnOOH) (Wards) were used as Mn(III) standards. Synthetic K-birnessite and colloidal MnO_2, synthesized by the method of Perez-Benito et al. (1996), were used as Mn(IV) standards.

Elemental compositions of the soils, determined by XRF (Chapter 1), were used in a McMaster calculation to determine the amount of soil placed in the sample holder. Scans were run on field moist soil as well as soils dried in the oven overnight at 80°C.

Pectora roborant cultus recti

4.3 Results

4.3.1 Extractable Mn

The manganese released after drying the soils from the A, B1 and B2 horizons at 40 and 80°C is shown in Figure 4.1a. In the A horizon drying results in a dramatic increase in exchangeable Mn, with a 10-fold increase after drying at 40°C and 20-fold increase after drying at 80°C. The B1 and B2 horizons are much less affected by the drying treatments, which suggests that organic matter may be playing a role in the release of Mn from the A horizon. As a comparison the effect of added acidity on Mn release is shown in Figure 4.1b. Added acidity increases the Mn release in all horizons. For the A horizon, however, drying has a much larger effect on Mn release, while the subsoils show the opposite effect.

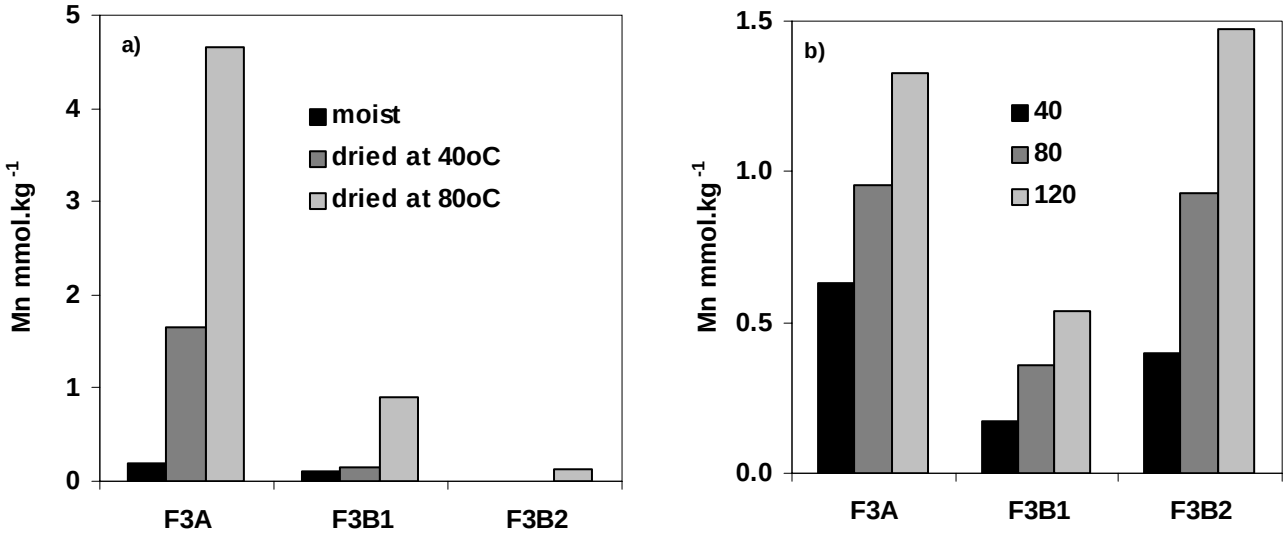

Figure 4.1 Exchangeable Mn extracted a) with 0.5 M $CaCl_2$ solution (1:20 soil solution ratio) from moist, and oven-dried soil at 40 and 80°C, b) with 0.5 M $CaCl_2$ after additions of HCl having the equivalent acidity of 40, 80 and 120 $mmol_c kg^{-1}$

The Mn and Fe concentrations extracted from moist and oven-dried (40°C) soils using Na-pyrophosphate are shown in Figure 4.2. The most striking feature of these data is the amount of metals extracted by pyrophosphate even while moist.

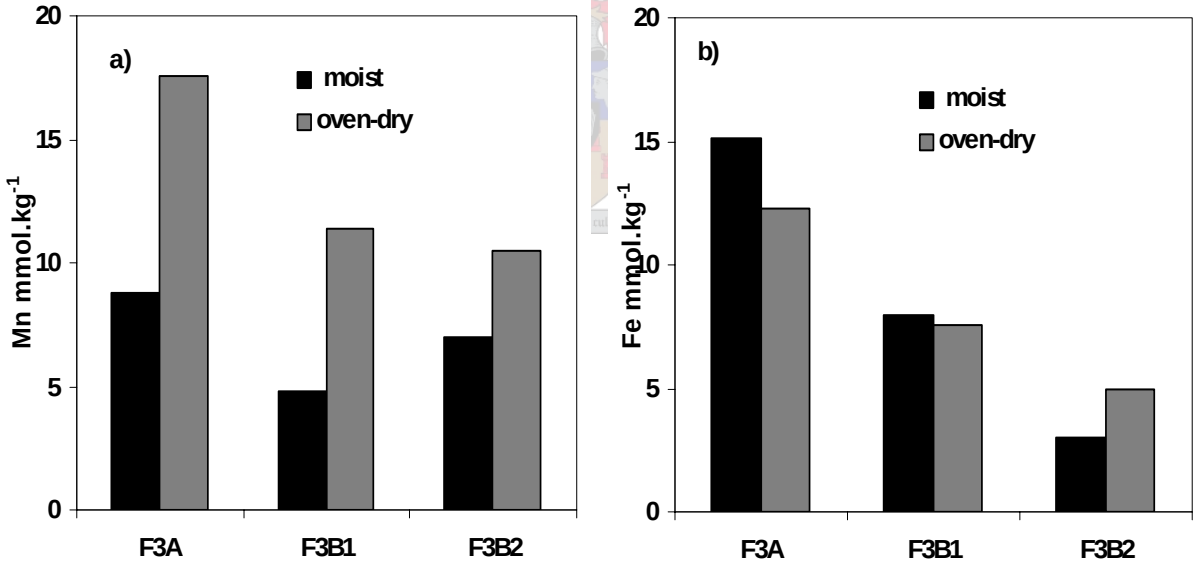

Figure 4.2 Concentrations of a) Mn and b) Fe in moist and oven-dried (40° C) soils extracted with 0.05 M, pH 5, Na-pyrophosphate (1:20 soil solution ratio).

Sodium-pyrophosphate is generally used to extract organically-bound metals (Iu et al., 1981), but certain complications arise due to dispersion and peptization (Loeppert and Inskeep, 1996). With this in mind it may make more sense to compare the relative metal concentration in extracts from moist and dried samples which were treated equally. The pH of the Na-pyrophosphate extract was kept similar to the soil pH (pH 5) in an attempt to

minimise pH related changes. The lower pH would also reduce the amount of clay dispersion reported for pH 10 Na-pyrophosphate.

The moist samples from the A horizon show higher pyrophosphate extractable Fe than Mn (Fig. 4.2). This could be indicative of the weak association Mn has with organic matter (McBride, 1978). The dry samples show a distinct increase in Mn while Fe shows no significant change. Once again the drying induced increase of Mn release is the most pronounced in the A horizon with the relative increase decreasing with depth. Extracts from four topsoils show similar trends in Fe and Mn release (Fig. B.1 Appendix B).

To assess the effect drying has on Al release, soils were air-dried at room temperature for 7 days, exchangeable Mn and Al were then measured in KCl extracts and compared with extracts taken from moist samples. The results are shown in Figure 4.3.

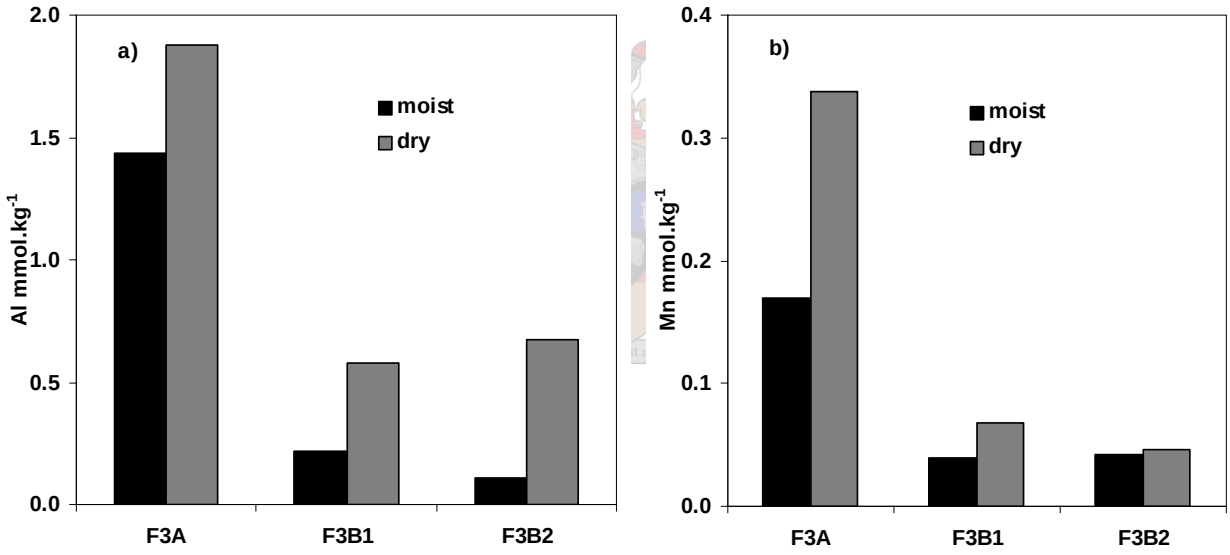

Figure 4.3 Extractable a) Al and b) Mn from moist and air-dried (7 days at 25°C) soils using 1M KCl (1:10 soil solution ratio).

Manganese once again shows the same response to drying and it appears that exchangeable Al also increases after drying. Similar results were obtained for the F4 profile (Fig. B.2 Appendix B). What is interesting is that drying causes a greater increase in Al release in the subsoils than in the topsoils. This could be a result of the decrease in pH of a drying surface, as will be shown in Chapter 5. The fact that the subsoils are more affected by drying with respect to Al release and the topsoil more affected with respect to Mn release may indicate that some factor other than or additional to pH is involved in controlling Mn release.

4.3.2 Redox status of dried soils

The reduction of Cr oxidising capacity accompanying soil drying has been frequently reported (Bartlett and James, 1979; Bartlett and James, 1980; Ross et al., 2001). To determine how the release of Mn relates to the decrease in Cr oxidising capacity subsamples from the A horizon were air-dried at room temperature for 7 days. Subsamples were removed each day and gravimetric water content, exchangeable Mn and Cr oxidizing capacity determined. The results are shown in Figure 4.4

Figure 4.4a shows Cr oxidation and Mn release as a function of gravimetric water content. The water content appears to decrease to 3% and then reach equilibrium. However, Mn release and Cr oxidation continue to change.

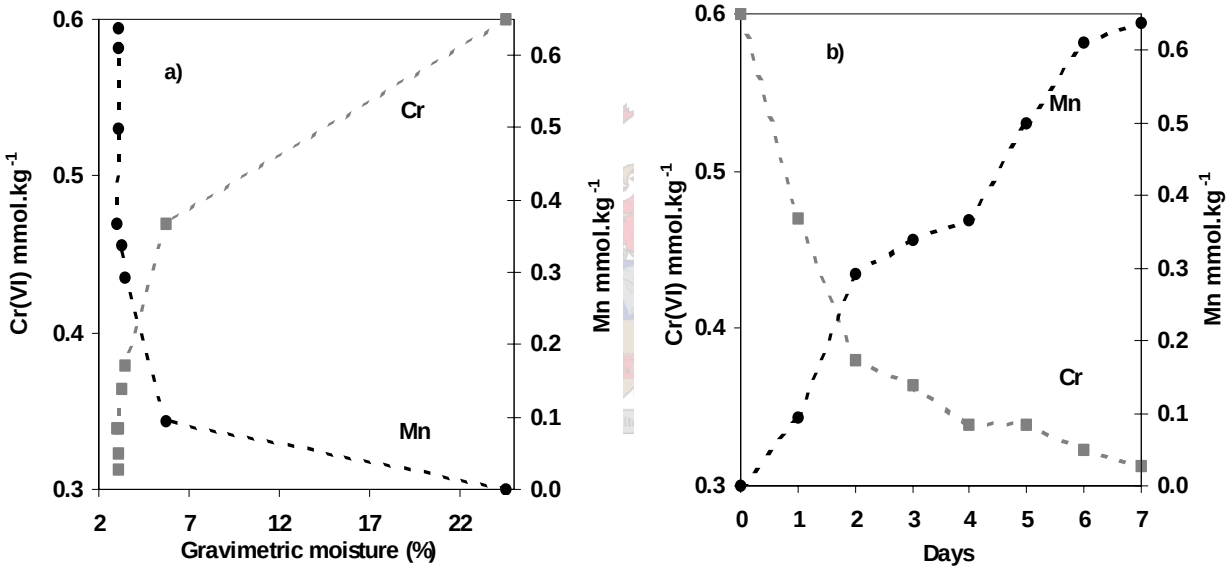

Figure 4.4 Manganese release and net Cr oxidized for soils dried at 25°C as a function of a) gravimetric moisture content and b) time.

The increase in Mn release with time shows a linear trend, while the decline of the Cr oxidation capacity is curvilinear. This trend was also observed by Ross et al. (2001a) who air-dried soils for 260 days. The data from their study as well as the present data suggest that the loss of Cr oxidising capacity is more sensitive to drying is the release of exchangeable Mn.

The effects of drying on net Cr oxidation and manganese electron demand (MED) were compared for soils of the F3 profile (Fig. 4.5). It is evident that in the moist soils, Cr oxidising capacity increases down the profile (Fig. 4.5a), which is understandable considering that any Cr(VI) measured is the net result of the Cr(III) oxidised by Mn oxides and the Cr(VI) reduced by organic matter (Bartlett and James, 1994).

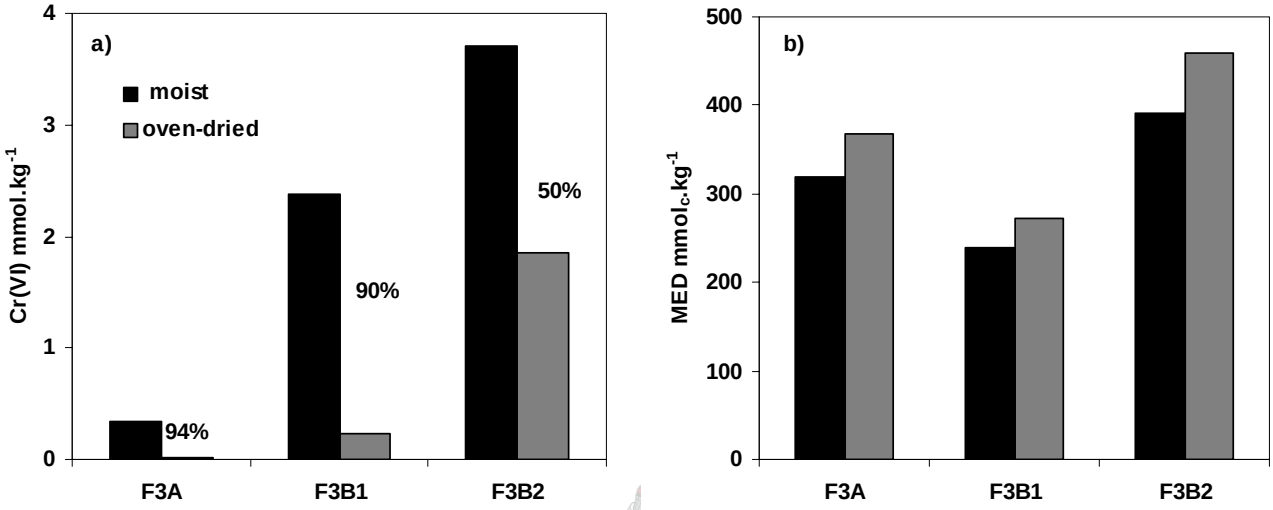

Figure 4.5 Redox tests performed on moist and oven-dried (40°C) soil showing a) net Cr oxidising capacity and b) manganese electron demand (MED).

Figure 4.6 shows Cr oxidizing capacity as a function of organic carbon and total Mn content. It appears from this that Cr oxidising capacity is more influenced by the decrease of organic carbon content than the total Mn in the soils

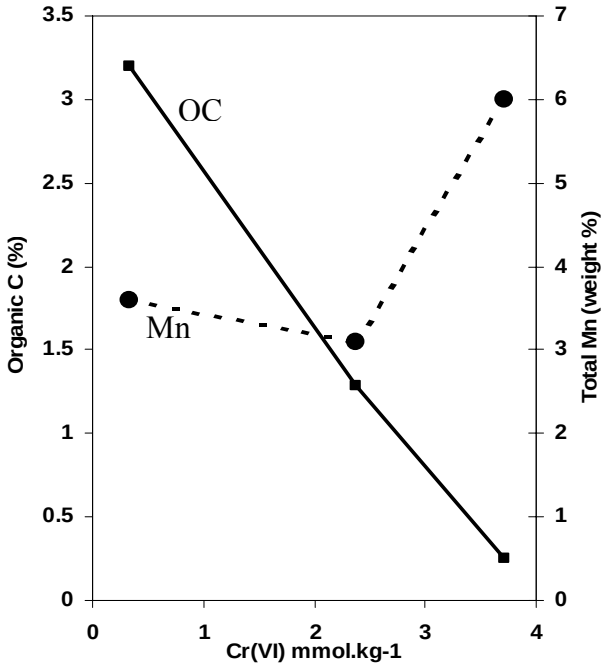

Figure 4.6 Cr oxidising capacity as a function of organic C and Mn both in weight %.

The Cr oxidizing capacity was profoundly influenced by soil desiccation with the A horizon suffering 94% loss of its original capacity (Fig. 4.5a). The B1 and B2 horizons show a similar decrease in Cr oxidation, with the magnitude of decline decreasing down the soil profile. The manganese electron demand (MED), as shown in Figure 4.5b, exhibits a very slight increase in I^- oxidation when the soils are dried. Similar results were obtained for soils in the F4 profile (Fig. B.3 Appendix B). Previous workers have not investigated the effects of drying on the MED and the current results appear contradictory, unless it is only the reducing capacity which is influenced by drying. This does not, however, explain the enhanced Mn release except if the released Mn is in fact not solely divalent.

To examine the oxidation state of the extractable Mn, oven-dried soils were washed with pH 5, Na-pyrophosphate. Sodium-pyrophosphate is generally used to extract organically bound metals (Iu et al., 1981). If trivalent Mn is present in soils it is most likely to be found complexed with organic ligands, thus using Na-pyrophosphate would serve the dual purpose of extracting and stabilizing any Mn(III). A potential problem with pyrophosphate, if present in sufficient concentrations, is its ability to complex and solublize Mn(III) from minerals containing trivalent Mn (Klewicki and Morgan, 1999). Further, oxidation of Mn^{2+} to Mn^{3+} may be initiated by the high pH (~10) of Na-pyrophosphate. To circumvent these problems the pH of the Na-pyrophosphate was adjusted to 5 and the concentration was kept low (0.05 M). At this pH no oxidation of added Mn^{2+} was observed in the pyrophosphate solution. If the pyrophosphate were to dissolve structural Mn(III), it would affect the moist and the dry samples equally so it was assumed any change observed in the pyrophosphate extract would be drying-induced.

Moist and oven-dried (40^{o}C) soils from the F3 profile were washed in Na-pyrophosphate and the oxidation state of the extract determined iodometrically. The results are shown in Table 4.1. The oxidation state of the moist soil extracts shows an O/Mn ratio of 0.8 for the A and B1 samples and 1.3 for the B2 sample (Table 4.1). The fact that the ratio is lower than unity can most likely be attributed to the overestimation of active Fe which was measured in the Na-pyrophosphate extract and included in the equation used to determine oxidation state (Murray, 1984). Drying results in a significant increase in O/Mn ratio for the A and B1 samples (Table 4.1). It appears then that in the A and B1 samples there is not only a change in the quantity of Mn released but perhaps also a change in the oxidation

state of the released Mn. The B2 sample shows an interesting result, with the oxidation state being greater than unity and unaltered by drying (Table 4.1). The extracts from both wet and dry soils were a light pink colour which is indicative of Mn(III)-pyrophosphate complexes (Bartlett and Ross, 1988). It is likely that the pyrophosphate extracted some Mn(III) present in the mineral phase. However, the higher oxidation state was consistent for the moist and dried samples, which suggests that the subsoil is less affected by drying. This concurs with much of the above data and further implies involvement of humic substances.

Table 4.1 Oxidation state of the pH 5, Na-pyrophosphate extracts, measured iodometrically

	O/Mn ratio	
	Moist	Dried
F3A	0.8	1.2
F3B1	0.8	1.2
F3B2	1.3	1.3

In the light of the most dramatic changes occurring in the A horizon, the oxidising capacity and free radical content of Na-pyrophosphate extracts from the four A horizons (F2A, F3A, F4A and F5A) were investigated. This was achieved using redox sensitive tetramethylbezidine (TMB) and the UV absorbance of the pyrophosphate extracts.

Tetramethylbezidine can be used as an electron transfer indicator because its final two-electron oxidation product has a different colour to its one-electron intermediate product. This has formed the basis of the TMB test for free radicals described by Bartlett (1988). During the oxidation of TMB a diamine is oxidized to a diimine (yellow product) by losing two electrons (Josephy et al., 1982). During this oxidation a charge transfer product forms which is blue in colour. This charge transfer product involves a π-π electron transfer between the diamine reagent and the diimine product. A second, intermediate, yellow free radical molecule can form which is distinctly different to the charge transfer complex but also indicates a one-electron transfer. This free radical molecule is in equilibrium with the charge transfer complex (Josephy et al., 1982). In a study of TMB sorbed onto hectorite (McBride, 1985) it was observed that at lower loadings of TMB, the diimine was the major product and increasing the loading resulted in a green colour developing, indicating a

mixture of the yellow diimine product and the blue charge-transfer complex which suggests that the higher the loading the less complete the oxidation. Bartlett (1988) has suggested that the colour sequence of TMB added to soils can be used to grade soils in oxidative potential. He suggests that it is the Mn(III) ion which oxidizes the TMB, through the one electron charge-transfer complex, to the yellow diimine product. If solely Mn(IV) is present the blue colour develops slowly because time is needed to produce the Mn(III) ions which can then react with the TMB. If an intense blue colour forms immediately on addition of TMB to the soil it means the Mn(III) ion is already present and if it is in excess it will oxidize the TMB all the way to the yellow diimine product. When an equivalent volume of TMB solution was added to the extracts from the moist and dry samples, the extracts from the moist soil turned blue-green while the extracts from the dry soil turned yellow immediately. This suggests that the moist soil extract, although having some oxidizing capacity, could not fully oxidize the diamine to the diimine, while the extract of the dry soil could complete that oxidation. These results, together with the oxidation state analysis, suggest that release of Mn from dried soils may be more complex than originally thought and there may be an involvement of Mn(III) in the dissolution reactions.

The redox behaviour of the Na-pyrophosphate extracts was further investigated by determining the Cr reducing capacity of the extracts. The results are shown in Table 4.2. These values represent the amount of Cr(VI) that is reduced after a known concentration of Cr(VI) was reacted with the Na-pyrophosphate extracts. The extracts from the dry soils show a marked increase in Cr reduction, compared to the moist soil extracts, which points towards an increased concentration of reducible organic substances. It is interesting to note that there is a direct correlation between the concentration of Mn and Cr reducing capacity in the dry soil extracts (Table 4.2).

Table 4.2 E_4/E_6 ratios and Cr(VI) reducing capacities determined on pH 5, 0.05 M Na-pyrophosphate extracts from moist and dried (40°C for 24 hrs) subsamples taken from the A horizons of the F2, F3, F4 and F5 profiles.

	E_4/E_6 ratio		Cr(VI) reducing capacity mmol.kg^{-1}		Extractable Mn mmol.kg^{-1}	
	Moist	Dry	Moist	Dry	Moist	Dry
F2A	6.3	6.7	0.2	0.8	13.3	24.0
F3A	6.2	6.6	0.2	0.6	10.2	20.5
F4A	7.0	7.4	0.01	0.4	5.5	15.3
F5A	5.8	7.0	0.01	0.2	2.0	7.3

Information about the nature of the organic substances extracted with the Na-pyrophosphate was obtained using light absorbance in the visible region. It has been shown that the free radical content, molecular mass and degree of aromatic carbon condensation can be obtained from the UV absorbance of organic matter extracts at certain wavelengths (Chen et al., 1977). The so-called E_4/E_6 ratio is the ratio of UV absorbance values measured at 460 and 660 nm in either a $NaHCO_3$ or Na-pyrophosphate extract (Chen et al., 1977; Schnitzer and Levesque, 1979). The E_4/E_6 ratios were measured in the Na-pyrophosphate extracts of the field-moist and air-dried topsoils. The optimum pH for determining the E_4/E_6 has been shown to be between 7 and 8 (Chen et al., 1977), but it was hoped that more information could be gathered on the pH 5, Na-pyrophosphate extracts used in the above experiments. As can be seen from Table 4.2, the E_4/E_6 ratio increases in the extracts of the dried soils. This may show tentative evidence that the free radical content of the organic matter has increased during drying. It does, however, indicate that there is a change in the nature of the soluble organic fraction which was also observed by Bartlett and James (1980) and Ross et al. (2001a).

The data obtained from the analysis of Na-pyrophosphate extracts seems contradictory. Comparing the Na-pyrophosphate extracts from moist and dried soils, it appears that drying increases the oxidation state slightly as well as the TMB oxidising capacity but at the same time enhances Cr(VI) reducing capacity. To gain further insight into changes in oxidation state, x-ray absorption spectroscopy was employed using the near-edge energy region to track oxidation state changes.

4.3.3 XANES analysis

An attempt was made to characterise the redox changes that occur with drying. X-ray absorption at near-edge structure (XANES) analysis was performed on oven-dried (50^{o}C) and moist samples. Unfortunately, only a bulk XAS beam line was available and so only the average oxidation state in the bulk soil could be evaluated.

Oxidation state standards used for the XANES investigation are shown in Figure 4.7. The values for the main-edge energies are in good accord with previous work (Schulze et al., 1995; Ross et al., 2001a; Guest et al., 2002).

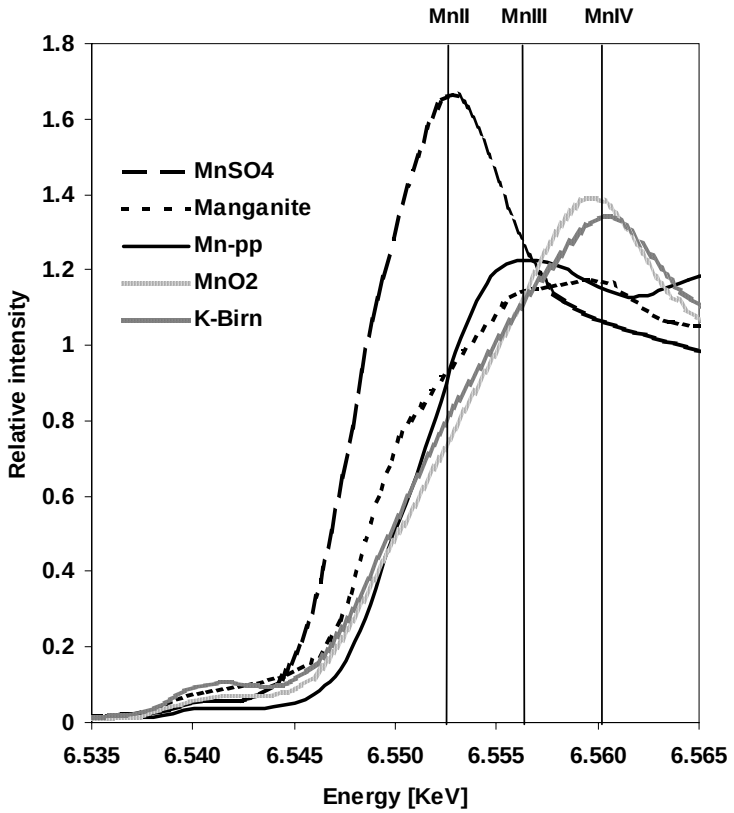

Figure 4.7 XANES spectra of Mn oxidation state standards normalized to the pre-edge feature at 6.539 KeV.

The main-edge for Mn(II) in $MnSO_4$ is at 6.553 KeV; for Mn(III), in Mn-pyrophosphate and manganite, at 6.556 KeV and for Mn(IV), in K-birnessite and polymeric MnO_2, at 6.560 KeV. The spectra of manganite and K-birnessite have a shoulder in the lower energy region which is most likely attributable to a fraction of Mn(II) in the mineral structure. However, the major absorption peaks are in good accord with the other standards. The polymeric MnO_2 shows a slightly lower energy edge than the K-birnessite which may indicate that K-birnessite has a higher Mn(IV) content than the polymeric MnO_2. It is evident from Figure 4.7 that the edge energy increases with oxidation state, with the difference in energy of Mn(II) and Mn(IV) being 7 eV.

The XANES spectra of the moist and oven-dried samples from the F3A and F3B1 horizons are shown in Figure 4.8. Each spectrum represents the arithmetic mean of 3 scans. The main-edge for the moist samples lies at 6.560 KeV, corresponding to the edge energy of Mn(IV) in the K-birnessite and MnO_2 standards. The spectra of the dry samples show a similar pattern but there is a visible spectral shift compared to the moist samples, especially evident in the linear portion of the edge (Fig 4.8). Stueben et al. (2004) used the near-edge region to calculate energy shifts, with a shift to lower energies representing a shift to lower oxidation states. Ross et al. (2001a) used the energies at 0.5 relative intensity to calculate shifts in XANES spectra and obtained a shift of 1.5 eV between a moist soil and a soil dried for an extended period of time. The shift between the moist and dry F3A sample at 0.5 relative intensity is 0.54 eV and an even smaller shift was observed for F3B1. Although small, these shifts are meaningful when it is considered that only 7 eV separates Mn(II) from Mn(IV), and the spectra were obtained on a bulk XAS beam line which measures average oxidation state throughout the sample. Thus to get a visible shift using bulk XAS the change in oxidation state needs to be significant.

Attempts to fit a linear combination of standards to the sample spectra was unsuccessful because the error involved with the linear fit was greater than the difference between the sample spectra. This seriously limits the amount of information that can be extracted from the XANES data. The shift to lower energies does indicate, however, that that the overall oxidation state of the Mn oxides has decreased and the fact that this was observed on a bulk XAS beam line indicates that the change was substantial.

Unfortunately, the XANES results cannot be used to confirm the formation of Mn(III). The micro-XANES study by Ross et al. (2001a), however, shows some more meaningful results. Firstly, it was noted that only samples that had been stored for an extended period of time showed any significant energy shift. Secondly, the spectrum that resulted from the long-term drying was most satisfactorily fitted when a contribution of 40-50% manganite was used in the linear combination fit. The authors commented that this proportion of manganite was very high. However, it may be realistic considering the above evidence for Mn(III) participation in the drying reactions.

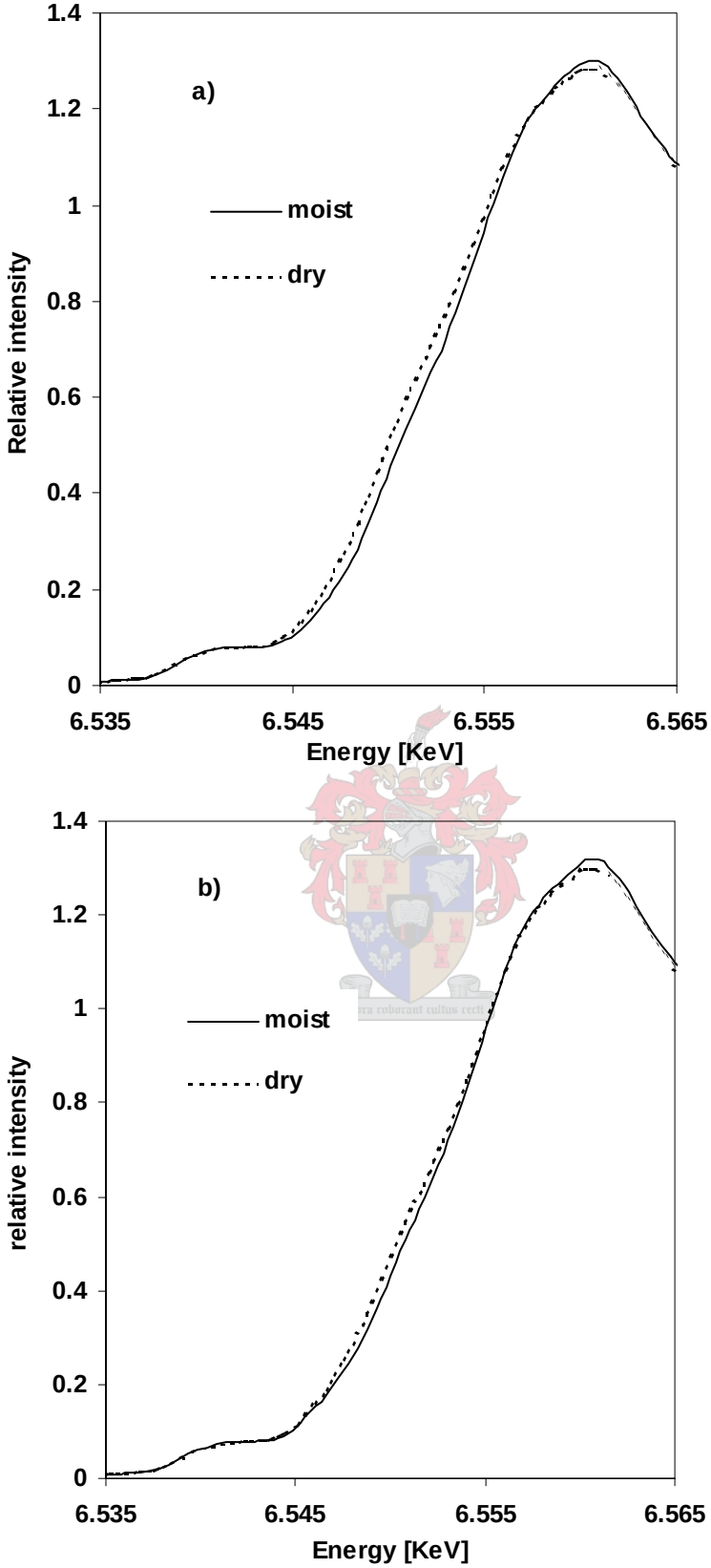

Figure 4.8 XANES spectra comparing moist and oven-dried (50°C) samples for a)F3A and b) F3B1.

4.4 Discussion

The results presented above show that the chemical changes which accompany drying are complex. It has been shown that drying has the greatest effect on the A horizon and least effect on the deeper subsoil. In the topsoil drying markedly enhances the exchangeable Mn fraction and decreases the Cr oxidising capacity of the soil. Little change is observed, however, in the manganese electron demand. This seemly contradictory redox behaviour of dried soils may provide clues to some of the chemical changes that occur during drying. The Cr test is sensitive to reduction by organic substances while the MED only measures oxidising capacity (Bartlett, 1988). It would seem apparent then that drying has its effect in increasing the reducing capacity rather than decreasing the oxidising capacity. This supports the view of Bartlett and James (1980) who suggested that the loss of Cr oxidizing capacity in dried soils stemmed from the increase in concentration of soluble organic compounds. It does not, however, rule out the hypothesis of Ross et al. (2001) that the reduced Mn(II) ions block the sites for Cr bonding and oxidation, because I^- , used in the MED determination, is an anion and would bind to sites different to those binding Cr^{3+}.

An apparent paradox is the small effect which drying has on the MED, although there is a dramatic increase in exchangeable Mn. This may require us to reassess the assumption that the exchangeable Mn is divalent. Bartlett (1988) conducted a study which investigated reduction of soil Cr oxidising capacity after Mn^{2+} and citrate were added, in combination and as separate treatments, to a soil containing Mn oxides. Independent additions of citrate and Mn^{2+} both resulted in a decrease of net Cr oxidation, but the greatest decrease was observed when citrate and Mn^{2+} were added to the soil in conjunction. The MED was largely unaffected by the treatments suggesting that a change in reducing capacity was involved. It was suggested that the addition of Mn^{2+} and citrate in combination resulted in reverse disproportionation of Mn via the reaction:

$$MnO_2 + Mn^{2+} + 3(COOH)_2 \rightarrow 2Mn(COO)_3 + 2H_2O + 2H^+ \quad [1]$$

Usually, Mn(III) is highly unstable in solution and rapidly undergoes disproportionation following the equation:

$$2Mn^{3+} + 2H_2O \rightarrow MnO_2 + Mn^{2+} + 4H^+ \quad [2]$$

in which a Mn(III) ion either accepts an electron or donates an electron, with the forward reaction being thermodynamically spontaneous (log K = +9.1; Bartlett, 1999). However, reaction (1) can occur spontaneously through the formation of a Mn(III)-citrate complex (Bartlett, 1988). These Mn(III)-citrate complexes then act as strong reducing agents which reduce Cr more effectively than citrate alone. The proposed theory for the increased reducing capacity of Mn(III)-citrate complexes involves the partial oxidation of the organic ligand by a one-electron transfer from the Mn(III) to the citrate as depicted by the reaction:

$$Mn(III)\text{-}C_2O_4^- \rightarrow Mn(II) + CO_2^{-}\cdot + CO_2 \qquad [3]$$

This results in a highly unstable organic free radical which will readily give up its unpaired electron, thus making it a strong reducing agent (Bartlett, 1988).

The observations in the above-mentioned study are very similar to the results obtained in this study where the Cr oxidising capacity is dramatically decreased while the MED remains largely unchanged. The question may arise: could Mn(III)-organic complexes be forming as the soil surface dries and could this explain the role of organic matter in the drying effect?

It has generally been assumed that the Mn which is released from dry soils is divalent (Ross et al., 2001a) although this is rarely verified. Manganese(III) is usually considered unstable in solution although it has been found to form stable complexes with certain organic and inorganic ligands (Dion and Mann, 1946, Belcher and West, 1952; Klewicki et al., 1998). There has been growing interest in the occurrence of trivalent Mn in natural waters and soils as evidence of its stabilization by certain ligands is uncovered (Dion and Mann, 1946; Kostka et al., 1995; Klewicki and Morgan, 1998). If Mn is extracted from the soil using a non-complexing salt such as $CaCl_2$, any Mn(III) present would rapidly undergo disproportionation following equation 2. If, however, an extraction agent like pyrophosphate was used, any organically bound Mn(III) would be stabilized.

Sodium-pyrophosphate was used to extract organically bound Mn from dried and moist soils. If drying were to induce the formation of Mn(III)-organic complexes, it might be expected that the Na-pyrophosphate extracts from the dried soil would show an increase in oxidation state. This is indeed the case for the A and B1 horizon, where the organic matter

content is the highest and Mn(III) stabilization may be most favourable (Table 4.1). The increase in oxidising capacity with drying was further illustrated by reacting Na-pyrophosphate extracts from wet and dried topsoil samples with TMB. The extracts from the dry soils showed a positive, yellow TMB test for Mn(III) while the moist soil extracts turned dark blue, indicative of partial oxidation. Quite conversely, the extracts from the dried soils also showed the highest Cr(VI) reducing capacity (Table 4.2). This means the extracts from the dry soil were able to oxidise iodide and TMB yet reduce Cr(VI). This seemingly contradictory result fits well with the behaviour of free radicals which can be strong oxidising agents as well as strong reducing agents by donating their unpaired electron or accepting a mate for their odd electron (Bartlett and James, 1994). According to this definition, Mn(III) is a free radical and may be responsible for the Cr reducing capacity as well as the TMB oxidation observed in the dry soil extracts.

The formation of Mn(III)-citrate complexes as well as their decomposition is favoured by a low pH (Bartlett, 1999). It will be shown in Chapter 5 that the pH of a drying surface can be extremely low. This may favour the formation and decomposition of Mn(III)-organic complexes. If drying were to favour the formation of Mn(III)-organic complexes this may explain the release of Mn from dry soils in its divalent state or its intermediate trivalent state. It would also explain the reduction in Cr oxidising capacity and the unaltered MED status as well as the enhancement of the drying effects in topsoils where the organic content is the highest.

The practical implications of the chemical changes that occur with drying may be important in the case of the Graskop soils where the A horizon is rich in Mn oxides. The A horizon will be the most affected by surface conditions and the top few centimetres of soil may experience very low moisture levels during extended dry periods. This drying effect could therefore be an important consideration in determining the factors which affect Mn mobility. The continual removal of water from the transpiring evergreen plantations throughout the dry season may cause significant desiccation of the topsoil and chlorosis in the pine needles, which has been observed towards the end of the dry season, may be related to an increase in plant available Mn. Grassland soils may also be expected to be influenced by drying especially with the frequent *veld* fires in late winter which may cause heating and desiccation in the top few centimetres of soil. When the spring rains come it is usually observed that re-growth from burnt areas is more vigorous that in unburnt areas.

This is usually attributed to microbial stimulation, what is commonly referred to as the Birch effect (Birch, 1958). If free radicals were to form during soil desiccation, it is interesting to speculate what effect this could have on redox sensitive nutrients such as nitrogen.

4.5 Conclusions

Drying has an important effect on the release of Mn from the solid phase. The effects are more noticeable in topsoils than in subsoils which suggests that humic substances may be involved in the reactions taking place during drying. The enhancement of extractable Mn from dried soils was accompanied by a large loss of Cr oxidising capacity although MED was little affected. This could be an indication that drying enhances the reducing capacity of the soil. Pyrophosphate extracts from dried soil show an increase in both oxidising and reducing capacities compared to extracts from moist soil. This is characteristic of free radicals, and perhaps the conditions on the drying soil surface are conducive to the formation of Mn(III)-organic complexes which can act as strong oxidising and reducing agents. This may explain the Mn release as well as the contradictory redox results. It also may explain why the chemical changes induced by drying decrease with distance from the organic-rich topsoil horizon.

The effect of drying may cause the mobility of Mn in some of the forest soils, and may be a contributor to the chlorosis observed in *Pinus* foliage towards the end of the dry season. The frequent *veld* fires in the grasslands may cause severe desiccation of the top few centimetres of soil and drying could play a major role in releasing Mn from the solid phase in the grassland soils. The fact that drying has its largest effect on surface soils has important practical implications not only for the Graskop soils but also soils in arid environments, where the topsoils can become really dry. One example of this is the soils of the Swartland, along the west coast of South Africa. These soils contain a fair amount of Mn, often associated with carbonate or silica hardpans. The xeric climate is conducive to extremely hot, dry conditions during summer which will certainly dry out the surface soils. This may influence Mn plant availability to wheat crops planted in autumn.

CHAPTER 5

5 Spectroscopic investigation into the changes which accompany the drying of a manganiferous clay surface

5.1 Introduction

The results of the preceding chapter have highlighted the complexity of reactions that occur with drying. It appears that drying not only affects the quantity of exchangeable Mn released from dried soils but it may also change the speciation of the exchangeable Mn. These deductions have been made through comparing the changes that occur in soils before and after the soils have been dried. However, it is difficult to identify the actual mechanism involved due to the lack of surface specific techniques that can be applied under normal conditions of temperature and pressure. X-ray photoelectron spectroscopy (XPS) is a powerful technique for probing the chemical status of surface and surface-bound species. It requires evacuation of the analytical chamber, however, which would cause water to be lost from the surface. X-ray absorption spectroscopy also provides information pertaining to the chemical environment of the solid, but it is not surface-specific. Thus observation of the drying reactions in real time have been challenging. Attenuated total reflectance (ATR) Fourier transform infrared (FTIR) spectroscopy is a surface specific technique which may be ideal for probing the chemical changes that occur on a drying surface as it can be performed *in situ*, at ambient temperatures and pressures. Further, rapid scans of the drying surface can be obtained allowing real time investigation of the drying soil-water interface. This chapter highlights the changes that occur in pH and sorbed oxalate as water is gradually removed from a clay film.

Mortland and Raman (1968) used the conversion of NH_3 to NH_4^+ on a smectite surface to indicate the effect drying has on surface pH. This was achieved by observing peak shifts in the hydrated and dehydrated state. Surface acidity of minerals can also be determined with the use of Hammett indicators dissolved in a non-polar medium (Benesi, 1956; Hemni and Wada, 1974; Frenkel, 1975), although this method has limited used in tracking pH changes as free water is removed from a fully hydrated surface. Attenuated total reflectance Fourier transform infrared (ATR-FTIR) spectroscopy provides the ability to investigate the drying mineral surface *in situ* under ambient conditions, allowing insight into some of the anomalies associated with water removal from the mineral-water interface. Vibration

spectroscopy, specifically in the infrared, is extremely sensitive to absorbance caused by the presence of water and is therefore a sensitive probe for the degree of surface hydration. The ATR-FTIR technique is correspondingly sensitive to species adsorbed at the solid-water interface and is capable of analyzing the surface for reactivity promoted by the drying process.

Organic matter has been implicated as being involved in the release of Mn from the solid phase (Bartlett and James, 1980; Ross et al., 2001a). The present study has also shown strong involvement of organics, with drying induced changes always being the most dramatic in the A horizon and decreasing with depth. In this light it was thought instructive to investigate the changes that occurred to a simple organic molecule, sorbed onto the clay surface as the surface was gently dried. To achieve this oxalate was sorbed onto the clay and changes in the consecutive sequence of IR spectra were observed as water was gradually evaporated.

Oxalate is a simple ubiquitous organic species and is a common microbial metabolite (Stone 1987). Reduction of Mn oxides by oxalate has been extensively researched (Stone and Morgan, 1984; Stone, 1987; Xyla et al., 1992; Perez-Benito et al., 1996; Banerjee and Nesbitt, 1999) although the results of these studies are not all unanimous. Most workers propose that oxalate completely reduces MnO_2 to Mn^{2+} with itself being oxidised to CO_2 (Stone and Morgan, 1984; Stone, 1987; Xyla et al., 1992; Perez-Benito et al., 1996) while more recent work using XPS shows little evidence of Mn^{2+} generation (Banerjee and Nesbitt, 1999). In the latter study, it was found that oxalate reduced Mn(IV) to Mn(III) and stable Mn(III)-oxalate complexes were formed suggesting that one-electron transfer takes place between Mn(IV) and oxalate. It is clear from these disagreements that the interaction between Mn oxides and oxalate is still not fully understood and it may not be ideal to introduce the added complexity of drying, but oxalate has IR bands that mostly fall outside the region of the water bands, and a fair amount of research has been conducted on oxalate-oxide systems which would aid in the interpretation of the data.

5.2 Materials and methods

The clay fraction of F3B2 horizon was separated from the bulk soil by shaking and sedimentation after lowering the pH of the aqueous suspension to 4 with HCl. After

restoring the pH of the suspension to pH 5 with NaOH, the dispersed clay fraction was flocculated by adding a few drops of 0.5 M $MgSO_4$ and washed multiple times with ultra-pure deionized (DI) water. The clay was re-suspended and diluted to a concentration of approximately 30 mg/L in 30:70 ethanol:water solution. A thin clay film was air-dried on a germanium (Ge) internal reflection element (IRE) for examination by ATR-FTIR spectroscopy using a Thermo Electron® Nexus 670 spectrometer fitted with a liquid N_2 - cooled MCT-A detector and a Horizontal ATR flow-through assembly (PIKE Technology). The Ge IRE was chosen due to the effective pH at the surface potentially decreasing below the solubility limit of the more commonly used ZnSe IRE.

The dry clay film was re-hydrated in the flow cell with ultra-pure DI water and a background scan was collected of the fully hydrated clay. All subsequent scans were ratioed against the hydrated-clay background, allowing peak intensity due to water loss and the sorbed indicator to be observed. A pH 5.6 solution of thymol blue ($C_{27}H_3O_5S$) was injected into the flow cell to give a final concentration in contact with the clay surface of 5 x 10^{-5} M. The above procedure was repeated for the oxalate experiment using 5 x 10^{-5} M, pH 5.6 Na-oxalate. This concentration is well below the infrared detection limit for aqueous species on the IRE used in ATR-FTIR (Duckworth and Martin, 2001; Borda et al., 2003) permitting any thymol blue or oxalate detected to be considered surface-bound. The clay film with sorbed indicator or oxalate was allowed to dry gradually at room temperature using the dry-air purge of the spectrometer. During the entire drying period spectra were collected every minute using 64 co-added scans at 4 cm^{-1} resolution.

Standard spectra of 0.025 M solutions of thymol blue at pH 5.6 and 1.2 (deprotonated and protonated, respectively) were collected on a clean Ge crystal. This was repeated for oxalate using 0.025 M Na-oxalate (pH 5.6) and oxalic acid (pH 1.5). A set of control spectra were collected on 5 x 10^{-5} M solutions of thymol blue and Na-oxalate that were allowed to dry on the clean Ge crystal. The only observable change in the control spectra were concentration-dependent peak intensity increases due to the evaporation of water and subsequent increase in the activity of solution species. No new peaks, or shifts in peak positions, were observed in the control experiment.

5.3 Results and discussion

The spectra of the drying clay film, before any sorbates were added, are shown in Figure 5.1.

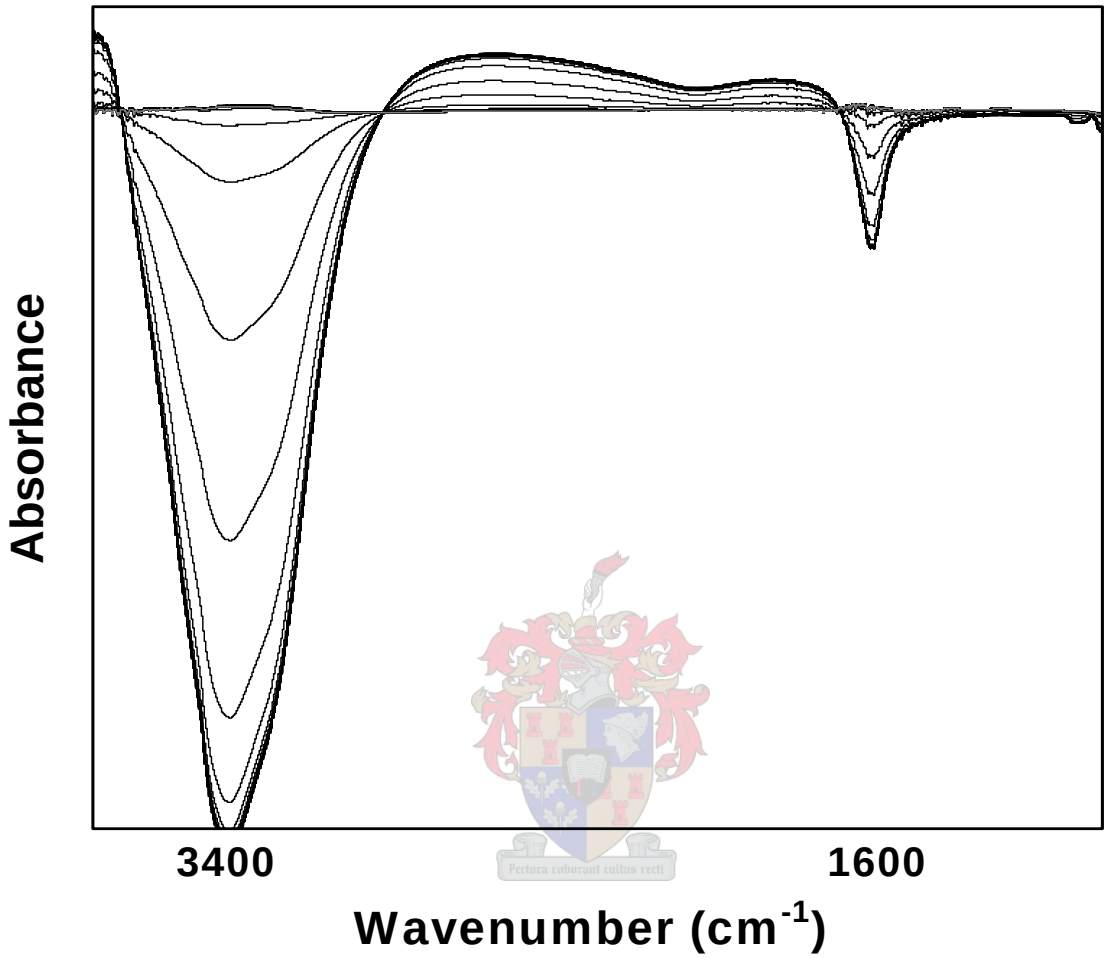

Figure 5.1 Selected spectra showing water removal as a wetted clay film was evaporated over an 8 hr period on a Ge crystal. The negative absorption bands around 3400 and 1600 cm^{-1} signify loss of water relative to the fully hydrated clay background.

Two water bands are present, one in the 3200 -3500 cm^{-1} region and a second at approximately 1600 cm^{-1}. The broad spectral intensity in the 3200 – 3500 cm^{-1} region is due to the υ_1 symmetric stretching mode for water along with OH stretching modes from surface functional groups. The peak at approximately 1600 cm^{-1} is due to the υ_2 bending mode of water. This bending mode is therefore a much more direct indication of surface dryness because there are no vibrational band overlaps due to surface functional groups. The intensity of the 1600 cm^{-1} peaks become increasingly more negative with drying, until the peaks superimpose, indicating the loss of free water from the surface.

5.3.1 Surface pH

Spectra for the protonated and deprotonated thymol blue standard solutions are shown in Figure 5.2. The region between 1120 and 1280 cm^{-1} shows the largest spectral difference between the protonated and deprotonated forms of the indicator which was interpreted as the protonation/deprotonation of the sulfonate (SO_3H) group (pK_a = 1.65; Kolthoff et al., 1967) on the thymol blue molecule.

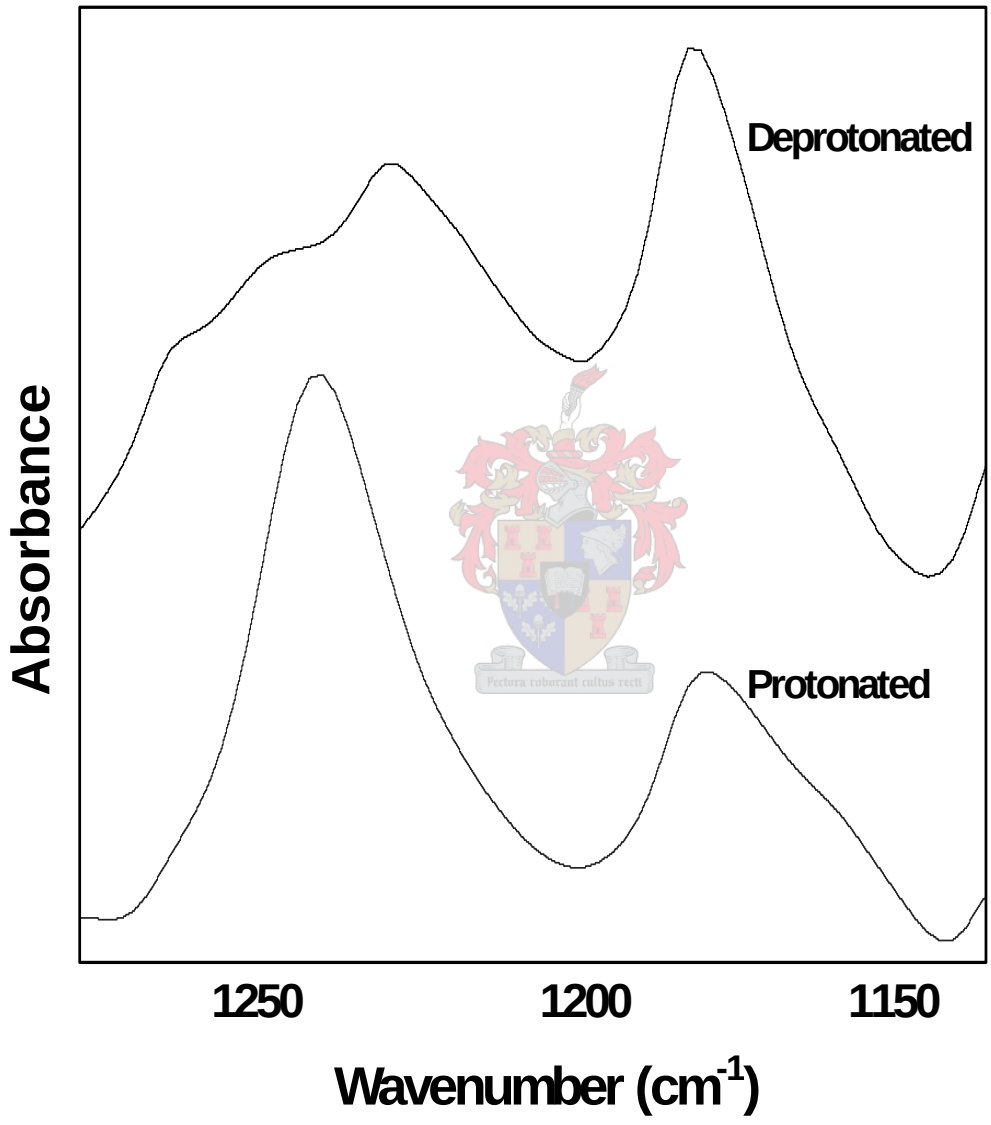

Figure 5.2 IR spectra of protonated and deprotonated thymol blue standards using 0.025 M solutions equilibrated on a clean Ge crystal

Figure 5.3 shows a time series of spectra collected during the drying of thymol blue-treated clay. More than 1000 scans were collected over an 8 hr period, however, for clarity only a selection of the spectra has been included. Two distinctly different spectral patterns are

apparent: those representing the hydrated surface (upper group), and those representing the dry surface (lower group). The change in the lower spectral pattern coincided with the bunching of negative water bands (as illustrated in Fig. 5.1) indicating that the transformation is linked to the removal of free water by evaporation.

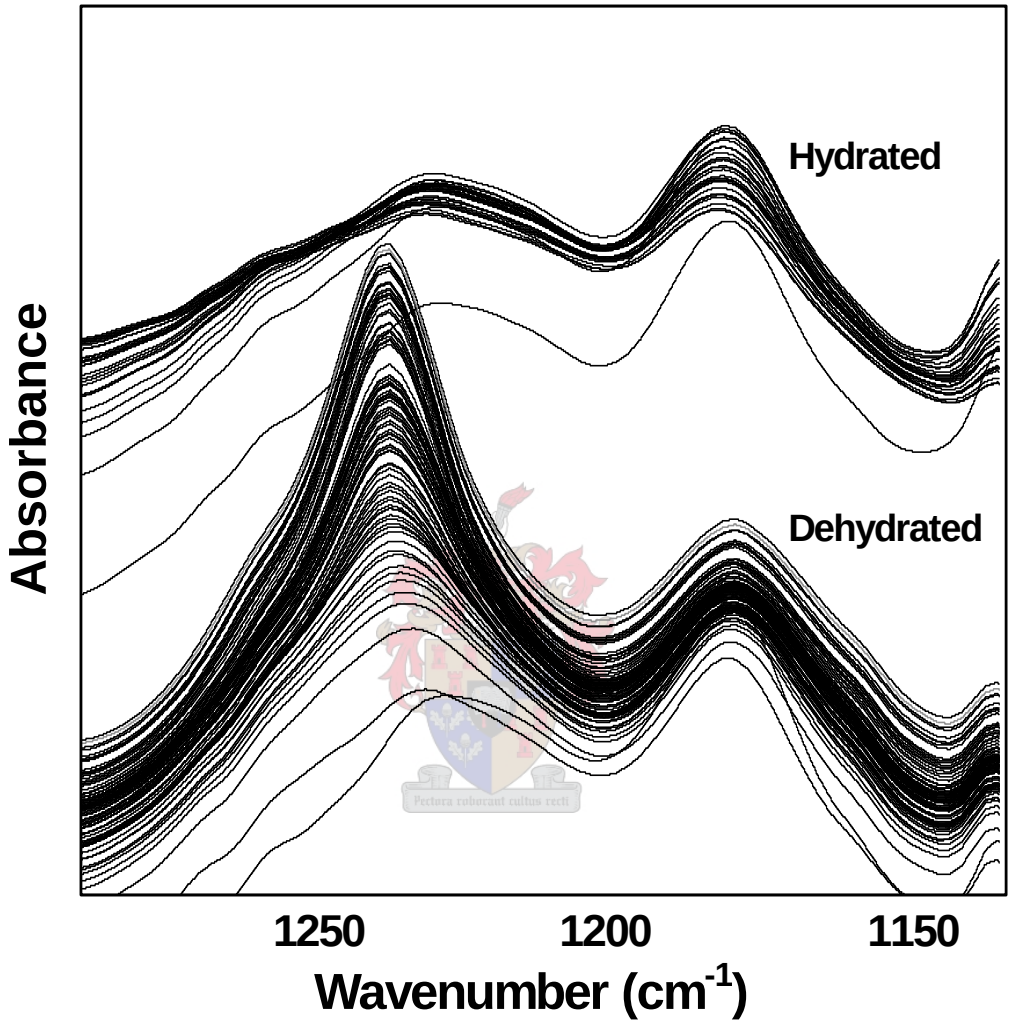

Figure 5.3 Selected spectra for thymol blue sorbed on to a clay film which was allowed to air-dry over an 8 hr period during which a spectrum was collected every minute. Assignment of hydrated and dehydrated regions is based on changes in the water bands at 1600 cm^{-1}.

In Figure 5.3, the spectra for the wet, thymol blue-treated clay are similar to the spectrum for the deprotonated form, as would be expected at the ambient soil pH, whereas spectra from the dried clay have the appearance of the protonated indicator (Fig. 5.2). Other regions of the spectra (not shown) were not affected by drying, suggesting that spectral changes brought about in the sulfonate region by drying are caused by the protonation of the indicator at the soil surface. These results provide valuable spectroscopic evidence for the acidifying effect of drying the clay surface and considering the unanimous spectral shift

it can be concluded that the indicator is in its fully protonated state, inferring that the pH has dropped to at least 1.65.

5.3.2 Response of adsorbed oxalate to drying

The IR spectrum for aqueous oxalate is dominated by strong asymmetric (C-O) and symmetric (C=O) stretching bands at ~1570 and ~1308 cm^{-1}, respectively (Mehrotra and Borha, 1983). Coordination of a carboxyl group is usually associated with loss of symmetry, appearing in IR spectra as an increased number of peaks and increased separation ($\Delta\nu$) between the asymmetric (ν_{as}) and symmetric (ν_s) carboxyl stretching bands (Dobson and McQuillan, 1999). Protonation of the carboxylate group results in a significant change in IR absorption, especially the splitting of the asymmetric peak and appearance of a new peak around 1240cm^{-1} (Axe and Persson, 2001). Coordination of carboxyl groups with metal ions will also reduce symmetry and result in peak shifts. Previous use has been made of $\Delta\nu$ to elucidate the coordination environment of carboxylates (Duckworth and Martin, 2001; Dobson and McQuillan, 1999; Nara et al., 1996).

Table 5.1 Frequency (cm^{-1}) of absorption maxima in IR spectra of 25 mM aqueous solutions of Na-oxalate (pH 5.6) and oxalic acid, and in spectra of the hydrated and dehydrated clay film with oxalate sorbed from a $5x10^{-5}$ M, pH 5.6 Na-oxalate solution, compared with bands for oxalate sorbed on other materials.

Na-oxalate(aq)	Oxalic acid(aq)	Hydrated surface	Dehydrated surface	Al_2O_3[a]	Fe_2O_3[b]
	1733				
				1720	1720
		1672	1690	1695	1701
1570	1623				
		1427	1423	1424	1423
			1366		
1307		1303	1305	1297	1305
	1231		1240		

[a] Dobson and McQuillan, 1999.

[b] Duckworth and Martin, 2001.

The most important IR frequencies of the aqueous oxalate and oxalic acid standards used in this study (Table 5.1) are in good accord with published data (Axe and Persson, 2001; Duckworth and Martin, 2001; Dobson and McQuillan; 1999; Kubicki *et al*., 1999; Hug and

Sulzberger, 1994). The aqueous oxalate standard has its absorption maxima at 1570 and 1307 cm^{-1}. The changes due to protonation were observed in the aqueous oxalic acid standard, having peaks at 1733, 1623 and 1231 cm^{-1} (Table 5.1).

Figure 5.4 shows selected spectra from the time sequence as the clay-oxalate surface was dried. In the moist state the oxalate-clay system shows peaks at 1672, 1427 and 1303 cm^{-1} (Fig. 5.4; Table 5.1). The adsorbed oxalate peak at 1303 cm^{-1} is very similar to that of aqueous oxalate (Table 5.1). The broad peak at 1670 cm^{-1} is shifted relative to the asymmetric aqueous oxalate peak and a new peak is evident at 1427 cm^{-1} (Table 5.1)

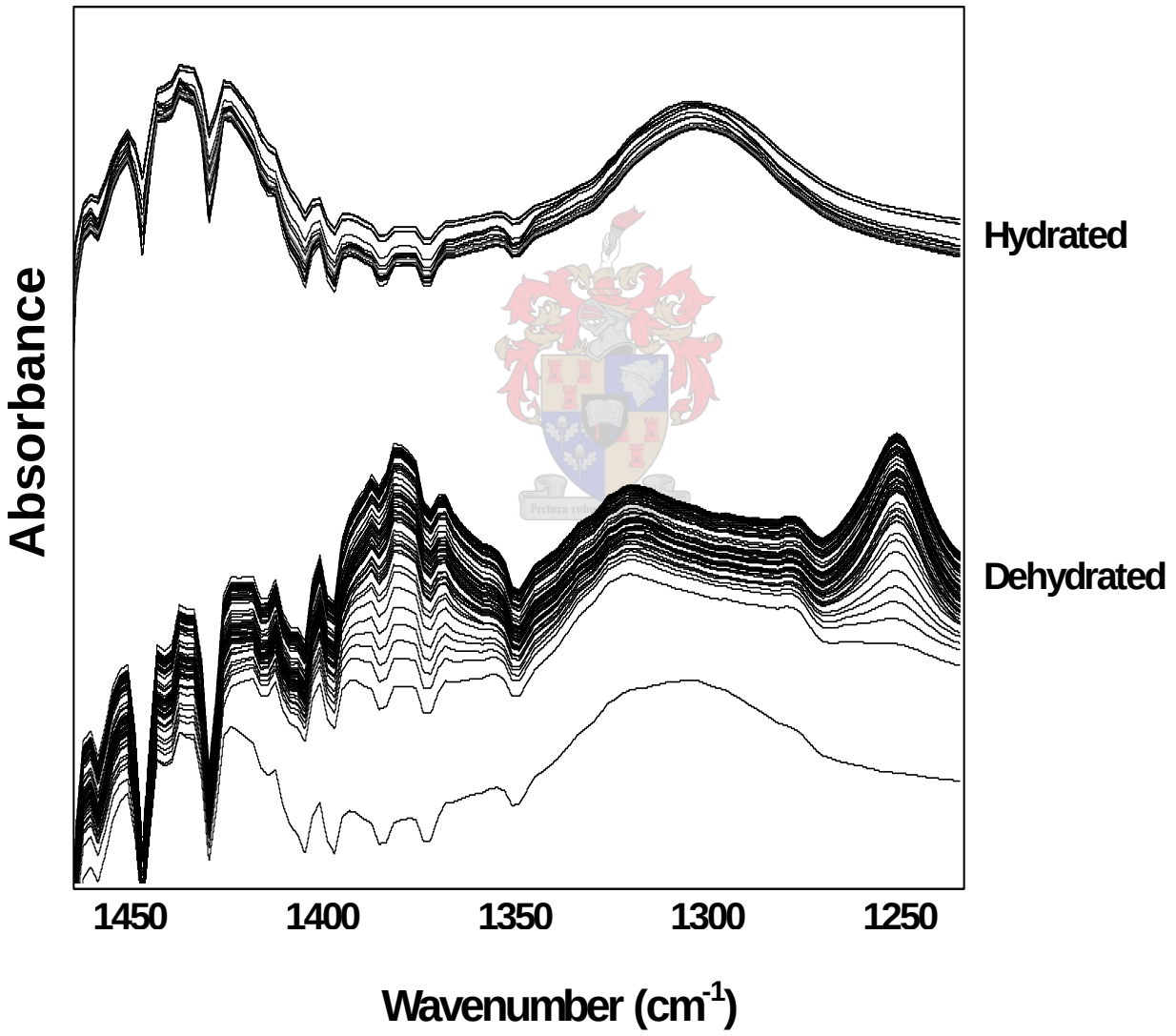

Figure 5.4 Selected spectra for Na-oxalate sorbed on to a clay film which was allowed to air-dry over an 8 hr period during which a spectrum was collected every minute. Assignment of hydrated and dehydrated regions is based on changes in the water bands at 1600 cm^{-1}.

Work done on oxides of Zr, Ti and Al (Dobson and McQuillan, 1999) and Fe (Duckworth and Martin, 2001) has revealed that inner sphere sorption of oxalate to the oxide surface causes significant changes in the IR spectra, namely the appearance of a peak around 1420 cm^{-1} paired with a large shift in the asymmetric stretch region, usually around 1710 cm^{-1}. The symmetric stretch frequency also shifts slightly to between 1270 and 1297 cm^{-1}. The IR spectrum of the current clay-oxalate system appears to show a hybrid between inner sphere- and outer sphere-bonded oxalate because peaks corresponding to both aqueous and coordinated species can be identified (Table 5.1; Fig. 5.4). It was interesting to note that there is little evidence of CO_2 evolution in the IR spectra of the fully hydrated system (data not shown) which suggests that at the concentrations of oxalate used in this experiment there appears to be little oxidation of $C_2O_4^{2-}$ to CO_2.

While the clay film was still hydrated there was little change in the spectra but once free water had been removed there was a clear change in peak positions. The transition is shown from hydrated (upper) to dehydrated spectra (lower group) in Figure 5.4. The large negative water bands result in the loss of information in the 1500 –1700 cm^{-1} region. To overcome this, a background scan of the dry clay was collected prior to oxalate treatment and this dry background was then used to correct a spectrum taken of the dry clay-oxalate system (Fig. 5.5).

Pectora roborant cultus recti

Although noisy, the spectrum allows the peak position of the asymmetric stretch to be determined in the dehydrated state and compared with the position of the peak in the hydrated state. Figures 5.4 and 5.5 both highlight the changes that occur with drying, the most discernible being the appearance of two new peaks at 1240 and 1366 cm^{-1} and the loss of intensity in the 1305 cm^{-1} peak. Borda et al. (2003) reported peaks at 1365 and 1245 cm^{-1} when oxalate was reacted with $Fe_2(SO_4)_3$ in solution. These peaks were assigned to the decrease in symmetry of the oxalate ion with the formation of a FeC_2O_4 complex. Similar Mn oxalate complexes forming on the clay surface may account for the occurrence of two peaks at 1366 and 1240 cm^{-1}. Drying may aid the formation of such complexes for two reasons: firstly, evaporation will markedly increase the concentration of oxalate in solution, thus increasing the tendency for inner sphere complexation and secondly, the decreasing thickness of hydration spheres associated with both ligand and metal centres may aid inner sphere coordination. Protonation may also be responsible for the 1240 cm^{-1} peak, but it cannot explain the 1366 cm^{-1} peak. The peak at 1240 cm^{-1} was also present

when a clay film wetted only with distilled water was dried (data not shown). This may represent either protonation, or metal complexation of carboxyl groups in the natural humic substances and although the peak was evident in the untreated clay spectrum, the oxalate-treated clay showed a distinct enhancement of this peak.

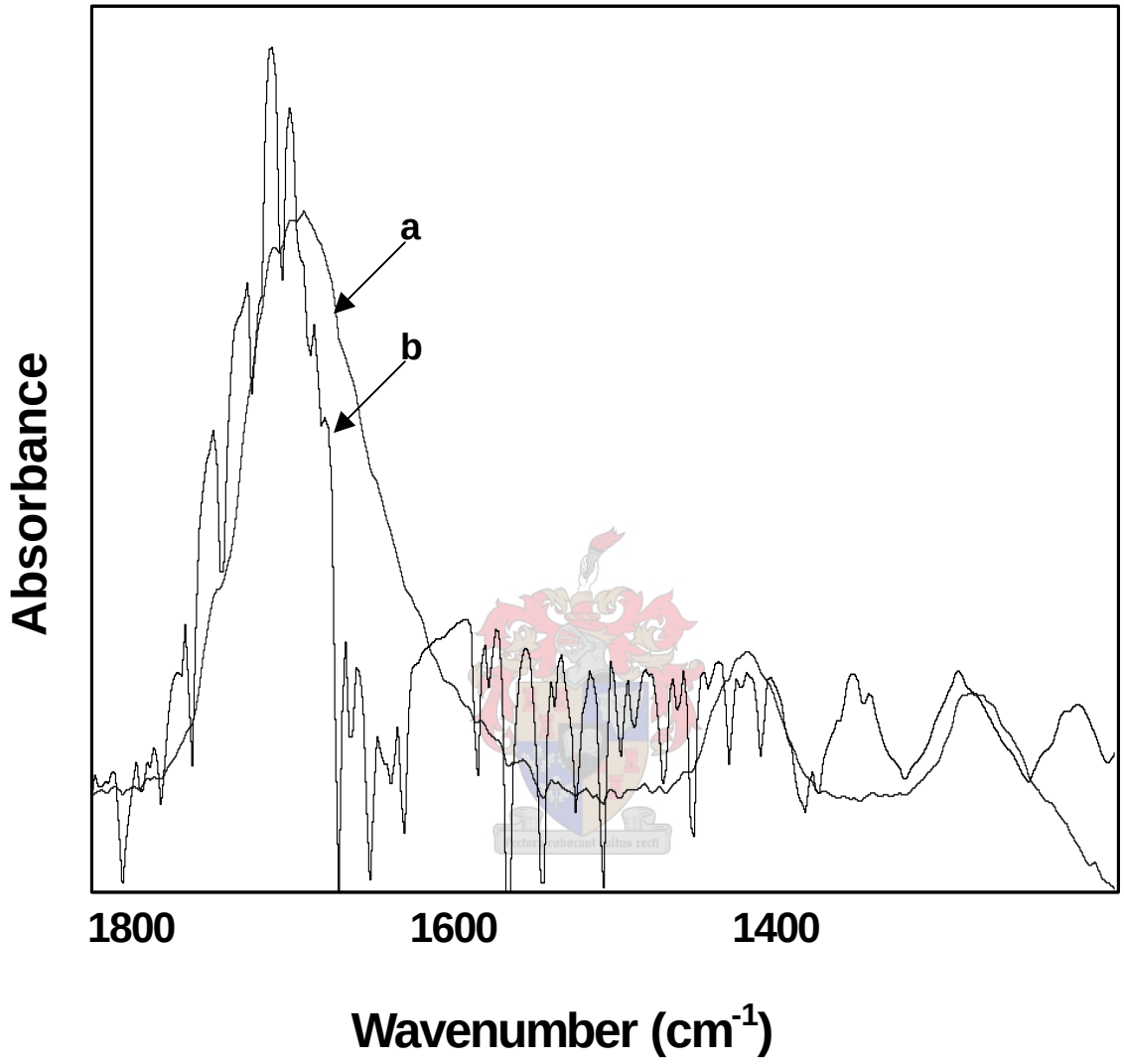

Figure 5.5 Spectra for sorbed oxalate (a) background corrected using a hydrated clay background and (b) background corrected using a dehydrated background.

From peak maxima in Figure 5.5, $\Delta\nu$ (ν_{as}-ν_s) could be determined for the hydrated and dehydrated systems. Spectra of the hydrated clay film show $\Delta\nu$ = 360 cm^{-1}. Two ν_s frequencies were used for the dehydrated sample: the 1305 cm^{-1} peak, which although diminished is still present, and the lower frequency 1240 cm^{-1} peak. These gave a $\Delta\nu$ of 380 and 450 cm^{-1}, respectively. Increase in $\Delta\nu$ indicates loss of symmetry, being lowest for dissolved ions and bidentate coordination and highest for monodentate coordination (Nara

et al., 1996; Duckworth and Martin, 2001). Drying the surface brings about an increase in $\Delta\nu$ which adds evidence for a change in the coordination of the ligand.

These results show evidence of a change in coordination environment accompanying the removal of free water from the clay surface. It appears that drying results in a more inner sphere type of association between the metal centre and the oxalate ligand. This could provide valuable insight into understanding the interaction of organic-metal interactions that may take place in drying soils. Inner sphere coordination at the oxide surface may facilitate metal-ligand charge transfer between an oxidant such as Mn and the organic ligand. There is little evidence of total oxalate oxidation which would result in significant decease of peak intensity as the oxalate is oxidised to CO_2. The results from Chapter 4 provide evidence to support the role of Mn(III)-complexes in the drying reactions. Inner sphere coordination between certain organics and the Mn oxide surface may favour the formation of Mn(III)-organic complexes by two mechanisms: i) a one-electron transfer between Mn(IV) and the organic ligand, or ii) reverse disproportionation. These are shown in the reactions below:

i) $2MnO_2 + C_2O_4^{2-} + 2H^+ \rightarrow 2Mn(III) + 2CO_2$

$Mn(III) + C_2O_4^{2-} \rightarrow Mn(III)\text{-}C_2O_4$

ii) $MnO_2 + Mn^{2+} + 3(COOH)_2 \rightarrow 2Mn(COO)_3 + 2H_2O + 2H^+$

Both of these mechanisms are favoured by low pH (Davies, 1969; Banerjee and Nesbitt, 1999, respectively), which might further explain the role of drying in initiating either process.

Proton and ligand promoted dissolution of Mn oxides cannot be ruled out considering the data obtained in these experiments. Proton and ligand promoted dissolution are favoured by low pH and inner sphere ligand coordination (Zinder et al., 1986) both of which are satisfied by the chemical environment of the drying clay surface. Guest et al. (2002) proposed that reducing the pH in solution caused solid state reduction of Mn(IV) to Mn(III) without the release of Mn(II) into solution. Considering the low pH reached at the clay surface this could quite possibly be occurring during drying. It does not, however, explain

the observed release of Mn, unless ligand promoted dissolution were involved in liberating structural Mn(II) or Mn(III) into solution.

Although the present study may provide more questions than answers regarding the release of Mn from dried soils, it does illustrate a novel technique for observing changes that may be responsible for some of the anomalies associated with drying in soils.

5.4 Conclusions

In this chapter it has been shown that the difference between the chemical environment of a dry surface and that of a fully hydrated surface can be elucidated spectroscopically using ATR-FTIR. The dramatic reduction in pH upon drying can be tracked by observing absorbance changes in thymol blue adsorbed to the clay surface. Inner sphere bonding of oxalate to the clay surface appears to intensify with drying. The fact that these changes were observed in a Mn oxide-rich clay known to exhibit enhanced Mn extractability following drying suggests that surface acidification and intensification of the bonding of humic substances with surface metal cations, may both be involved in mobilizing Mn. This may help to explain the apparent redox anomaly of exchangeable Mn concentrations being enhanced by drying. The fact that these chemical transitions can be demonstrated with air-drying at ambient temperatures suggests a new paradigm for interpreting some of the chemical changes that may take place with moisture fluctuations in geochemical environments.

GENERAL DISCUSSION

The objective of this study was to determine the factors which influence the stability of the manganiferous oxisols of Graskop and, in doing so, also investigate some of the fundamental chemical and mineralogical properties of the soils. In addition to the potential for drying to mobilize Mn in the Graskop soils, advantage was taken of the abundant Mn in an attempt to reveal some of the chemistry surrounding Mn release from dried soils. To achieve these goals the steps involved were: to look for signs of Mn mobility within the landscape and the profile, to assess the mineralogy, charge characteristics and buffer capacity of the soils, to look at the effects of acidification on metal release and then, finally, to try and uncover some of the chemical processes that account for the release of Mn in dried soils.

From field observations it would appear that Mn is mobile in the Graskop soils. This is apparent from the high nodule content of the upper subsoils and the mottled zone at greater depths which may imply incipient nodule formation. The general trend of increasing Mn concentration with depth suggests that manganese is being mobilized as a front of pedogenesis moves down the profile. However, the exact pedogenic process was not evident from field observations except to suggest that organic matter may be a contributing factor. The total Mn concentrations in these soils are exceeding high, being higher than those reported for the manganiferous oxisols of Hawaii (Fujimoto and Sherman, 1948), and the Graskop soils are probably some of the most Mn-enriched soils known. The high Mn content is accompanied by very high trace element concentrations which would almost classify the soil as contaminated if these trace elements were not native.

The mineralogy of the Graskop soils is typical of soils in an extremely advanced stage of weathering, with the clay fraction consisting predominantly of sesquioxides and kaolinite. The Al-hydroxy interlayered Mn oxide, lithiophorite dominates the mineralogy of the clay fraction, with accessory amounts of birnessite, gibbsite, goethite, hematite, maghemite, and kaolinite. In the weathering sequence of Mn oxides in soils, lithiophorite has been suggested as being the end member due to its relative stability in acid, weathered soils (Parc et al., 1989; Golden et al., 1993) which may explain its abundance in the Graskop soils.

The charge characteristics of the soils are very interesting with the pH of the soil being at or slightly lower than the point of zero charge. Perhaps these soils could be said to be in isoelectric equilibrium, with the net charge being at or very close to zero thereby justifying their classification as *Posic* (WRB) or *Anionic* (Soil Taxonomy). As expected, from soils at this stage of weathering, they have a very low buffer capacity especially in the organic-poor subsoil which commenced solid phase dissolution with the first increment of titrated acidity. This implies that the soils are highly sensitive to the addition of acidity and therefore metal release could be a serious issue under acid-generating crops. Manganese release showed a linear increase with added acidity, although the amount released was much less than expected considering the high Mn reserves. Aluminium on the other hand was released in substantial quantities in response to acidification and any Mn phytotoxity in these soils would probably be overshadowed by Al toxicity.

It would appear then that the Mn oxide phase in the Graskop soils may show a degree of resilience to added acidity which comes as a surprise considering that similar Hawaiian soils showed a 100-fold increase in soluble Mn per unit decrease in pH (Hue et al., 2001). This resilience of the Mn-rich Graskop soils is hard to explain, but it may have a lot to do with the Mn mineralogy. Lithiophorite is commonly found in acid, weathered soils (Taylor et al., 1964; Golden et al., 1993), which suggests it is one of the most stable Mn minerals under these conditions. A possible reason for this stability may be the relatively low concentration of Mn(II) in the mineral structure. Lithiophorite hosts Mn in its 3+ and 4+ state while birnessite hosts Mn in its 2+, 3+ and 4+ state (Post, 1999). It has been suggested that the observed Mn release from birnessite in acid conditions could originate from proton promoted dissolution of MnO housed in the structure (Banerjee and Nesbitt, 2001). If this suggestion is correct then it may follow that lithiophorite, with its lower Mn^{2+} content, will release less Mn in response to acidification and therefore be more stable under acidic conditions.

An alternative or additional explanation for the relative resilience of these soils may be solid state reduction of Mn within the oxide structure without the release of any Mn(II), as was shown to occur in soil Mn oxides as the pH was lowered from 7 to 3 (Guest et al., 2002). If acidification results in solid state reduction then perhaps the poise of the Graskop soils is so high that they will endure drops in pH by hosting and delocalising electrons

within the oxide structure without releasing large quantities of Mn into solution. In soils of lower Mn content the electron delocalising capacity would soon become saturated, whereafter Mn dissolution would begin. The Graskop soils, however, may provide such an abundance of electron acceptors that they can tolerate minor fluctuations in the redox potential before large-scale dissolution begins. It may be speculated then that the reason why these manganiferous oxisols have persisted for so long under the intense weathering regime, is because the oxides are superabundant and thus the soil environment is kept highly oxic even though the pH is low enough to cause Mn oxide instability. Despite this, pedogenic processes are gradually taking their toll, with Mn slowly being stripped from the upper soil horizons, probably through organically fuelled reductive dissolution, and being redistributed deeper in the profile. It would appear, however, that acidity from the acid-generating pine plantations may not affect the stability of the Mn oxide phase as much as originally anticipated. Aluminium mobility, however, is a foreseeable problem with the continued cultivation of acid-producing crops.

The effects of drying on Mn release were investigated in Chapters 4 and 5. These effects were not only studied to assess the possible impacts that drying could have on Mn mobility in the Graskop soils but also an attempt was made to provide some insight into the possible reaction mechanisms involved in this phenomenon. The ATR study in Chapter 5 showed that a severe drop in pH occurred on the mineral surface, accompanying the removal of free water from the clay film. Additionally, drying appeared to induce a shift in the coordination of oxalate from a more outer-sphere association to a more inner-sphere association. These two pieces of information may provide additional insight into the results obtained in Chapter 4, which showed evidence that Mn release during drying may involve the formation of Mn(III)-organic complexes. From these observations the following theory of Mn release from dried soils is proposed: as the soil dries there is a severe drop in pH at the mineral surface accompanied by a shift of certain outer-sphere organic associations to more inner-sphere associations. This provides the low pH and complexing organics that favour the reverse disproportionation of Mn^{4+} and Mn^{2+} to Mn^{3+}. This usually unfavourable reaction is driven by the free energy of complex formation between Mn(III) and an organic ligand (Bartlett, 1999). These Mn(III)-organic complexes may remain stable or, depending on the ligand, undergo a one-electron transfer between Mn(III) and the organic ligand, resulting in organic free radicals capable of reducing redox species such as Cr(VI). Of course, the formation of Mn(III)-complexes does not have to involve reverse

disproportionation reactions. The inner-sphere bonding of organics to the Mn oxide surface may facilitate metal-ligand charge transfer which could also result in Mn(III)-organic complexes. This proposed mechanism would account for the enhancement of exchangeable Mn, the decline in Cr oxidising capacity as well as the minor change observed in the manganese electron demand. It would also provide an explanation for the influence of organic matter, as is implied by the fact that the drying induced changes decrease down the profile.

Under both grassland, with fires and greater exposure to sunlight and wind, and forest plantations, with continuous evapotranspiration throughout the dry season, considerable desiccation can be expected in the surface horizon. This desiccation could be an important factor in determining seasonal changes in Mn solubility.

This study has only scraped the surface of the some of the pedological mysteries surrounding these soils which definitely warrant further investigation. One very interesting aspect that this study has uncovered is the unique trace element composition of the Graskop soils. This, together with their high sesquioxide content, makes them ideal for investigating trace element partitioning among mineral phases. Using techniques like X-ray microdiffraction in conjunction with X-ray microfluorescence, mineral and element maps could be compiled and superimposed which might provide useful information on mineral-trace element associations in soils. Further, because of the abundant nodule content of the soils it would also be of interest to look at the partitioning of trace elements between the nodules and the soil matrix.

Further spectroscopic work on drying reactions may also prove insightful. For example, the mechanism of Cr(VI) reduction on a drying surface could be probed. With the redox changes that have been shown to accompany drying, the fate of many redox-sensitive compounds may be altered though drying. It has been shown in this study that attenuated total reflectance spectroscopy provides a simple, novel approach for investigating drying-induced changes under conditions of normal pressure and temperature. Apart from gaining further insight into Mn release, this technique opens a lot of other exciting opportunities for geochemical studies. Most of our understanding of geochemical systems comes from studies in fully hydrated systems. However, the release of Mn from a dried soil is an indictor that important chemical changes occur on the drying mineral-water interface and,

in limiting our investigations to fully hydrated systems, we may only be seeing half the picture. Using attenuated total reflectance spectroscopy we may be able to gain a more holistic understanding of geochemical reactions taking place in terrestrial environments which are exposed to continuous cycles of wetting and drying.

REFERENCES

Adams, S.N., K.G. Honeysett, K.G. Tiller, and K. Norrish. 1969. Factors controlling the increase of cobalt in plants following the addition of a cobalt fertilizer. Australian Journal of Soil Research 7:29-42.

Asghar, M., and Y. Kanehiro. 1981. The fate of applied iron and manganese in an oxisol and ultisol from Hawaii. Soil Science 131:53-55.

Axe, K., and P. Persson. 2001. Time-dependent surface speciation of oxalate at the water-boehmite (γ–AlOOH) interface: Implications for dissolution. Geochimica Cosmochima Acta 65:4481-4492.

Banerjee, D., and H.W. Nesbitt. 1999. XPS study of reductive dissolution of birnessite by oxalate: Rates and mechanistic aspects of dissolution and redox processes. Geochimica Cosmochima Acta 63:3025-3038.

Banerjee, D., and H.W. Nesbitt. 2001. XPS study of dissolution of birnessite by humate with constraints on reaction mechanisms. Geochimica Cosmochima Acta 65:1703-1714.

Bartlett, R.J. 1981. Nonmicrobial nitrate to nitrite transformation in soils. Soil Science Society of America Journal 45:1054-1058.

Bartlett, R.J. 1988. Manganese redox reactions and organic interactions in soils, p. 59-73, *In* D. G. Graham and et al., eds. Manganese in soils and plants. Kluwer Academic Publishers, Netherlands.

Bartlett, R.J. 1999. Characterizing soil redox reactions, p. 371-397, *In* D. L. Sparks, ed. Soil physical chemistry, second ed. CRC Press, Baco Raton, Florida.

Bartlett, R.J., and B.R. James. 1979. Behaviour of chromium in soils: III. Oxidation. Journal of Environmental Quality 8:31-35.

Bartlett, R.J., and B.R. James. 1980. Studying, dried stored soil samples - some pitfalls. Soil Science Society of America Journal 44:721-724.

Bartlett, R.J., and D.S. Ross. 1988. Colorimetric determination of oxidizable carbon in acid soil solution. Soil Science Society of America Journal 52:1191-1192.

Bartlett, R.J., and B.R. James. 1994. Redox chemistry in soils. Advances in Agronomy 50:151-208.

Bartlett, R.J., and B.R. James. 1995. System for categorizing soil redox status by chemical field testing. Geoderma 68:211-218.

Belcher, R., and T.S. West. 1952. Trivalent manganese as an oxidimetric reagent. Analytica Chimica Acta 6:322-332.

Benesi, H.A. 1956. Acidity of catalyst surfaces. I. Acid strength from colours of adsorbed indicators. Journal of the American Chemical Society 78:5490-5494.

Berndt, G.F. 1988. Effect of drying and storage conditions upon extractable soil manganese. Journal of the Science of Food and Agriculture 45:119-130.

Bigham, J.M., R.W. Fitzpatrick, and D.G. Schulze. 2002. Iron Oxides, *In* J. B. Dixon and D. G. Schulze, eds. Soil mineralogy with environmental applications. Soil Science Society of America, Madison, Wisconsin.

Birch, H.F. 1958. The effect of soil drying on humus decomposition and nitrogen availability. Plant and Soil 10:9-31.

Bloom, P.R. 1982. Metal-organic matter interactions in soil, p. 129-149, *In* R. H. Dowdy and e. al, eds. Chemistry in the soil environment, Vol. ASA Spec. Publ. 40. ASA-SSSA, Madison, USA.

Bloom, P.R. 2000. Soil pH and pH buffering, p. B-333- B-352, *In* M. E. Sumner, ed. Handbook of soil science. CRC Press, Boca Raton, Florida.

Bloom, P.R., M.B. McBride, and R.M. Weaver. 1979. Aluminum organic matter in acid soils: salt extractable aluminum. Soil Science Society of America Journal 43:813-815.

Blume, H.P. 1967. Zum Mechansimus der Marmorierung und Konkretionsbildung in Stauwasserboden. Zeitschrift Pflanzenernahrung und Bodenkunde:124-134.

Borda, M.J., D.R. Strongin, and M.A. Schoonen. 2003. A novel vertical attenuated total reflectance photochemical flow-through reaction cell for Fourier transform infrared spectroscopy. Spectrochimica Acta 59:1103-1106.

Buhmann, C. 1986. Investigation of 2:1 layer silicates in selected South African soils. PhD thesis, University of Natal, South Africa.

Bunzl, K., W. Schimmack, P. Schramel, and M. Suomela. 1999. Effects of sample drying and storage time on extraction of fallout Pu239+240, Cs-137 and natural Pb-210 as well as of stable Cs, Pb and Mn from soils. Analyst 124:1383-1387.

Chao, T.T. 1972. Selective dissolution of manganese oxides from soils and sediments with acidified hydroxylamine hydrochloride. Soil Science Society of America Proceedings 36:764-768.

Chen, Y., N. Senesi, and M. Schnitzer. 1977. Information provided on humic substances by E_4/E_6 ratios. Soil Science Society of America Journal 41:352-358.

Coleman, N.T., G.W. Thomas, F.H. leRoux, and G. Bredell. 1964. Salt-exchangeable and tritratable acidity in bentonite-sesquioxide mixtures. Soil Science Society of America Proceedings 28:35-37.

Cotton, F.A., and G. Wilkinson. 1966. Advanced inorganic chemistry. Interscience, New York.

Davies, G. 1969. Some aspects of the chemistry of manganese(III) in aqueous solution. Coordination Chemistry Reviews 4:199-224.

De Waal, S.A. 1978. The ferromanganese deposit at Lisbon Falls near Graskop, Transvaal, and its similarity to ferromanganese nodules of the ocean floor. Transactions of the Geological Society of South Africa 80:121-136.

Dion, H.G., and P.J.G. Mann. 1946. Three-valent manganese in soils. Journal of Agricultural Science 36:239-245.

Dixon, J.B. 1988. Todorokite, birnessite and lithiophorite as indicator minerals in soils. Manganese Symposium,Adelaide.

Dixon, J.B., and H.C.W. Skinner. 1992. Manganese minerals in surface environments, *In* H. C. W. Skinner and R. W. Fitzpatrick, eds. Biomineralisation processes of iron and manganese. Verlag, Cremlingen.

Dixon, J.B., and G.N. White. 2002. Manganese oxides, p. 367-388, *In* J. B. Dixon and D. G. Schulze, eds. Soil mineralogy with environmental applications. Soil Science Society of America, Madison, Wisconsin.

Dobson, K.D., and A.J. McQuillan. 1999. In situ infrared spectroscopic analysis of the adsorption of aliphatic carboxylic acids to TiO_2, ZrO_2, Al_2O_3 and Ta_2O_5 from aqueous solutions. Spectrochimica Acta 55:1395-1405.

du Toit, B. 1993. Soil acidification under forest plantations and the determination of the acid neutralising capacity of soils. Msc thesis, University of Natal, South Africa.

Duckworth, O.W., and S.T. Martin. 2001. Surface complexation and dissolution of hematite by C_1-C_6 dicarboxylic acids at pH = 5.0. Geochimica Cosmochima Acta 65:4289-4301.

FAO. 1998. World Reference Base for Soils Food and Agricultural Organization of the United Nations, Rome.

Fendorf, S.E., R.J. Zasoski, and R.G. Burau. 1993b. Competing metal ion influences of chromium(III) oxidation by birnessite. Soil Science Society of America Journal 57:1508-1515.

Fendorf, S.E., D.L. Sparks, J.A. Franz, and D.M. Camaioni. 1993a. Electron paramagnetic resonance stopped-flow kinetics study of manganese(II) sorption-desorption on birnessite. Soil Science Society of America Journal 57:57-62.

Fey, M.V. 1981. Hypothesis for the pedogenic yellowing of red soil materials. Poceedings 10th Nat. Cong. Soil Sci. Soc. Southern Africa. East London.Tech. Commn No 180 Department of Agriculture.130-136.

Fitzpatrick, R.W., and U. Schwertmann. 1981. The distribution and nature of secondary magnetic minerals in sesquioxidic soils along the eastern seaboard of South Africa. Poceedings 10th Nat. Cong. Soil Sci. Soc. Southern Africa. East London.Tech. Commn No 180 Department of Agriculture.pp167-168.

Fox, R.L., N.V. Hue, R.C. Jones, and R.S. Yost. 1991. Plant-soil interactions associated with acid weathered soils. Plant and Soil 134:65-72.

Frenkel, M. 1974. Surface acidity of montmorillonites. Clays and Clay Minerals 22:435-441.

Frenkel, M. 1975. Use and abuse of some Hammett indicators for the determination of surface acidity. Analytical Chemistry 47:598-599.

Fujimoto, C.K., and D. Sherman. 1945. The effect of drying, heating, and wetting on the level of exchangeable manganese in Hawaiian soils. Soil Science Society of America Proceedings 10:107-112.

Fujimoto, C.K., and D. Sherman. 1948. Behaviour of manganese in the soil and the manganese cycle. Soil Science 66:131-145.

Furrer, G., and W. Stumm. 1986. The coordination chemistry of weathering: I. Dissolution kinetics of δ-Al_2O_3 and BeO. Geochimica Cosmochima Acta 50:1847-1860.

Goldberg, S.P., and K.A. Smith. 1984. Soil manganese: E Values, distribution of manganese-54 among soil fractions, and effects of drying. Soil Science Society of America Journal 48:559-564.

Golden, D.C., J.B. Dixon, and Y. Kanehiro. 1993. The manganese oxide mineral, lithiophorite, in an oxisol from Hawaii. Australian Journal of Soil Research 31:51-66.

Goodman, B.A., and M.V. Cheshire. 1987. Characterization of iron-fulvic acid complexes using Mossbauer and EPR spectroscopy. Science of the Total Environment 62:229-240.

Gotoh, S., and W.H. Patrick. 1972. Transformation of manganese in a waterlogged soil as affected by redox potential and pH. Soil Science Society of America Proceedings 36:738-741.

Guest, C.A., D.G. Schulze, I.A. Thompson, and D.M. Huber. 2002. Correlating manganese X-ray absorption near-edge structure spectra with extractable soil manganese. Soil Science Society of America Journal 66:1172-1181.

Hawker, L.C., and J.G. Thompson. 1988. Weathering sequence and alteration products in the genesis of the Graskop manganese residua, Republic of South Africa. Clays and Clay Minerals 36:448-454.

Haynes, R.J., and R.S. Swift. 1991. Concentrations of extractable Cu, Zn, Fe, and Mn in a group of soils as influenced by air-drying and oven-drying and wetting. Geoderma 49:319-333.

Healy, T.W., A.P. Herring, and D.W. Fuerstenau. 1966. The effect of crystal structure on the surface properties of a series of manganese dioxides. Journal of Colloid and Interface Science 21:435-444.

Hendershot, W.H., and L.M. Lavkulich. 1978. The use of zero point of charge (ZPC) to assess pedogenic development. Soil Science Society of America Journal 42:468-472.

Henmi, T., and K. Wada. 1974. Surface acidity of imogolite and allophane. Clay Minerals 10:231-245.

Herselman, J.E., C.E. Steyn, and M.V. Fey. 2004. Baseline concentrations of 7 trace elements in surface soils of South Africa and implications for environmental management. South African Journal of Science. In review.

Holmgren, G.G.S. 1967. A rapid citrate-dithionite extractable iron procedure. Soil Science Society of America Proceedings 31:210-211.

Hsu, P.H. 1989. Aluminum hydroxides and oxyhydroxides, *In* J. B. Dixon and S. B. Weed, eds. Minerals in the soil environment, second ed. Soil Science Society of America, Madison, Wisconsin.

Hue, N.V., G.R. Craddock, and F. Adams. 1986. Effect of organic acids on aluminum toxicity in subsoils. Soil Science Society of America Journal 50:28-34.

Hue, N.V., R.L. Fox, and W.W. McCall. 1987. Aluminium, Ca, and Mn concentrations in macadamia seedlings as affected by soil acidity and liming. Communications in Soil Science and Plant Analysis 18:1253-1267.

Hue, N.V., S. Vega, and J.A. Silva. 2001. Manganese toxicity in a Hawaiian oxisol affected by soil pH and organic amendments. Soil Science Society of America Journal 65:153-160.

Hug, S.T., and B. Sulzberger. 1994. In situ Fourier infrared spectroscopic evidence for the formation of several different surface complexes on TiO_2 in the aqueous phase. Langmuir 10:3587-3597.

Hunter, R.J. 1981. Zeta potential in colloid science, principles and applications. Academic Press, Sydney.

Iu, K.L., I.D. Pulford, and H.J. Duncan. 1981. Influence of waterlogging and lime or organic matter additions on the distribution of trace metals in an acid soil. Plant and Soil 59:317-326.

Jackson, M.L., C.H. Lim, and L.W. Zelazny. 1986. Oxides, hydroxides and aluminosilicates, p. 101-150, *In* A. Klute, ed. Methods of soil analysis. Part 1, Second ed. ASA-SSSA, Madison, USA.

Johnson, D.W., and D.E. Todd. 1987. Nutrient export by leaching and whole tree harvesting in a loblolly pine and mixed oak forest. Plant and Soil 102:99-109.

Josephy, P.D., T. Eling, and R.P. Mason. 1982. The horseradish peroxidase-catalysed oxidation of 3,5,3',5'-tetramethyl benzidine. The Journal of Biological Chemistry 257:3669-3675.

Kabata-Pendias, A., and H. Pendias. 2001. Trace elements in soils and plants. CRC Press, Boca Raton.

Keltjens, W.G., and E. van Loenen. 1989. Effects of aluminium on growth and nutritional composition of hyrodroponically grown seedlings of five different forest species. Plant and Soil 119:39-50.

Kennedy, C., D.S. Smith, and L.A. Warren. 2004. Surface chemistry and relative Ni sorptive capacities of synthetic hydrous Mn oxyhydroxides under variable wetting and drying regimes. Geochimica et Cosmochimica Acta 68:443-454.

Kim, J.G., J.B. Dixon, C.C. Chusuei, and Y. Deng. 2002. Oxidation of chromium(III) to (VI) by manganese oxides. Soil Science Society of America Journal 66:306-315.

Klewicki, J.K., and J.J. Morgan. 1998. Kinetic behaviour of Mn(III) complexes of pyrophosphate, EDTA and citrate. Environmental Science and Technology 32:2916-2922.

Klewicki, J.K., and J.J. Morgan. 1999. Dissolution of β-MnOOH particles by ligands: Pyrophosphate, ethylenediaminetetraacetate, and citrate. Geochimica Cosmochima Acta 63:3017-3024.

Kolthoff, I.M., M.K. Chantooni, Jr, and S. Bhowmik. 1967. Acid-base constants in acetonitrile. Analytical Chemistry 39:315-320.

Kosta, J.E., G.W. Luther, and K.H. Nealson. 1995. Chemical and biological reduction of Mn(III)-pyrophosphate complexes: Potential importance of dissolved Mn(III) as an environmental oxidant. Geochimica Cosmochima Acta 59:885-894.

Kubicki, J.D., L.M. Schroeter, B.N. Nguyen, and S.E. Apitz. 1999. Attenuated total reflectance Fourier-transform infrared spectroscopy of carboxylic acids adsorbed onto mineral surfaces. Geochimica Cosmochima Acta 63:2709-2725.

le Roux, J. 1973. Quantitative mineralogical analysis of Natal soils. Soil Science 115:137-144.

Lindsay, W.L. 1979. Chemical equilibria in soils John Wiley & Sons, New York.

Loeppert, R.H., and W.P. Inskeep. 1996. Iron, *In* D. L. Sparks, ed. Methods of soil analysis. Part 3. Chemical methods. Soil Science Society of America, Madison, Wisconsin.

Louw, J.H. 1995. Site classification and evaluation for commercial forestry in the Crocodile River catchment eastern Transvaal. MSc thesis, University of Stellenbosch, South Africa.

Lutz, H.J., and R.F. Chandler. 1946. Forest soils Wiley, New York.

Makino, T., S. Hasegawa, Y. Sakurai, S. Ohno, H. Maejima, and K. Momohara. 2000. Influence of soil-drying under field conditions on exchangeable manganese, colbalt, and copper contents. Soil Science and Plant Nutrition 46:581-590.

Manceau, A., S. Llorca, and G. Calas. 1987. Crystal chemistry of cobalt and nickel in lithiophorite and asbolane from New Caledonia. Geochimica Cosmochima Acta 51:105-113.

Manceau, A., A.I. Gorshkov, and V.A. Drits. 1992. Structural chemistry of Mn, Fe, Co, and Ni in manganese hydrous oxides: Part II. Information from EXAFS spectroscopy and electron and X-ray diffraction. American Mineralogist 77:1144-1157.

Manceau, A., N. Tamura, R.S. Celestre, A.A. Macdowell, N. Geoffroy, G. Sposito, and H.A. Padmore. 2003. Molecular-scale speciation of Zn and Ni in soil

ferromanganese nodules from loess soils of the Mississippi basin. Environmental Science and Technology 37:75-80.

Marques, J.J., D.G. Schulze, N. Curi, and S.A. Mertzman. 2003. Trace element geochemistry in Brazilian Cerrado soils. Geoderma in press.

McBride, M.B. 1978. Transition metal bonding in humic acid: An ESR study. Soil Science 126:200-209.

McBride, M.B. 1982. Electron spin resonance investigation of Mn^{2+} complexation in natural and synthetic organics. Soil Science Society of America Journal 46:1137-1143.

McBride, M.B. 1985. Surface reactions of 3,3'5,5'-tetramethyl benzidine on hectorite. Clays and Clay Minerals 33:510-516.

McBride, M.B. 1994. Environmental Chemistry of Soils Oxford University Press, New York.

McKenzie, R.M. 1970. The reaction of cobalt with Manganese dioxide minerals. Australian Journal of Soil Research 8:97-106.

McKenzie, R.M. 1971. The synthesis of birnessite, cryptomelane, and some other oxides and hydroxides of manganese. Mineralogical Magazine 38:493-502.

McKenzie, R.M. 1972. The manganese oxides in soils - a review. Zeitschrift Pflanzenernahrung und Bodenkunde 131:221-242.

McKenzie, R.M. 1977. Manganese Oxides and Hydroxides, *In* J. B. Dixon and S. B. Weed, eds. Minerals in soil environments. Soil Science Society of America, Madison, Wisconsin.

McKenzie, R.M. 1980. The adsorption of lead and other heavy metals on oxides of manganese and iron. Australian Journal of Soil Research 18:61-73.

Mehrota, R.C., and R. Bohra. 1983. Metal Carboxylates Academic Press, New York.

Mortland, M.M., and K.V. Raman. 1968. Surface acidity of smectites in relation to hydration, exchangeable cation and structure. Clays and Clay Minerals 16:393-398.

Murray, J.W. 1974. The surface chemistry of hydrous manganese dioxide. Journal of Colloid and Interface Science 46:357-371.

Murray, J.W., and J.G. Dillard. 1979. The oxidation of cobalt(II) adsorbed on manganese dioxide. Geochimica Cosmochima Acta 43:781-787.

Murray, J.W., L.S. Balistrieri, and B. Paul. 1984. The oxidation state of manganese in marine sediments and ferromanganese nodules. Geochimica Cosmochima Acta 48:1237-1247.

Nara, M., H. Torii, and M. Tasumi. 1996. Correlation between the vibrational frequencies of carboxylate group and the types of its coordination to a metal ion: An *ab initio* molecular orbital study. Journal of Physical Chemistry 100:19812-19817.

Neaman, A., B. Waller, F. Mouele, F. Trolard, and G. Bourrie. 2004. Improved methods for selective dissolution of manganese oxides from soils and rocks. European Journal of Soil Science 55:47-54.

Norvell, W.A. 1988. Inorganic reactions of manganese in soils, p. 37-58, *In* R. D. Graham and et al., eds. Manganese in soils and plants. Kluwer Academic Publishers, Netherlands.

Nowicki, T.E. 1997. The impact of Pinus spp. on the chemical properties of soils and stream waters in South African upland catchments. PhD thesis, University of Cape Town.

Ostwald, J. 1984. Two varieties of lithiophorite in some Australian deposits. Mineralogical Magazine 48:383-388.

Ovington, J.D., and H.A.I. Madgwick. 1957. Afforestation and soil reaction. Journal of Soil Science 8:141-149.

Parc, S., D. Nahon, Y. Tardy, and P. Vieillard. 1989. Estimated solubility products and fields of stability for cryptomelane, nsutite, birnessite, and lithiophorite based on natural weathering sequences. American Mineralogist 74:466-475.

Parks, G.A., and P.L. De Bruyn. 1962. The zero point of charge of oxides. Journal of Physical Chemistry 66:967-973.

Partridge, T.C., and R.R. Maud. 1987. Geomorphic evolution of southern Africa since the Mesozoic. South African Journal of Geology 90:179-208.

Paterson, E., B.A. Goodman, and V.C. Farmer. 1991. The chemistry of aluminium, iron and manganese oxides in acid soils, p. 97-124, *In* B. Ulrich and M. E. Sumner, eds. Soil Acidity. Springer-Verlag, Berlin.

Perez-Benito, J.F., C. Arias, and E. Amat. 1996. A kinetic study of reduction of colloidal manganese dioxide by oxalic acid. Journal of Colloid and Interface Science 177:288-297.

Post, J.E. 1999. Manganese oxide minerals: Crystal structures and economic and environmental significance, pp. 3447-3454 Geology, Mineralogy and Human Welfare. Proceedings of the National Academy of Science ,Irvine, CA, Vol. 96.

Post, J.E., and D.L. Bish. 1988. Rietveld refinement of the todorokite structure. American Mineralogist 78:861-869.

Potter, R.M., and G.R. Rossman. 1979a. The tetravalent manganese oxides: identification, hydration, and structural relationships by infrared spectroscopy. American Mineralogist 64:1199-1218.

Raveh, A., and Y. Avnimelech. 1978. The effect of drying on the colloidal properties of humic compounds. Plant and Soil 50:545-552.

Richter, D.D. 1986. Sources of acidity in some forested Udults. Soil Science Society of America Journal 50:1584-1589.

Ross, D.S., and R.J. Bartlett. 1981. Evidence for nonmicrobial oxidation of manganese in soil. Soil Science 132:153-160.

Ross, D.S., T.R. Wilmot, and J. Larsen. 1994. Testing sugarbush soils- effects of sampling storage and drying. Communications in Soil Science and Plant Analysis 25:2899-2908.

Ross, D.S., H.C. Hales, G.C. Shea-McCarthy, and A. Lanzirotti. 2001a. Sensitivity of soil manganese oxides: Drying and storage cause reduction. Soil Science Society of America Journal 65:736-743.

Ross, D.S., H.C. Hales, G.C. Shea-McCarthy, and A. Lanzirotti. 2001b. Sensitivity of soil manganese oxides: XANES spectroscopy may cause reduction. Soil Science Society of America Journal 65:744-752.

Ross, S.J., D.P. Franzmeir, and C.B. Roth. 1976. Mineralogy and chemistry of manganese oxides in some Indiana soils. Soil Science Society of America Journal 40:137-143.

Ruth, A., B.B. Johnson, and T.J. Fowler. 1998. Geomorphic controls on aluminium in acid soils of the Axe Creek catchment, Victoria. Australian Journal of Soil Research 36:951-962.

Schnitzer, M., and M. Levesque. 1979. Electron spin resonance as a guide to the degree of humification of peats. Soil Science 127:140-145.

Schulze, D.G., S.R. Sutton, and S. Bajt. 1995. Determining manganese oxidation state in soils using X-ray absorption near-edge structure (XANES) spectroscopy. Soil Science Society of America Journal 59:1540-1548.

Schutz, C.J. 1990. Site relationships for Pinus *patula* in the eastern Transvaal escarpment area. PhD thesis, University of Natal, South Africa.

Schwertmann, U., and R.M. Taylor. 1977. Iron Oxides, p. 145-180, *In* J. B. Dixon and S. B. Weed, eds. Minerals in soil environments. Soil Science Society of America, Madison, Wisconsin.

Silvester, E., A. Manceau, and V.A. Drits. 1997. Structure of synthetic monoclinic Na-rich birnessite and hexagonal birnessite: II. Results from chemical studies and EXAFS spectroscopy. American Mineralogist 82:962-978.

Soil Classification Working Group. 1991. Soil Classification: A Taxonomic System for South Africa. Department of Agricultural Development, Pretoria.

Soil Survey Staff. 1999. Soil Taxonomy. Second ed. United States Department of Agriculture, Washington DC.

Sparks, D.L. 2003. Environmental soil chemistry. Second ed. Academic Press, Orlando, Florida.

Sparrow, L.A., and N.C. Uren. 1987. Oxidation and reduction of Mn in acidic soils: Effect of temperature and soil pH. Soil Biology and Biochemistry 19:143-148.

Stone, A.T. 1987. Microbial metabolites and the reductive dissolution of manganese oxides: oxalate and pyruvate. Geochimica Cosmochima Acta 51:919-925.

Stone, A.T., and J.J. Morgan. 1984a. Reduction and dissolution of manganese(III) and manganese(IV) oxides by organics.1 Reaction with hydroquinone. Environmental Science and Technology 18:450-456.

Stone, A.T., and J.J. Morgan. 1984b. Reduction and dissolution of manganese(III) and manganese(IV) oxides by organics.2 Survey of the reactivity organics. Environmental Science and Technology 18:617-624.

Stueben, B.L., B. Cantrelle, J. Sneddon, and J.N. Beck. 2004. Manganese K-edge XANES studies of Mn speciation in Lac des Allemands as a function of depth. Microchemical Journal 76:113-120.

Sumner, M.E., M.V. Fey, and A.D. Noble. 1991. Nutrient Status and toxicity problems in acid soils, p. 149-182, *In* B. Ulrich and M. E. Sumner, eds. Soil Acidity. Springer-Verlag, Berlin.

Taylor, R.M., R.M. McKenzie, and K. Norrish. 1964. The mineralogy and chemistry of manganes in some Australian soils. Australian Journal of Soil Research 2:235-248.

Tokashiki, Y., J.B. Dixon, and D.C. Golden. 1986. Manganese oxide analysis in soils by combined X-ray diffraction and selective dissolution methods. Soil Science Society of America Journal 50:1079-1084.

Tokashiki, Y., T. Hentona, M. Shimo, and L.P. Vidhana Arachchi. 2003. Improvement of the successive selective dissolution procedure for the separation of birnessite, lithiophorite and goethite in soil manganese nodules. Soil Science Society of America Journal 67:837-834.

Turner, S. 1982. A structural study of tunnel manganese oxides by high-resolution transmission electron microscopy. PhD thesis, Arizona State University.

Uehara, G., and G.P. Gillman. 1982. The mineralogy, chemistry and physics of tropical soils with variable charge clays. Westview Press, Boulder, CO.

Ulrich, B. 1991. An ecosystem approach to soil acidification, p. 28-79, *In* B. Ulrich and M. E. Sumner, eds. Soil Acidity. Springer-Velag, Berlin.

Uzochukwu, G.A., and J.B. Dixon. 1986. Manganese oxide minerals in nodules of two soils of Texas and Alabama. Soil Science Society of America Journal 50:1358-1363.

Vega, S., M. Calisay, and N.V. Hue. 1992. Manganese toxicity in cowpea as affected by soil pH and sewage sludge amendment. Journal of Plant Nutrition 15:219-231.

Viljoen, M.J., and W.U. Reimold. 1999. An introduction to South Africa's geological and mining heritage Mintek, Johannesburg, South Africa.

Von Christen, H.C. 1964. Some observations on the forest soils of South Africa. Forestry in South Africa 1:91-104.

White, J.L., and C.B. Roth. 1986. Infrared spectroscopy, p. 291-330, *In* A. Klute, ed. Methods of soil analysis Part 1 Physical and mineralogical methods, Second ed. ASA-SSSA, Madison Wisconsin.

Xyla, A.G., B. Sulzberger, G.W. Luther, J.G. Hering, P. Van Cappellen, and W. Stumm. 1992. Reductive dissolution of manganese (III,IV) (hydr)oxides by oxalate: The effect of pH and light. Langmuir 8:95-103.

Yang, D.S., and M.K. Wang. 2003. Characterization and a fast method for synthesis of sub-micron lithiophorite. Clays and Clay Minerals 51:96-101.

Zinder, B., G. Furrer, and W. Stumm. 1986. The coordination chemistry of weathering: II. Dissolution of Fe(III) oxides. Geochimica Cosmochima Acta 50:1861-1869.

APPENDIX A- supplementary data relating to Chapter 2

This Appendix shows XRD patterns of powdered, whole soil, samples from the subsoils of F2, F4 and F5 profiles. Soil material was ground and placed in aluminium sample holders for XRD analysis. Details of defractometer settings are provided in section 2.2.2. Dithionite-citrate treated sample was prepared by the method described in Table 2.1. The substantial difference in the kaolinite/quartz and mica/quartz ratios of the two patterns in Figure A.1 may be attributed the removal of Mn and Fe materials after the DC treatment resulting in a 'cleaner' pattern of the remaining clay minerals.

F2-subsoil

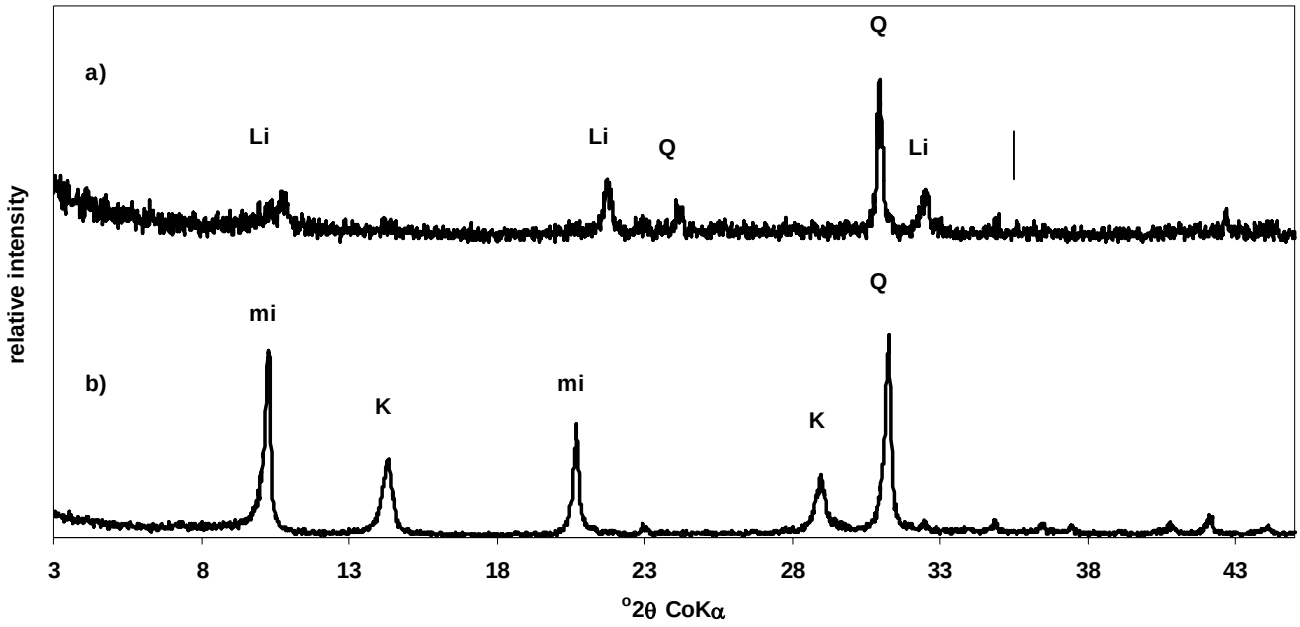

Figure A.1 Powder X-ray diffraction patterns of a) untreated, and b) dithionite-citrate (DC) treated soil material from F2 profile (F2B2), k= kaolinite (7.16, 3.57, 2.34 Å); mi= mica (10.0, 4.98, 3.34 Å); Li = lithiophorite (4.71, 9.43, 2.37, 3.14 Å); Q = quartz (3.34; 4.26 Å).

F4- subsoil

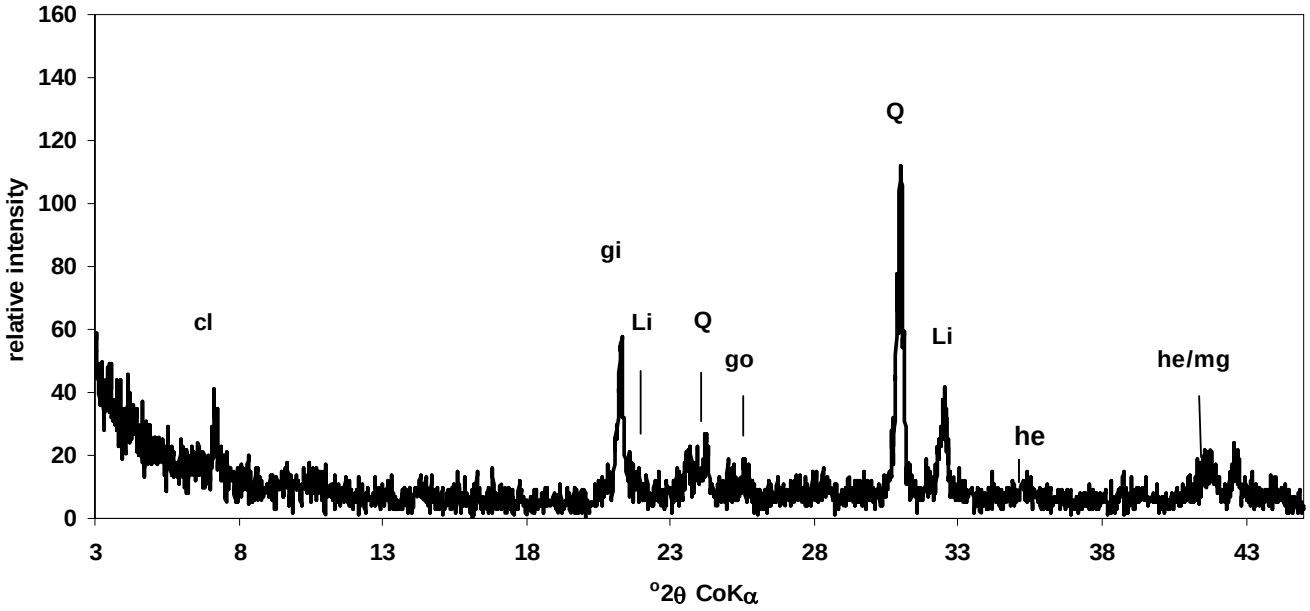

Figure A.2 Power XRD pattern of soil material taken from the subsoil of the F4 profile (F4B2), gi= gibbsite (4.85, 4.37, 4.32 Å); Li = lithiophorite (4.71, 9.43, 2.37, 3.14 Å); Q = quartz (3.34; 4.26 Å); go = goethite (4.18, 2.69, 2.43 Å); mg = magnetite/maghemite (2.52, 2.95 Å) and he = hematite (2.69, 3.68, 2.52 Å).

F5-subsoil

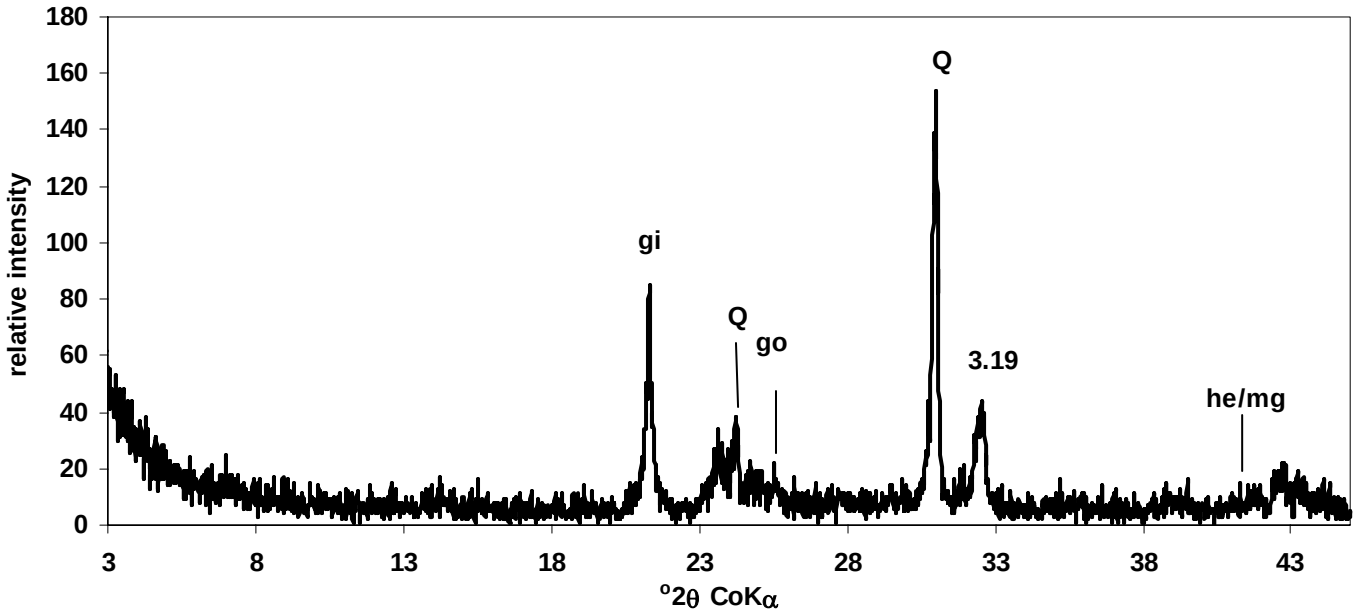

Figure A.3 Powder XRD pattern of soil material taken from the subsoil of the F5 profile (F5B2) gi= gibbsite (4.85, 4.37, 4.32 Å); Q = quartz (3.34; 4.26 Å); go = goethite (4.18, 2.69, 2.43 Å); mg = magnetite/maghemite (2.52, 2.95 Å) and he = hematite (2.69, 3.68, 2.52 Å).

APPENDIX B Supplementary data relating to Chapter 4

The data in the ensuing figures show the reproducibility of certain results obtained in Chapter 4, using soil material from different profiles. The corresponding figures in chapter 4 are indicated in the figure captions.

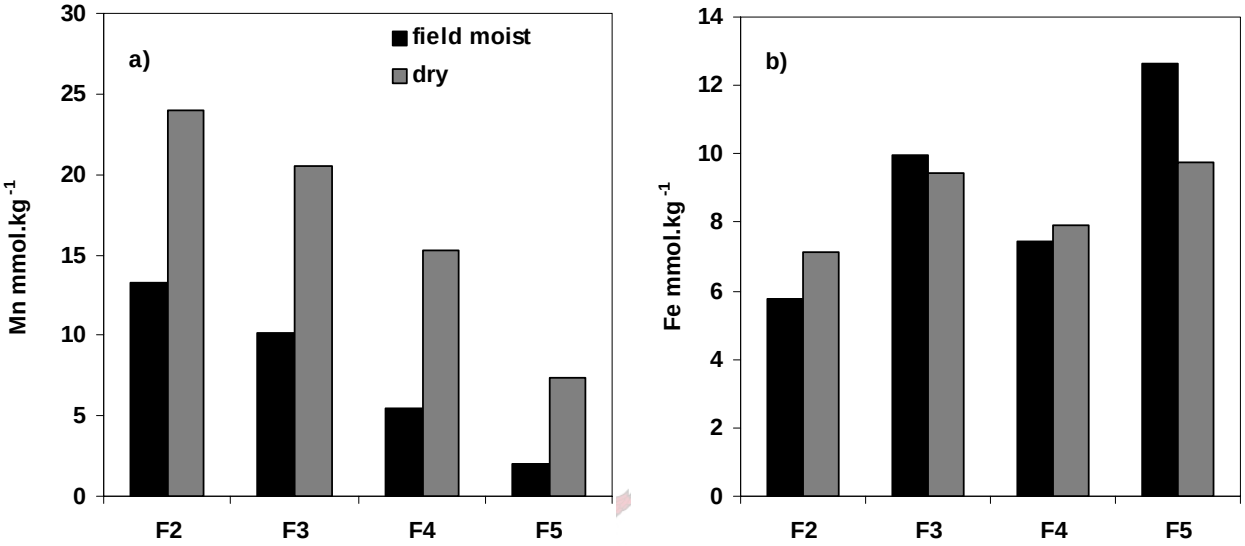

Figure B.1 Concentrations of a) Mn and b) Fe in moist and oven-dried (40^{o} C) topsoil samples, from F2, F3, F4 and F5 profiles, extracted with 0.05 M, pH 5, Na-pyrophosphate (1:20 soil solution ratio). See Figure 4.2.

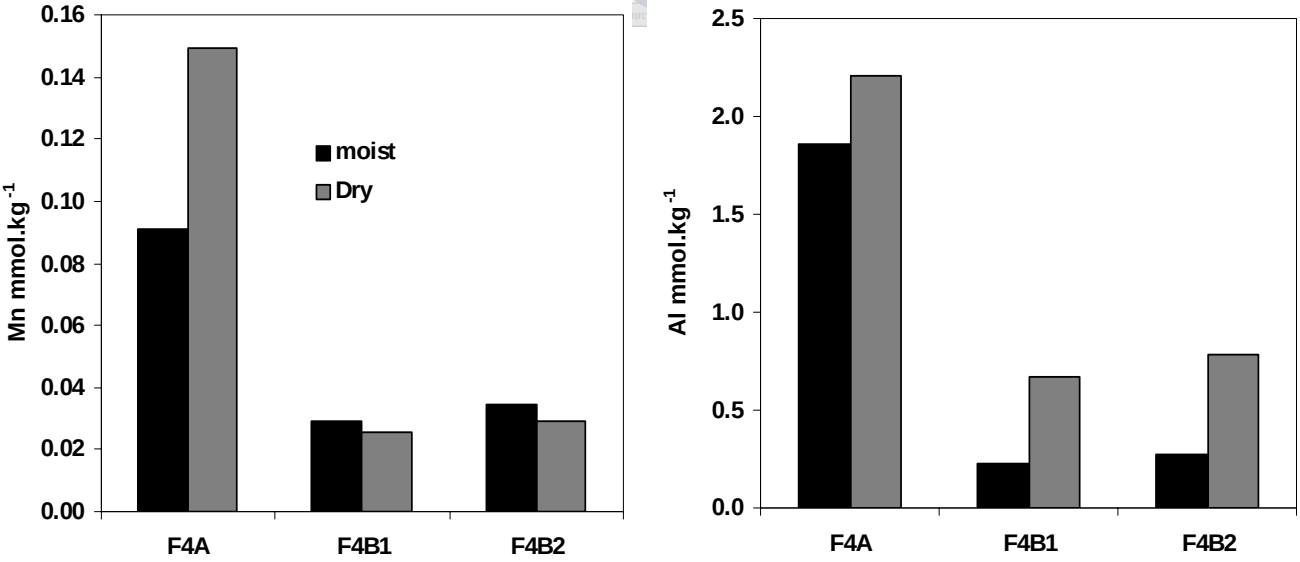

Figure B.2 Extractable a) Al and b) Mn from moist and air-dried (7 days at 25^{o}C) soils from the F4 profile using 1M KCl (1:10 soil solution ratio). See Figure 4.3.

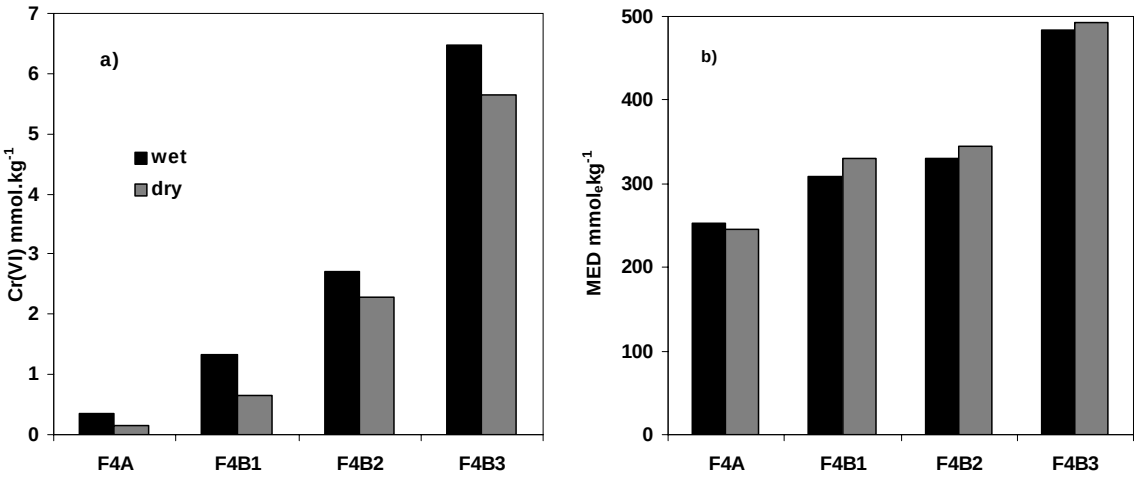

Figure B.3 Redox tests performed on moist and oven-dried (40^{o}C) soil from the F4 profile showing a) net Cr oxidising capacity and b) manganese electron demand (MED). See Figure 4.5